THE ROLE OF THE ARYL HYDROCARBON RECEPTOR AND THE LIVER X RECEPTOR IN GENE REGULATION AND METABOLIC HOMEOSTASIS

by

Jung Hoon Lee

Bachelor of Science, Dongguk University, 2001

Master of Science, Seoul National University, 2003

Submitted to the Graduate Faculty of

School of Pharmacy in partial fulfillment

of the requirements for the degree of

Doctor of Philosophy

University of Pittsburgh

2009

UNIVERSITY OF PITTSBURGH

School of Pharmacy

This thesis was presented

by

Jung Hoon Lee

It was defended on

April 07, 2009

and approved by

Regis R. Vollmer, PhD., Professor, Pharmaceutical Sciences

Song Li, MD., PhD., Associate Professor, Pharmaceutical Sciences

Zhou Wang, PhD., Professor, Urology

Yuan-Pu (Peter) Di, PhD., Assistant Professor, Environmental and Occupational Health

Dissertation Advisor: Wen Xie, MD., PhD., Associate Professor, Pharmaceutical Sciences

THE ROLE OF THE ARYL HYDROCARBON RECEPTOR AND THE LIVER X RECEPTOR IN GENE REGULATION AND METABOLIC HOMEOSTASIS

Jung Hoon Lee, PhD

University of Pittsburgh, 2009

The aryl hydrocarbon receptor (AhR) is a PAS domain transcriptional factor also known as the "dioxin receptor" or "xenobiotic receptor." My thesis work has uncovered an endobiotic role for AhR in hepatic steatosis and other metabolic functions. Activation of AhR induced spontaneous hepatic steatosis, which is characterized by the accumulation of triglycerides. The steatotic effect of AhR was likely due to the combined upregulation of fatty acid translocase CD36/FAT, suppression of fatty acid oxidation, inhibition of hepatic export of triglycerides, and an increase in the mobilization of peripheral fat. Promoter analysis established CD36 as a novel transcriptional target of AhR. Moreover, the steatotic effect of an AhR agonist was inhibited in mice deficient of CD36. Results from this study may help to establish AhR and its target fatty acid translocase CD36 as attractive targets for intervention in fatty liver disease.

The liver X receptors (LXRs), both the α and β isoforms, are nuclear receptors identified as sterol sensors that modulate cholesterol and lipid metabolism and homeostasis. In the second part of my thesis research, I report a novel LXR-mediated mechanism of androgen deprivation. Genetic or pharmacological activation of the liver X receptor (LXR) *in vivo* lowered androgenic activity by inducing the hydroxysteroid sulfotransferase 2A1 (SULT2A1), an enzyme essential for the metabolic deactivation of androgens. Activation of LXR also inhibited the expression of steroid sulfatase (STS) in the prostate, which may have helped to prevent the local conversion of sulfonated androgens back to active metabolites. At the physiological level, activation of LXR in

mice inhibited androgen-dependent prostate regeneration in castrated mice. Treatment with LXR agonists inhibited androgen-dependent proliferation of prostate cancer cells in LXR- and SULT2A1-dependent manner. The ability of LXRs to regulate androgen metabolism makes them novel therapeutic targets for the treatment and prevention of hormone-dependent prostate cancer.

Taken together, my work has revealed novel functions of AhR in lipid metabolism and LXR in androgen deprivation. It is hoped that understandings of the endobiotic functions of AhR and LXR may establish these two receptors as therapeutic targets for the management of metabolic disease in humans.

TABLE OF CONTENTS

LIST OF TABLES

LIST OF FIGURES

PREFACE

This thesis is dedicated to my loving husband, Min Jae, without whom none of this could have been possible; to my dad, who has always believed in your daughter as a scientist; and to my mom, who has always been proud of your daughter. Thank you.

Abbreviation

ACC-1, acetyl CoA carboxylase 1; **AhR**, aryl hydrocarbon receptor; **AR**, androgen receptor; **Arnt**, aryl hydrocarbon receptor nuclear translocator; **ARE**, androgen receptor responsive element; **BrdU**, bromodeoxyuridine; **DHEA**, dehydroepiandrosterone; **DHT**, dihydrotestosterone; **DRE**, dioxin responsive element; **EMSA**, eletrophoretic mobility shift assay; **EST**, estrogen sulfotransferase; **FABP**, fatty acid binding protein; **FAS**, fatty acid synthase; **FAT**, fatty acid translocase; **FATP**, fatty acid transporter protein; **FBS**, fetal bovine serum; **FFA**, free fatty acid; **FICZ**, 6-formylindolo [3,2-b]carbazole; **3β-Hsd**, 3β-hydroxysteroid dehydrogenase; **17β-Hsd**; 17β- hydroxysteroid dehydrogenase; **LH**, luteinizing hormone; **LDLR**, low density lipoprotein receptor; **LRP**, LDLR related protein; **LXR**, liver X receptor; **3-MC**, 3-methylchoranethrene; **NAFLD**, non-alcoholic fatty liver disease; **NCoR**; nuclear receptor corepressor; **PAPS**, 3'-phosphoadenosine-5'-phosposulfate; **PAS**, period-Arnt-single minded; **PCNA**, proliferating cell nuclear antigen; **PSA**, prostate specific antigen; **RIP140**, nuclear receptor interacting protein 1; **RXR**, retinoid X receptor; **SCD-1**, stearoyl CoA desaturase-1; **SHP**, short heterodimer partner; **SMRT**, silencing mediator or retinoid and thyroid receptors; **SR**, scavenger receptor; **SRC**, steroid receptor coactivator; **Sts**, steroid sulfatase; **SULT**, sulfotransferase; **T**, testosterone; **TCDD**; 2,3,7,8-tetrachlorodibenzo-*p*-dioxin; **TG**, transgenic; **VLDL**, very low density lipoprotein; **VLDLR**, very low density lipoprotein receptor; **VP**, viral protein 16; **WAT**, white adipose tissue; **WT**, wild type

CHAPTER I

1.0 INTRODUCTION

1.1 AN OVERVIEW OF AHR AND LXR AS XENOBIOTIC AND ENDOBIOTIC SENSORS

The expression of many genes involved in xenobiotic and endobiotic metabolism is regulated by the aryl hydrocarbon receptor (AhR) and the orphan nuclear receptors, such as the liver X receptor (LXR). Both AhR and LXR are ligand-dependent transcription factors that sense endogenous or xenobiotic signals and subsequently regulate the expression of their target genes. The regulation of target genes is achieved by binding of the receptors to DNA responsive elements in enhancer or promoter regions of target genes. The regulation of target gene in turn will affect the homeostasis of numerous xenobiotics and endobiotics, such as bile acids, lipids, hormones, glucose, fat-soluble vitamins and mediators of the inflammatory process (Pascussi et al., 2008).

AhR belongs to the basic helix-loop-helix (bHLH) PER-ARNT-SIM (PAS) family (Figure 1). The prototypical AhR ligand is an environmental contaminant 2,3,7,8-tetrachlorodibenzo-p-dioxin (TCDD), therefore it is also called ‘dioxin receptor’ (Hoffman et al., 1991). AhR binds structurally diverse xenobiotic chemicals, such as 3-methylcholanthrene (3-MC) and endobiotic chemicals, such as indigo and 6-formylindolo[3,2b]carbazole (FICZ). Prior

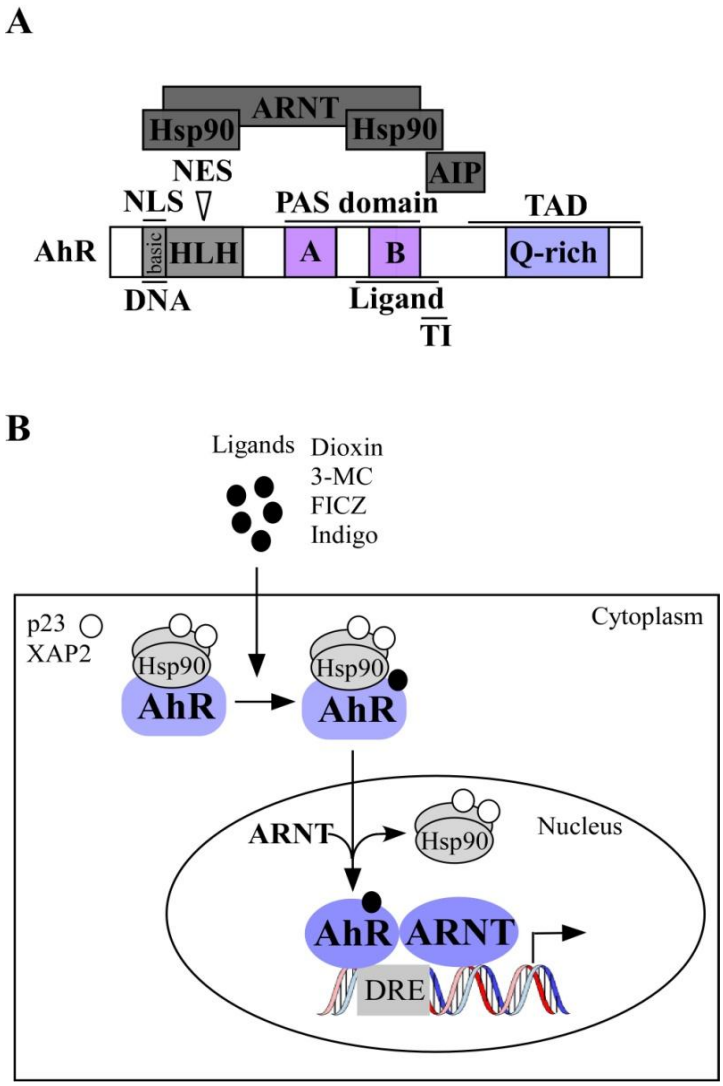

Figure 1 Functional domain of aryl hydrocarbon receptor (AhR) and AhR pathway **(A)** Schematic illustration of structural and functional organization of AhR. NLS, nuclear localization signal; NES, nuclear export signal; HLH, helix-loop-helix; Hsp90, heat shock protein 90; ARNT, AhR nuclear translocator; DNA, DNA binding domain; Ligand, ligand binding domain; PAS, PER-ARNT-SIM; AIP, AhR interacting protein; TAD, transactivation domain; TI, transcription inhibitory domain **(B)** Model of AhR signaling. AhR normally resides in the cytoplasm, stably associated with two heat shock protein 90 (Hsp90). AhR regulatory proteins, including p23 and XAP2 also stabilize AhR in cytoplasm. On activation by ligands results in AhR translocation into the nucleus where AhR is heterdimerized with AhR nuclear translocator (ARNT). The AhR-ARNT heterodimer regulates its target genes by binding to dioxin responsive element (DRE) present in the promoter region.

to ligand binding, AhR is located in the cytoplasm, associating with HSP90, X-associated protein

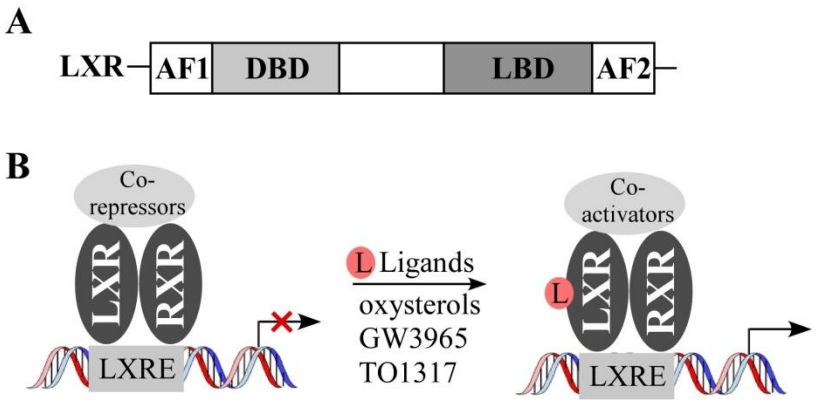

Figure 2 Structural domain of liver X receptor (LXR) and LXR-mediated regulation of gene. **(A)** Domain structures of nuclear receptors. AF1 and 2, activation domain 1 and 2; DBD, DNA binding domain; LBD, ligand binding domain **(B)** Liver X receptor (LXR) pathway. Within the nucleus, LXR/RXR heterodimers are bound to LXREs in the promoters of target genes and in complex with corepressors, such as SMRT and NCOR. Ligand binding recruits coactivators, leading to induction of target gene expression.

2 (XAP2, also known as ARA9 or AIP), and HSP90 co-chaperone p23 (Carlson and Perdew, 2002). Binding of a ligand to AhR triggers nuclear translocation and allows heterodimerization with the AhR nuclear translocator (ARNT) (Reyes et al., 1992). AhR-ARNT heterodimers bind to dioxin responsive element (DRE) in the promoter region of target genes. The consensus DRE is TNGCGTG (Gu et al., 2000).

The liver X receptors LXRα and LXRβ are lipid-activated nuclear receptors that were first identified as cholesterol sensors. LXRs, like many other nuclear receptor superfamily members, consist of a N-terminal DNA-binding domain (DBD) and a C-terminal ligand-binding domain (LBD) (Figure 2). It is generally believed that in the absence of ligands, LXRs recruit complexes of corepressors, including NCoR, SMRT, RIP140, and SHP, that silence the transcription of target genes (Gronemeyer et al., 2004). Upon ligand binding, increased transcription is achieved by conformational changes of the receptors that lead to exchanges of corepressors with coactivators, such as the p160 family of coactivators (SRC-1, SRC-2/GRIP1, and SRC-3/ACTR/AIB1) (McKenna and O'Malley, 2002) and heterodimerization with retinoid

X receptors (RXRs). LXR-RXR heterodimers bind to DNA-responsive elements that contain direct repeats (DRs) of the consensus motifs AG(G/T)TC(A/C) separated by four base pair (DR-4) (Chawla et al., 2001) or inverted repeats separated by no base pairs IR-0 (Uppal et al., 2007). LXR agonists include the endogenous cholesterol metabolites, such as 24(S),25-epoxycholesterol, 24(S)-hydroxycholesterol, 22(R)-hydroxycholesterol (Repa and Mangelsdorf, 2002), as well as synthetic agonists, such as TO0901317 (TO1317) (Schultz et al., 2000) and GW3965 (Collins et al., 2002).

My thesis work has established AhR as a key modulator of lipid metabolism (Chapter II) and LXRs as a regulator of androgen metabolism, which links to prostate cancer (Chapter III).

1.2 GENERAL SIGNALING AND FUNCTION OF AHR AND LXR

1.2.1 AhR

Vertebrates have developed a general strategy to protect themselves from adverse chemical environments by up-regulating batteries of xenobiotic metabolizing enzymes (XMEs), thus decreasing the biological half-life of the insulting chemicals. XMEs include phase I, phase II metabolizing enzymes and phase III transporters. They are present in abundance either at the basal or inducible levels in response to xenobiotics exposures. It has long been observed that a number of XMEs are regulated by ligand-dependent transcription factors, including the PAS domain transcription factor AhR, and nuclear hormone receptors, constitutive androstane receptor (CAR), and pregnane X receptor (PXR). AhR can induce the expression of the microsomal cytochrome P450-dependent monooxygenase 1 (CYP1) genes in response to

halogenated aromatic hydrocarbons (HAHs) and polycyclic aromatic hydrocarbons (PAHs). Phase II glutathione S-transferases (GSTs) and UDP-glucuronosyltransferases (UGTs) have also been shown to be regulated by AhR. Most of these enzymes appear to have metabolic activity toward PAHs, such as benzo[a]pyrene and 3-methylcholantherene, and are believed to decrease their biological half-life. Therefore, AhR function is believed to be an adaptive response to the cellular environmental and a sensor to xenobiotic signals. However, it has become clear that in addition to its role in regulating drug metabolizing enzymes, AhR is also a primary mediator of HAHs and PAHs-induced toxicity. Sustained activation of AhR by HAH and PAH mediates a pleiotropic effect of species- and tissue-dependent toxicities, including cancer, immunosuppression, liver damage, and birth defects. The HAHs and PAHs-mediated toxic effects appear to be AhR-dependent since the responses to benzo[a]pyrene or dioxin were abrogated by the genetic ablation of AhR (Fernandez-Salguero et al., 1995; Schmidt et al., 1996; Shimizu et al., 2000). Although the mechanisms underlying these toxic effects are largely unsolved, it has been hypothesized that AhR-mediated induction of CYP1A and 1B1 contributes to the metabolic activation of carcinogens. These enzymes catalyze the epoxidation of PAHs, resulting in the generation of highly reactive intermediate that are capable of binding covalently to specific residues of DNA. The formation of DNA adduct causes mutation, birth defects and toxicity followed ultimately by carcinogenesis. In contrast to PAHs that undergo metabolic conversion into DNA-reactive intermediates, dioxin and other HAHs are non-genotoxic compounds that fail to form a DNA adduct but show carcinogenic effects. A link between AhR and dioxin toxicity has been established with the use of $AhR^{-/-}$ mice, however, the mechanisms behind a wide range of toxic effects by dioxin remain unresolved.

Although AhR has been identified as a 'xenobiotic receptor', emerging evidence has pointed to an equally important role of AhR as an 'endobiotic receptor'. Subsequent studies, mainly through the characterization of $AhR^{-/-}$ mice, suggest that AhR also has endobiotic functions by affecting physiology and tissue development. For example, $AhR^{-/-}$ mice had smaller livers (Fernandez-Salguero et al., 1995; Schmidt et al., 1996) and vascular abnormalities (Lahvis et al., 2000). The most abnormal vascular pattern reported in $AhR^{-/-}$ mice is a patent Ductus Venosus (DV) (Lahvis et al., 2000) which is a porto-systemic shunt allowing portal blood to reach the systemic circulation without first passing through the liver. The endobiotic function of AhR has also been supported by recent identification of endogenous AhR agonists, such as indoles (Adachi et al., 2001), arachidonic acid metabolites (Seidel et al., 2001), modified LDL (McMillan and Bradfield, 2007), and leukotrine A4 metabolites (Chiaro et al., 2008). Therefore, the AhR functions can be classified into: 1) adaptive response which results in the detoxification of toxicants by enhanced metabolism, 2) toxic response through the induction of genes involved in metabolic activation of toxicants, and 3) developmental effects which are likely resulted from activation of the receptors by endogenous ligands.

1.2.2 LXR

LXRs, both the α and β isoforms, were known as sterol sensors that regulate cholesterol and lipid metabolism and homeostasis (Willy et al., 1995). LXRα is highly expressed in the liver, but its expression is also found in adipose tissues, intestine, macrophages, lung and kidney. LXRβ is expressed ubiquitously (Zelcer and Tontonoz, 2006). LXRα and LXRβ are highly conserved, sharing 76% and 78% sequence homology in their DNA binding domain (DBD) and ligand

binding domain (LBD), respectively. LXRα and LXRβ share many of the DNA response elements as well as endogenous and exogenous ligands. LXRs possess diverse functions, ranging from cholesterol efflux to lipogenesis and anti-inflammation. For this reasons, LXRs have been explored as a therapeutic target for atherosclerosis, diabetics, and Alzheimer's disease in animal models. In rodents, activation of LXRα increases cholesterol catabolism. LXRα deficient mice exhibited a marked increase in cholesteryl ester accumulation and LDL cholesterol levels in their livers but a decrease in HDL cholesterol levels when challenged with a high-cholesterol diet (Peet et al., 1998). In contrast, LXRβ deficient mice do not display an obvious phenotype in the response to high-cholesterol challenge (Alberti et al., 2001), implying that LXRα plays a more prominent role in hepatic cholesterol metabolism. The first target gene in cholesterol metabolism induced by LXR was identified as cholesterol 7α-hydroxylase (Cyp7a1), the rate limiting enzyme in the synthetic pathway that catalyzes for the formation of bile acid from cholesterol (Peet et al., 1998). LXRs were later found to increase the expression of the ATP-binding cassette (ABC) superfamily of transporters, including ABCA1, ABCG5, ABCG8 and ABCG1, resulting in cholesterol secretion into the bile and limiting dietary cholesterol absorption (Repa et al., 2000b). Treatment with LXR ligands, such as TO1317 and GW3965, lowers cholesterol level and inhibits the development of atherosclerosis in mouse models (Barish and Evans, 2004; Repa and Mangelsdorf, 2002).

Despite their promise as anti-atherosclerotic targets, LXRs have also been linked to hepatic lipogenesis (Repa et al., 2000a; Schultz et al., 2000; Yoshikawa et al., 2001). Treatment of mice with LXR agonists elevates triglyceride levels in the liver as well as in the plasma (Repa et al., 2000a; Schultz et al., 2000). LXR activation increases plasma triglyceride levels through the transcriptional activation of SREBP-1c, a transcriptional factor known to regulate the

expression of a battery of lipogenic enzymes, including SCD-1, ACC-1 and FAS. Accumulating evidence suggests that LXRs may also promote steatosis in a SREBP-independent manner. For example, FAS (Joseph et al., 2002), ACC-1 (Talukdar and Hillgartner, 2006) and SCD-1 (Chu et al., 2006) can be directly regulated by LXR, instead of being mediated by SREBP activation. LXRs positively regulate several transcription factors involved in lipogenesis, including PPARγ (Seo et al., 2004) and carbohydrate response element-binding protein (ChREBP) (Cha and Repa, 2007), a glucose-sensitive transcription factor and a regulator of conversion to lipids from excess carbohydrates. Activation of LXR has also been reported to induce enzymes in lipoprotein remodeling, such as lipoprotein lipase (LPL) (Zhang et al., 2001), a rate-limiting enzyme for catabolism of triglyceride from VLDL and chylomicrons.

In macrophages, LXRs play an important role in innate immunity and inflammatory signaling (Glass and Ogawa, 2006; Zelcer and Tontonoz, 2006). LXR agonists enhance macrophage survival during bacterial infection. Mice lacking LXRs were highly susceptible to the intracellular pathogen *Listeria monocytogenes* infection and this phenotype was recapitulated by transplantation of bone marrow from LXR$\alpha\beta^{-/-}$ mice into WT mice, indicating LXRs are required for innate immune response (Joseph et al., 2004). In addition, activation of LXRs inhibits the lipopolysaccharide (LPS) induction of a number of proinflammatory genes such as inducible nitric oxide synthase (iNOS), cytokines such as interleukin-1β (IL1β), and chemokines such as monocyte chemoattractant protein-1 (MCP-1) (Joseph et al., 2003). These observations have established LXRs as key modulators of both lipid metabolism and inflammatory signaling. More recently, we showed that LXR can alleviate cholestasis by enhancing bile acid detoxification (Uppal et al., 2007), and promote estrogen deprivation by activating the estrogen sulfotransferase (EST) (Gong et al., 2007).

CHAPTER II

2.0 AN ENDOBIOTIC ROLE OF AHR IN HEPATIC STEATOSIS

2.1 BACKGROUND

Hepatic steatosis, or fatty liver, is a common medical problem strongly associated with metabolic syndrome, which is characterized by insulin resistance and a high risk for cardiovascular disease (Kotronen and Yki-Jarvinen, 2008; Postic and Girard, 2008). The liver plays a central role in fatty acid and triglyceride metabolism (Lee et al., 2008b; Shi and Burn, 2004) (see Figure 3). In the fed state, the liver ensures an adequate supply of fuel substrate from glucose, which is required for *de novo* fatty acid synthesis. The hepatic *de novo* fatty acid synthesis is controlled by the dedicated lipogenic transcriptional factor sterol regulatory element binding protein 1c (SREBP-1c) that regulates a battery of lipogenic enzymes, including fatty acid synthase (FAS), stearoyl CoA desaturase-1 (SCD-1) and acetyl CoA carboxylase 1 (ACC-1) (Horton et al., 2002). The carbohydrate responsive element binding protein (ChREBP), another transcriptional factor, also plays an important role in inducing hepatic lipogenesis (Uyeda and Repa, 2006).

Another major source of hepatic lipids is circulating free fatty acids (FFAs). Upon uptake by the hepatocytes, FFAs can be converted to triglycerides, when intrahepatic FFAs are in excess (Bradbury, 2006). As such, increased uptake of circulating FFA by hepatocytes can contribute to hepatic steatosis. The importance of FFAs in steatosis is supported by the clinical observation

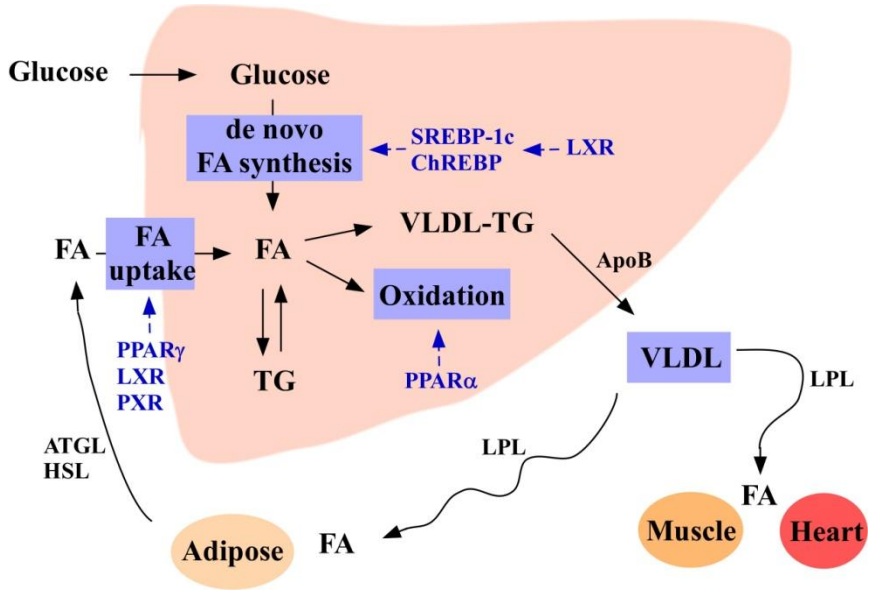

Figure 3 Hepatic lipid metabolism. In fed state, glucose is taken-up by liver to be metabolized, producing substrates required for de novo fatty acid synthesis. Within the liver, fatty acids are either oxidized or re-esterized into triglycerides for storage, which can be secreted as very-low density lipoprotein (VLDL) into blood stream. In turn, VLDL particles are directed toward difference tissues, such as muscle, heart and adipose tissues, depending on the tissue-specific availability of lipoprotein lipase (LPL). In addition, liver is responsible for uptake of triglyceride-derived free fatty acids. These actions of the liver are achieved by regulation of gene expression. The nuclear receptors and transcription factors involved in hepatic lipid metabolism are shown.

that their concentration in plasma is often increased in various disorders associated with hepatic steatosis (Bradbury, 2006).

Over 90% of plasma fatty acids are not free; they circulate as components of plasma lipoproteins (Figure 4). Very-density lipoproteins (VLDL) are the liver's primary vehicle for secreting triglyceride and transport lipids to peripheral tissues such as heart, skeletal muscle and adipose tissues. They undergo lipolysis, converting them to remnants, including intermediate-density lipoprotein (IDL), low-density lipoprotein (LDL) and oxidized LDL (ox-LDL). These remnants are returned to the liver. Chylomicrons, dietary fats formed in the intestine, are hydrolyzed by lipoprotein lipase (LPL) leading to fatty acid delivery to peripheral tissues. Chylomicron remnants are also taken up by the liver. Hepatic uptake of lipoproteins is mediated via receptors, including the

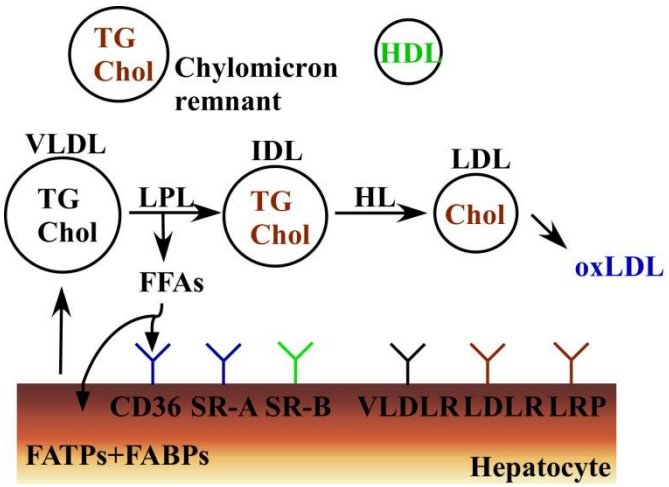

Figure 4 Hepatic lipid uptake. The liver obtains lipid via lipoproteins and free fatty acids. The lipids are repacked and secreted as triglyceride-rich VLDL from the liver. Following hepatic secretion, lipoprotein lipase (LPL) hydrolyzes VLDL to release triglyceride and fatty acids in various tissues, including blood stream, adipose, muscle and heart. It further shrinks into intermediate-density lipoprotein (IDL) by hepatic lipase (HL) and cholesterol-rich LDL. Hepatic uptake of lipoproteins is mediated by the receptors, such as the VLDL receptor (VLDLR), LDL receptor (LDLR), LDL receptor-related protein (LRP) and hepatic scavenger receptors including SR-A, SR-B and CD36. CD36 is also capable of taking up fatty acids. Fatty acids are also transported into hepatocyte by fatty acid transport proteins (FATPs) and fatty acid binding proteins (FABPs).

VLDL receptor (VLDLR), LDL receptor (LDLR), LDL receptor-related protein (LRP) and hepatic scavenger receptors including SR-A, SR-BI and CD36 (Figure 4).

The fatty acid translocase CD36/FAT is the most widely studied cell surface receptor responsible for uptake of FFA. CD36 belongs to class B scavenger receptor highly present on the surface of a number of nonheptic cells and tissues, including monocytes/macrophages, endothelium, smooth muscle cells and differentiated adipocytes (Collot-Teixeira et al., 2007). Therefore, its role mediating FFA uptake has been recognized in nonhepatic tissues (Collot-Teixeira et al., 2007; Febbraio and Silverstein, 2007). More recently, expression has been reported on hepatocytes under certain circumstances. For instance, CD36 has been documented to play an important role in hepatic steatosis due to its ability to translocate free fatty acids from the circulation into liver (Febbraio and Silverstein, 2007). In addition to CD36, fatty acid uptake can also be mediated by the liver fatty acid-binding protein (L-FABP) and fatty acid transport

protein (FATP) (Goldberg and Ginsberg, 2006). Mice deficient of L-FABP or FATP5 have been shown to be protective from Western diet-induced obesity and hepatic steatosis (Hubbard et al., 2006; Newberry et al., 2006).

Within the liver, fatty acids are either oxidized or re-esterized into triglycerides for storage. Fatty acids oxidation can occur in mitochondria, peroxisomes, or endoplasmic reticulum. Mitochondrial and peroxisomal oxidation is β-oxidation primarily mediated by carnitine palmitoyltransferase 1 (CPT-1) and palmitoyl acyl-coenzyme A oxidase 1 (ACOX-1), respectively. The oxidation that occurs in the endoplasmic reticulum is ω-oxidation, which is catalyzed by the CYP4A enzymes (Reddy and Hashimoto, 2001). The liver triglycerides can be secreted as very-low density lipoprotein (VLDL) into the blood stream. VLDL particles are then directed to peripheral tissues, such as muscle, heart and adipose tissues, depending on the tissue-specific availability of lipoprotein lipase (LPL).

Despite the appreciation by the characterization of AhR null mice and identification of endogenous AhR ligands for the endobiotic function of AhR, the molecular mechanisms by which AhR affects normal physiology remain largely unknown. In order to study the physiological function of the receptor, a mutant that bears the constitutively activated AhR (CA-AhR) was created by the deletion of the PAS-B domain in AhR and expressed in transgenic mice. CA-AhR expression driven by modified SV40 promoter caused the spontaneous development of stomach and liver cancer (Andersson et al., 2002; Moennikes et al., 2004). These mice also exhibited altered immune response (Andersson et al., 2003). T-cell specific expression of CA-AhR by CD2 promoter caused thymus involution and suppressed immunization-induced T-cell or B-cell expansion (Nohara et al., 2005). On the other hand, keratocyte-specific expression of CA-AhR by K14 promoter provoked an immune response accompanied by

inflammatory skin lesions (Tauchi et al., 2005). In this chapter, using genetic and pharmacological models of AhR activation, we showed that liver and intestine-specific activation of AhR had a marked effect on metabolic functions, including the induction of hepatic steatosis even when mice were maintained on a regular chow diet.

2.2 METHODS

Chemicals

TCDD (Cat#ED-901-C), Indigo (Cat#229296) and FICZ (Cat#GR206) were respectively purchased from Cambridge Isotope Laboratory (Andover, MA), Sigma (St Louise, MO) and BioMol (Plymouth Meeting, PA). Other chemicals were purchased from Sigma if not specified.

Animals, drug treatment, and body composition analysis

To generate the Tet-off transgenic system, CA-AhR was subcloned into the TetRE transgene cassette (Saini et al., 2004). Transgenic mice were produced at the University of Pittsburgh Transgenic Core Facility. The integration and copy numbers of the transgene were evaluated by Southern blot analysis. CA-AhR founder mice were bred with FABP-tTA transgenic mice (Line 71) to generate the TRE-CA-AhR/FABP-tTA bi-transgenic mice. When necessary, doxycycline (2 mg/ml) was given in drinking water containing 5% sucrose. $CD36^{-/-}$ mice (Febbraio et al., 1999) and $AhR^{-/-}$ mice (Fernandez-Salguero et al., 1995) in C57BL/6J background have been previously described. Transgenic mice and their same background and sex WT controls were used for all experiments. When necessary, mice received a single gavage of vehicle or TCDD (30 μg/kg, dissolved in corn oil) and were sacrificed 7 days later. Liver paraffin sections (5 μm)

and frozen sections (10 μm) were used for H&E and Oil-red O staining, respectively. Mouse body composition was analyzed by using EchoMRI-100™ from Echo Medical Systems (Houston, TX). The use of mice in this study was approved by the University of Pittsburgh Institutional Animal Care and Use Committee.

Plasmid constructs, reporter gene assay, and AhR siRNA transfection

CA-AhR was constructed as described by others (McGuire et al., 2001). Briefly, mouse AhR cDNA was amplified by PCR using primers designed to yield fragments of AhR encoding codons 1-287 and 422-805, respectively. The fragments were digested with SmaI/XhoI and XhoI/NheI, respectively and subcloned into the pCMX-PL2 expression vector. The human CD36 promoter (nt -1961 to +57) construct was PCR-amplified using the follow primers: 5'-GGTACCTCAAAATATGGTGGGTGCATAG-3' and 5'-CCCGGGCAATTCTTAATAGGATC-3'. The mouse CD36 promoter (nt -1411 to +56) was PCR-amplified using the following primers: 5'-GGCGCTAGCGTGTTGGAAACCTAGCTC-3' and 5'-GGCAAGCTTCTGTGAAGAAGAAAAAG-3'. The DRE mutant *CD36* promoters were generated by PCR extension (Zhou et al., 2006). All promoters were cloned into pGL3-basic vector containing a luciferase reporter gene. CV-1 and HepG2 cells were transfected in 48-well cell culture plates using DOTAP and polyethyleneimine polymer transfection agents, respectively (Lee et al., 2008a). Transfected cells were then treated with drugs in medium containing 10% charcoal/dextran-stripped FBS for 24 hrs before harvesting for luciferase and β-gal assays. Transfection efficiency was normalized against β-gal activity. AhR siRNA transfection was carried out using Lipofectamine 2000 as we have previously described (Lee et al., 2008a). The human AhR siRNA was added at the final concentration of 10nM in

transfection. The human AhR siRNA (Cat#SI02780148) and a control scrambled siRNA (Cat#1027280) were purchased from QIAGEN (Valencia, CA). Cells were transfected with siRNA for 5 hrs, and incubated in medium containing 10% FBS for 2 days.

Human and mouse primary hepatocyte preparation

Human primary hepatocytes isolated by collagenase perfusion were obtained from Dr. Steve Strom through the Liver Tissue Procurement and Distribution System (LTPDS). Mouse hepatocytes were prepared by collagenase perfusion (Wada et al., 2008). Cells were plated in 6-well plate or 6-cm dish and maintained in the hepatocyte maintenance medium from Cambrex BioScience (Walkersville, MA). After overnight incubation, cells were treated with appropriate drugs for 24 hrs before harvesting.

Northern blot and real-time RT-PCR analysis

Total RNA was isolated using the TRIZOL reagent from Invitrogen (Carlsbad, CA). Northern hybridization using ^{32}P-labeled cDNA probe was carried out as described (Lee et al., 2008a). For the real-time PCR analysis, reverse transcription was performed with random hexamer primers and Superscript RT III enzyme from Invitrogen. SYBR Green-based real-time PCR was performed with the ABI 7300 Real-Time PCR System. Data was normalized against control cyclophillin. Sequences of the real-time PCR probes are listed in Appendix A.

Western blot analysis

Liver extracts were prepared by homogenizing tissues in buffer A (20 mM Hepes pH=7.45, 150 mM KCl, 10% glycerol, 0.1 mM EDTA) containing protease inhibitor (Sigma, P8340). The

protein concentrations were determined by using the BCA kit from Pierce (Rockford, IL). For ApoB immunoblotting, 3 μl of plasma or 100 μg of liver extracts were separated on 6% SDS-PAGE gel and transferred onto nitrocellulose membrane. Membranes were blocked with 5 % non-fat milk in PBST (0.1 % Tween 20 in PBS) for 1 hr and then incubated with primary antibody overnight at 4°C. Antibody against ApoB100 (H-15, 1:200 dilution) and ApoB48 (S-18, 1:200 dilution) were purchased from Santa Cruz. For CD36 and PCNA immunoblotting, 100 μg of liver extracts were separated on 10% SDS-PAGE gel and transferred onto PVDF membrane and blotted with CD36 antibody (NB400-144, 1:1500 dilution) purchased from Novus Biologicals (Littleton, CO) and PCNA antibody (VP-P980, 1:500 dilution) from Vector (Burlingame, CA). For AhR immunoblotting, Huh-7 cells were harvested in lysis buffer (22 mM Tricine, 1% Triton X-100, 10 % glycerol, 5 mM DTT, 8 mM $MgCl_2$, 4 mM EGTA, 0.4 mM PMSF). Proteins were separated on 8% SDS-PAGE gel. After transfer to PVDF membrane, immunoblotting was performed using antibodies against AhR from BioMol (SA-210, 1:1000 dilution) and β-actin from Sigma (A1978, 1:5000 dilution).

Electrophoretic mobility shift assay (EMSA)

EMSA was carried out using receptor proteins by in vitro transcription/translation (TNT) as previously described (Saini et al., 2004). Oligonucleotide sequences for CD36/DREs and their mutant variants are labeled in the Figure 14A. Protein-DNA complex were resolved by electrophoresis through 8% polyacrylamide gel in 0.5 X TBE at 4 ℃ for 3-4 hrs.

Measurement of circulating and tissue lipids

Blood samples were collected into an EDTA containing tube and centrifuged at room temperature to collect plasma. Liver tissues were homogenized and lipids were extracted as previously described (Zhou et al., 2006). Briefly, 250 mg of liver was homogenized in 2 mL of buffer containing 18 mM Tris (pH 7.5), 300 mM mannitol, 50 mM EGTA, and 0.1 mM PMSF. Lipids were extracted by incubating 400 μL of homogenate overnight in chloroform/methanol mixture (2:1 v/v) followed by adding distilled water to separate the organic phase containing tissue lipids. The organic phase was dried under nitrogen gas. The lipid pellets were then dissolved in 120 μl of tert-butanol and 80 μl of Triton X 114:methanol (2:1 v/v) mixture. Plasma and liver concentrations of triglycerides and cholesterol were determined using assay kits from Stanbio (Boerne, TX). Plasma and liver free fatty acids were measured by using an assay kit from Biovision (Mountain View, CA). Plasma β-hydroxybutyrate was measured by an RANBUT kit from Randox (Crumlin, UK). Glucose levels were measured by using a glucometer.

Measurement of lipid peroxidation in liver

Tissue levels of malondialdehyde (MDA) were determined as an index of lipid peroxidation. Liver lipid homogenates were added to a reaction mixture containing 0.67% thiobarbituric acid (TBA), boiled for 1 h at 95°C, and then centrifuged at 3,000 g for 10 min. Supernatant absorbance was measured by spectrophotometry at 532 nm and compared with a standard curve prepared from different concentrations of 1,1,3,3-tetramethoxypropane.

TUNEL assay

Apoptosis was determined in liver paraffin sections by TUNEL assay using an assay kit (Cat # 11 684 795 910) from Roche Diagnostics (Indianapolis, IN). Apoptotic cells were detected by fluorescein staining, and the nuclei were counterstained with Propidium Iodide.

Measurement of intestinal fat absorption

Mice were fasted for 16hrs then orally given 10 ml/kg of olive oil. Plasma samples were collected at 0, 3, 6, 9, 12 hrs after olive oil administration. Plasma triglyceride levels were measured as described above.

Free fatty acid uptake experiment

Huh-7 cells were seeded into chamber slides (Cat#154526) from Nalge (Naperville, IL) at a density of 2.5×10^4/per well and incubated overnight before treatment with TCDD for 24 hrs. Primary mouse hepatocytes were seeded into 6-cm culture dishes and incubated overnight before treatment with DOX for 24 hrs. Cells were then serum starved for 3 hrs and rinsed with PBS. Cells were then incubated with 500 nM of 4,4-difluoro-5,7-dimethyl-4-bora-3α, 4α-diaza-*s*-indacene-3-hexadecanoic acid (BODIPY-C16) from Molecular Probes/Invitrogen for 3 mins in PBS, rinsed with ice-cold PBS three times, and fixed in ice-cold 4% paraformaldehyde (pH 7.4) for 30 mins. After washing with PBS twice, cells were cover slipped in mounting medium containing DAPI. The fluorescence intensity was quantified by using the NIH Image J software (http://rsbweb.nih.gov/ij).

Measurement of peroxisomal β-oxidation

Liver tissues were homogenized in 0.25 M sucrose (20% w/v) and homogenates were used for determination of peroxisomal β-oxidation by monitoring the rate of NAD+ reduction to NADH at 340 nm using palmitoyl-CoA as a substrate in the presence of KCN, which completely inhibits mitochondrial β-oxidation. The assay mixture contained 50 mM Tris-HCl buffer (pH 8.0), 0.2 mM NAD, 0.01 mM FAD, 0.1 mM CoA, 12 mM DTT, 0.15 mg/ml BSA, 0.01% Triton X-100, 1.0 mM KCN and 0.01 mM palmitoyl-CoA as previously described (Lazarow and De Duve, 1976; Youssef et al., 1997). NADH formation was quantitated using an extinction coefficient of 6.22 cm^{-1} mM^{-1}.

Measurement of VLDL secretion rate

VLDL secretion rate *in vivo* was measured as previously described (Merkel et al., 1998; Uchiyama et al., 2006). Briefly, 16 hr-fasted mice were injected with Triton WR1339 (500 mg/kg in saline) via the tail vein. Plasma samples were collected at 0 and 90 min after Triton WR1339 injection, and triglyceride levels were then measured as described above.

Statistical analysis

Results were presented as means ± SD. Animal numbers are shown in figure or figure legends. Comparisons between groups were performed using the Student's *t* test or one-way ANOVA where appropriate. * $P<0.05$ was considered statistically significant. N.S. represents statistically not significant.

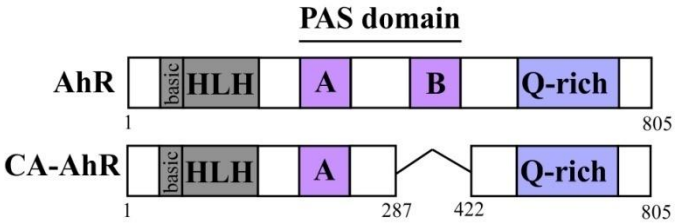

Figure 5 Schematic representation and domain structure of the wild type (WT) AhR and constitutively activated (CA-AhR) AhR. bHLH, basic helix-loop-helix, PAS, Per-Arnt-Sim.

2.3 RESULTS

2.3.1 Creation and characterization of the constitutively activated AhR (CA-AhR)

We constructed a constitutively activated AhR (CA-AhR) by deleting the minimal ligand-binding domain (amino acids 287-422) of the AhR (Figure 5). This mutant AhR has been shown to be constitutively activated (McGuire et al., 2001). Expression levels of CA-AhR were comparable to those of wild type AhR (Figure 6A). CA-AhR displayed an efficient binding to the dioxin response element (DRE) derived from the Cyp1a1 gene, as shown by eletrophoretic mobility shift assay (EMSA) (Figure 6B).

To determine functionality of the CA-AhR mutant protein, CV-1 cells were transiently transfected with the DRE-driven luciferase reporter gene pGud-luc (Han et al., 1994), together with expression vectors of AhR and Arnt. As shown in Figure 6C, CA-AhR activated the reporter gene in the absence of an exogenously added AhR ligand, and addition of the AhR ligand 3-methylchoranethrene (3-MC) (Denison and Nagy, 2003) had little further effect. This was in contrast to the wild type AhR receptor, which exhibited substantial ligand-dependent activation as expected (Figure 6C). CA-AhR also activated the pGud-luc reporter gene without a ligand treatment when both plasmids were transfected in vivo into mouse liver by a

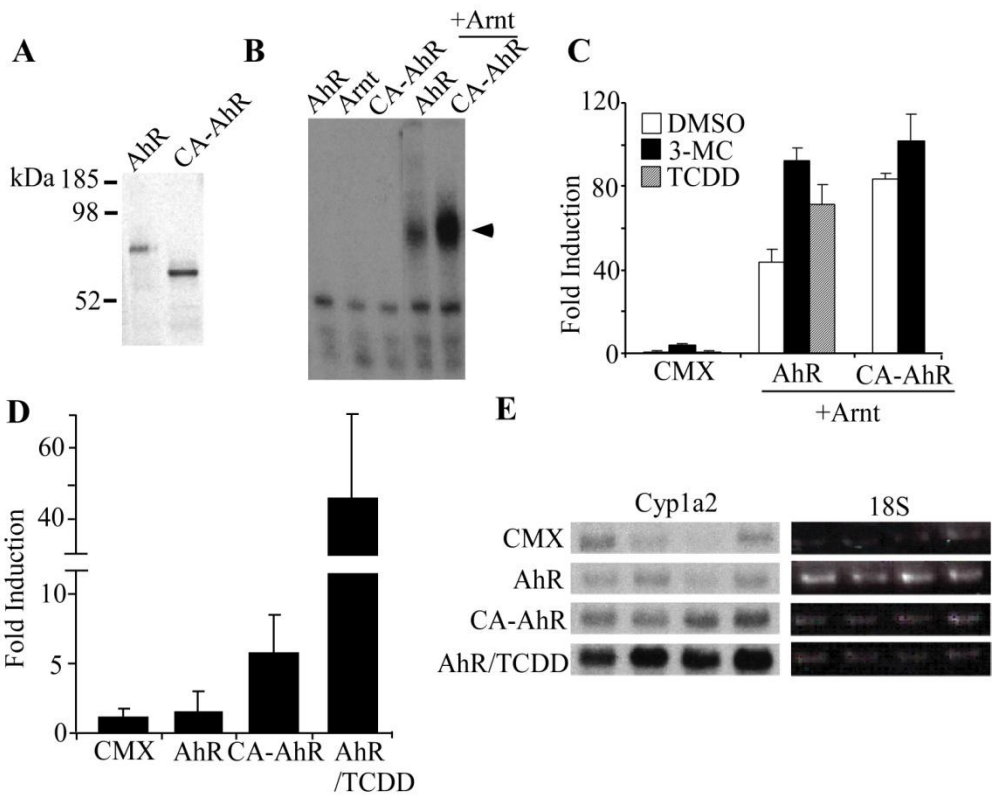

Figure 6 Characterization of a constitutively activated AhR (CA-AhR). **(A)** In vitro translated, [^{35}S]methionine-labeled wild type AhR or CA-AhR proteins. The positions of protein markers are shown on the left. **(B)** CA-AhR-Arnt heterodimers bind to Cyp1a1/DRE as shown by EMSA. Arrowhead indicates specific bands. **(C)** CA-AhR activates the AhR-responsive pGud-Luc reporter gene in a ligand independent manner. 3-MC, 3-methylchoranethrene. The drug concentration is 2 μM. **(D and E)** Eight week-old CD-1 female mice were treated with i.p. injection of DMSO or TCDD (50μg/kg). After one hour, mice were injected via the tail vein with 5μg of AhR or CA-AhR and 10μg of pGud-luc in saline. Six hours after injection of DNA, mice were sacrificed, the liver was collected, luciferase activity in extracts was measured (D) and the expression of Cyp1a2 was detected by Northern blot (E). The control lane (Ctrl) represents activity from reporter gene alone and empty expression vector.

hydrodynamic gene delivery system (Figure 6D and 6E). The reporter gene activity was increased ~5 fold by CA-AhR in the absence of TCDD compared to transfecting wild type AhR (Figure 6D) and the AhR-responsive gene Cyp1a2 mRNA levels were increased in mice injected with CA-AhR, as compared to wild type AhR (Figure 6E). Thus, CA-AhR transgene is transcriptionally active with ligand-independent manner in vitro and in vivo.

2.3.2 Generation of conditional tetracycline inducible transgenic mice expressing CA-AhR in the liver and intestine

To examine the biological consequences of AhR activation *in vivo*, we generated tetracycline inducible CA-AhR transgenic mice expressing the constitutively activated AhR (CA-AhR) (Figure 7A). Our "Tet-off" transgenic system is composed of two transgenic lines with one line (TetRE-CA-AhR) expressing CA-AhR under the control of a minimal cytomegalovirus promoter (P_{CMV}) fused to the tetracycline responsive element (TRE), and the other line (FABP-tTA) expressing the tetracycline transcriptional activator (tTA) constitutively and exclusively in liver and intestine under the control of the fatty acid binding protein (FABP) promoter (Zhou et al., 2006). We predict that in mice carrying both transgenes, tTA will bind to TRE and induce the expression of CA-AhR in the absence of doxycycline (DOX). In the same animals, treatment with DOX will dissociate tTA from TRE, leading to the silencing of CA-AhR expression (Figure 7A). To determine whether CA-AhR is transcriptionally active under tetracycline inducible system, we analyzed reporter gene activity by transient transfection of TRE-CA-AhR and Arnt, together with CMX-tTA or CMX-rtTA that expresses the reverse tTA in CV-1 cells (Figure 7B). Coexpression of tTA with TRE-CA-AhR resulted in induction of reporter gene expression in the absence of DOX, however DOX treatment failed to stimulate reporter gene activity (Figure 7B). The dependence of DOX for induction of CA-AhR was also confirmed by expression of rtTA, which binds to TRE in the presence of DOX resulting in induction of CA-AhR (Figure 7B).

Pronuclear microinjection of the FABP-tTA transgene yielded four founder mice that led to the establishment of four independent tTA lines, among which Line 71 was chosen for subsequent cross-breeding due to the high expression of tTA in both the liver and intestine (data not shown). Microinjection of the TRE-CA-AhR transgene produced six founders determined by

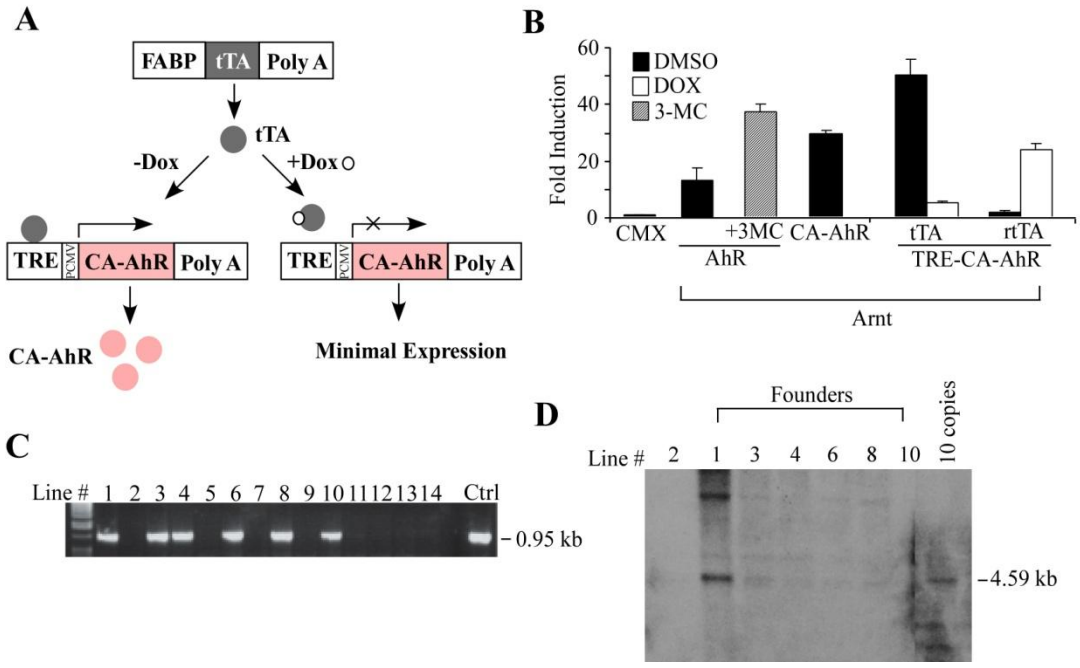

Figure 7 Conditional expression of CA-AhR under the tetracycline inducible system. **(A)** Schematic representation of the Tet-off FABP-tTA/TRE-CA-AhR transgenic system. DOX, doxycycline; FABP, fatty acid binding protein; PCMV, minimal CMV promoter; TRE, tetracycline responsive element; tTA, tetracycline transcriptional activator. **(B)** CV-1 cells were transiently transfected with pGud-luc and TRE-CA-AhR together with expression vectors of either tTA or rtTA (reverse tetracycline transcription activator: "Tet-On") in the presence/absence of DOX (1μg/mL). The reporter gene expression by AhR or CA-AhR was included as controls. The control lane (Ctrl) represents activity from reporter gene alone and empty expression vector. **(C and D)** Generation of TRE-CA-AhR transgenic mice. Integration and copy number of transgene was verified by PCR (C) and Southern blot analysis (D) of genomic DNA from tail.

PCR (Figure 7C). The integration and copy numbers of the transgene were evaluated by Southern blot analysis (Figure 7D). Cross-breeding of the TRE-CA-AhR founders with FABP-tTA mice yielded four bi-transgenic lines, among which Lines 4 and 6 were found to express *CA-AhR* in the liver and small intestine of both sexes (Figure 8A). The bi-transgenic mice also showed an increased mRNA expression of *Cyp1a2*, a known AhR target gene (Figure 8A). Interestingly, Line 3 expressed *CA-AhR* in the liver but not in the intestine, whereas Line 8 expressed *CA-AhR* in the liver and intestine of males but not females (Figure 8A). Line 4 was chosen for further characterization and most of the subsequent experiments.

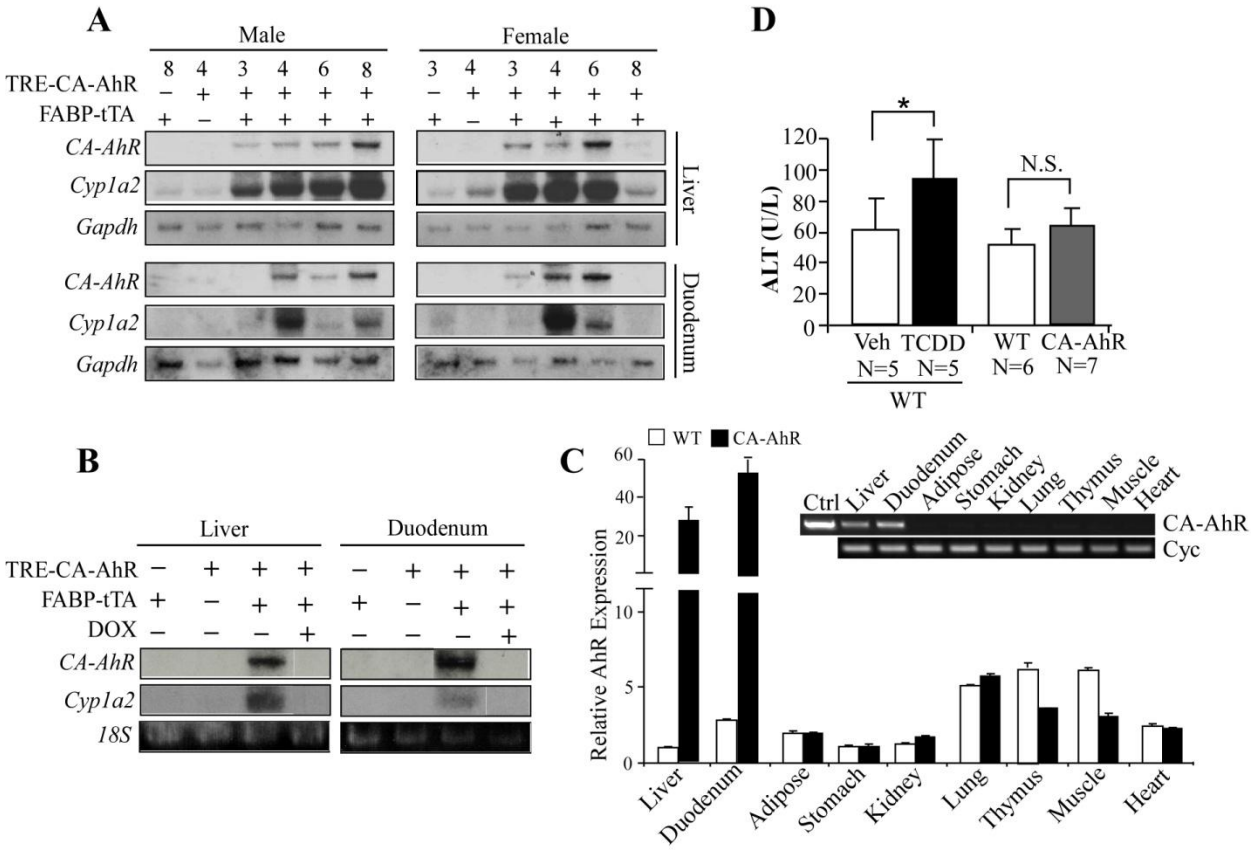

Figure 8 Generation of transgenic mice expressing CA-AhR in the liver and intestine. **(A)** Hepatic and intestinal expression of CA-AhR and induction of Cyp1a2 as shown by Northern blot analysis. Gapdh was shown for loading control. **(B)** Treatment of bi-transgenic mice with DOX for 1 week silenced both the expression of CA-AhR and induction of Cyp1a2. **(C)** CA-AhR transgene is not expressed in a panel of tissues outside of the liver and intestine of the transgenic mice, as determined by real-time PCR and semi-quantitative RT-PCR (insert). Cyclophilin is included as a loading control. **(D)** Activation of AhR in CA-AhR mice was not associated with obvious hepatotoxicity at 5-6 weeks of age. Serum levels of ALT were measured in female mice. Mice in TCDD treated group received a single p.o. dose of TCDD (30mg/kg) and sacrificed 7 days after.

As expected, the expression of *CA-AhR* and induced *Cyp1a2* gene expression were abolished when mice were given DOX-laced drinking water for one week (Figure 8B). *CA-AhR* was specifically expressed in liver and intestine, consistent with the tissue specificity of the FABP promoter (Zhou et al., 2006). No transgene expression was detected in several other AhR-expressing tissues, such as adipose tissue, stomach, kidney, lung, thymus, muscle and heart (Figure 8C). The transgenic mice were viable and fertile. The serum level of alanine aminotransferase (ALT), an indicator of hepatotoxicity, was not significantly increased in the

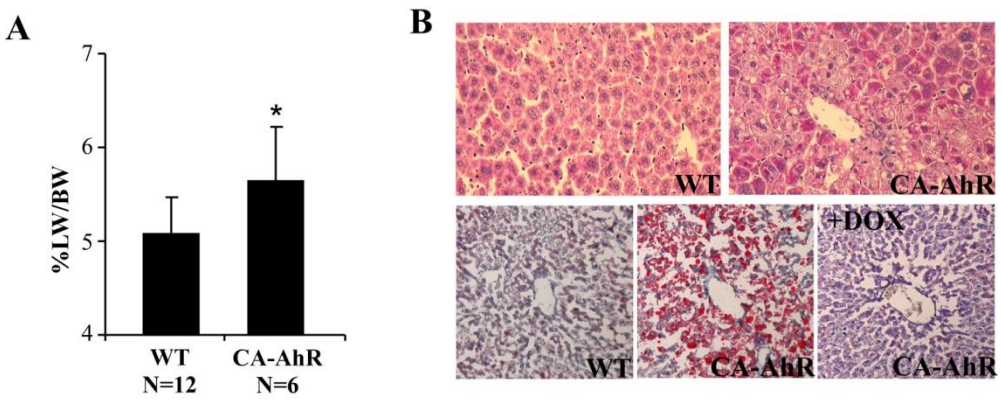

Figure 9 CA-AhR transgenic mice showed phenotype of hepatic steatosis. **(A)** The liver weight (LW) was measured as percentage of the total body weight (BW). **(B)** Liver sections of wild type (WT) and CA-AhR mice were stained with H&E (upper panels) or Oil-Red-O (lower panels).

transgenic mice (Figure 8D), suggesting that the genetic activation of AhR was not associated with obvious hepatotoxicity. This is in contrast to the known toxicity in mice treated with the xenobiotic AhR agonist TCDD (Figure 8D and (Walisser et al., 2005)).

2.3.3 CA-AhR transgenic mice developed hepatic steatosis and showed decreased body weight and fat mass

The CA-AhR transgenic mice showed hepatomegaly. At 5 weeks, the liver accounted for 5.08% of total body weight in WT females, and 5.64% in transgenic females, an increase of 11% (Figure 9A). H&E staining showed the hepatocytes from transgenic mice had a vacuolated-cytoplasmic appearance (Figure 9B), suggestive of lipid deposition. Oil-red O staining confirmed the increased lipid droplets in hepatocytes of transgenic mice (Figure 9B). Liver tissue triglyceride, but not cholesterol and free fatty acid, increased in concentration by 2.5 fold in transgenic mice (Figure 10A). The steatotic phenotype depended on AhR activation, because treatment of transgenic mice with DOX for 2 weeks normalized the liver Oil-red O staining and triglyceride content (Figure 9B and 10A). Hepatic steatosis was also observed in Line 3, in

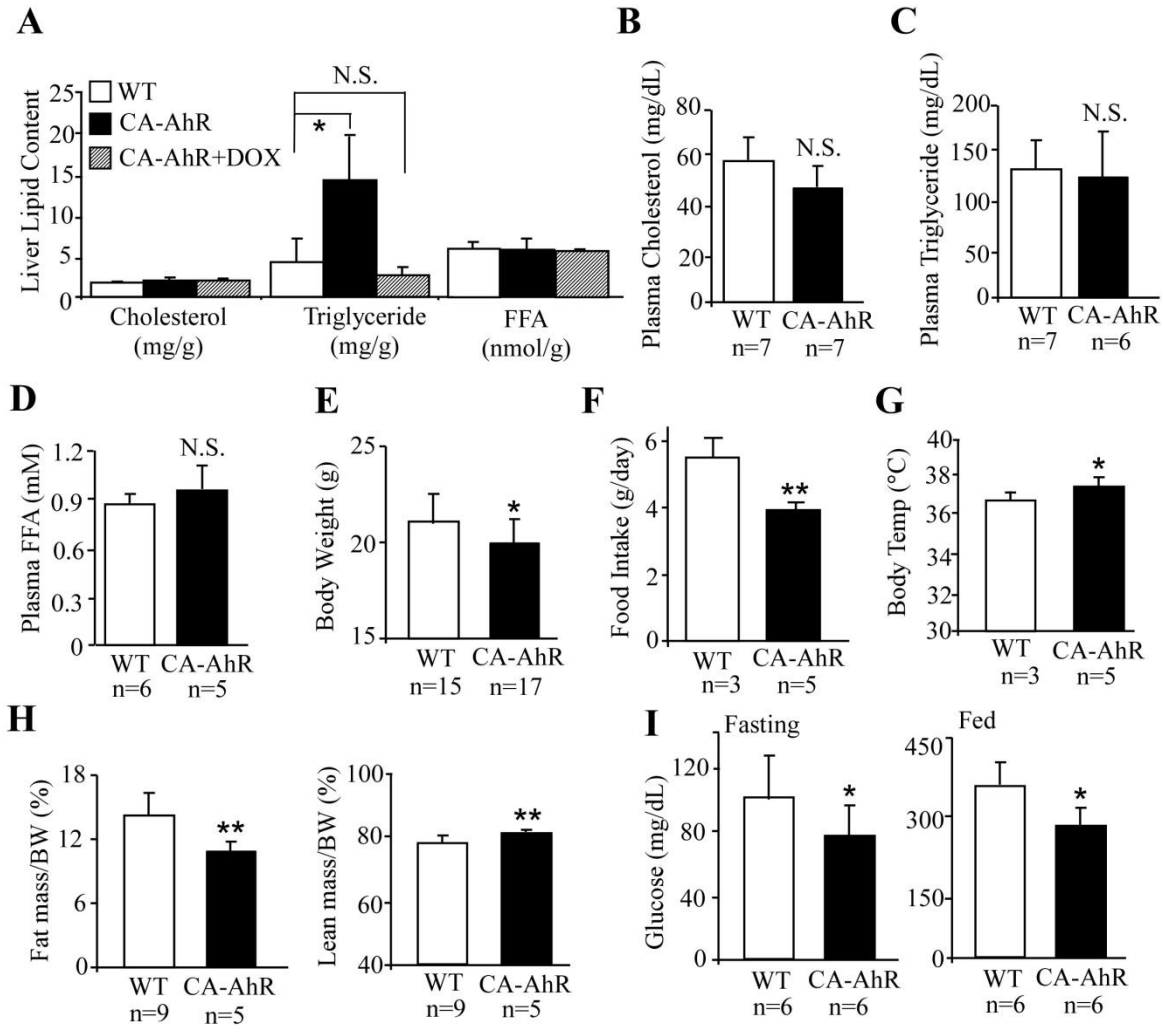

Figure 10 CA-AhR transgenic mice showed metabolic abnormalities. **(A)** Measurements of hepatic cholesterol, triglyceride and free fatty acid (FFA) in the liver. n=4 per each group **(B-D)** Plasma cholesterol (B), triglyceride (C) and FFA (D) levels were measured in overnight fasted mice. **(E)** Body weight **(F)** Food intake. Repeated 4 times **(G)** Rectal body temperature, repeated 4 times **(H)** Percentage of whole-body fat content and lean body mass were analyzed by MRI. **(I)** Circulating glucose levels were determined from fasting and fed mice. (A-D) 5-6 week-old female mice were used. (E-I) Two-month old female mice were used. Mice numbers are labeled.

which CA-AhR was expressed only in the liver (data not shown), suggesting that activation of AhR in the liver was sufficient for the development of steatosis. As consistent with hepatic cholesterol levels, plasma cholesterol levels were unchanged in CA-AhR mice (Figure 10B). Interestingly, despite hepatic accumulation of triglycerides, the plasma level of triglycerides was

not increased in the transgenic mice (Figure 10C). Plasma free fatty acid levels remained unchanged in the transgenic mice (Figure 10D).

The transgenic mice also showed other metabolic abnormalities. The transgenic mice, which were in the FVB background and fed with a standard rodent chow, had modest but significantly decreased body weight compared to their WT littermates (Figure 10E). CA-AhR mice were hypophagic (Figure 10F). Body temperature was increased in CA-AhR mice (Figure 10G). Body composition analysis by MRI showed that the transgenic mice had a 23% decrease in fat mass and 4% increase in lean mass when measured as percentages of body weight (Figure 10H). Circulating glucose levels were significantly lower in both fasted and fed transgenic mice (Figure 10I).

2.3.4 Activation of AhR induced fatty acid translocase CD36 and uptake of fatty acid

To understand the mechanism by which AhR promotes steatosis, we profiled the expression of genes in the liver and intestine by Affymetrix microarray analysis. The microarray results showed that 2.9% and 2.3% of genes were upregulated and downregulated in the livers of CA-AhR mice, respectively (Appendix B and Table 1). The microarray results on the intestine are summarized in Appendix C and Table 2. Our initial Affymetrix microarray analysis showed that the expression of CD36, a scavenger receptor capable of high affinity uptake of fatty acids, was induced in the liver of CA-AhR transgenic mice. In contrast, the expression of Srebp-1c and its target lipogenic enzymes Fas, Acc and Scd-1 was unchanged (data not shown). The microarray induction of hepatic *CD36* mRNA expression by AhR was confirmed by both real-time PCR (Figure 11A) and Northern blot analysis (Figure 11B). Consistent with the inducible levels in CD36 mRNA expression, CD36 protein expression (Figure 11C) was significantly increased in

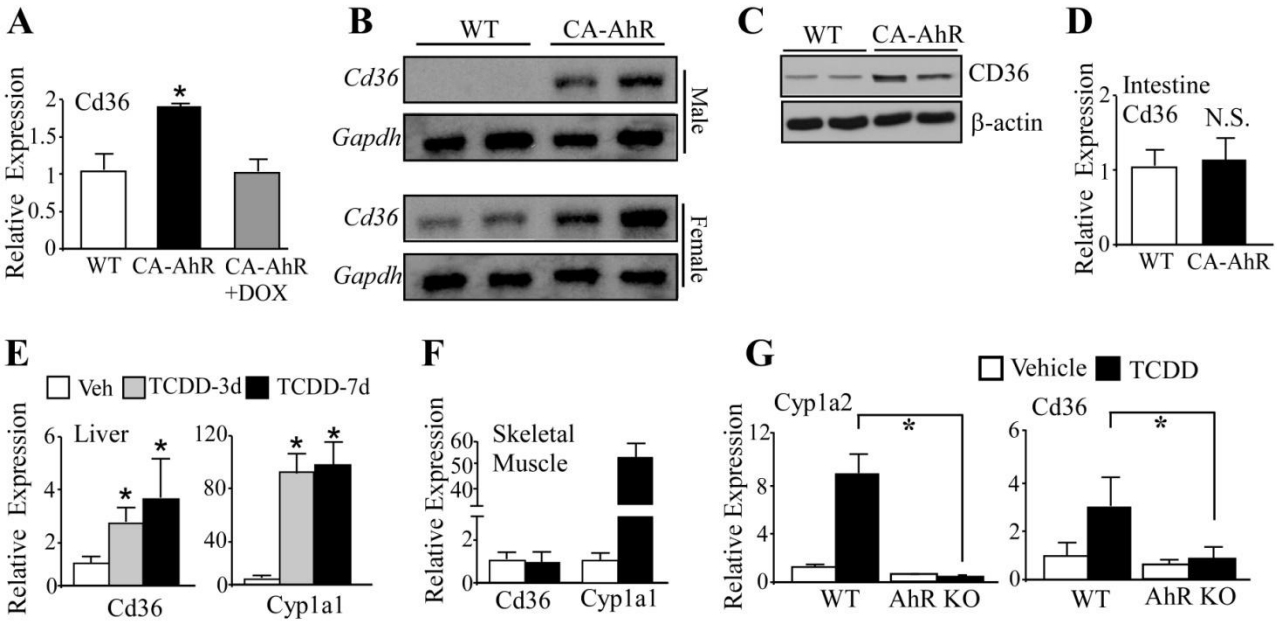

Figure 11 Activation of AhR induced expression of CD36 in liver. (A-B) Real-time PCR analysis (A) and Northern blot analysis (B) on the hepatic expression of CD36 mRNA in two-month-old female CA-AhR mice. When applicable, mice were treated with DOX (2 mg/ml in drinking water) for 2 weeks before sacrificing. N=4 for each group. **(C)** Western blot analysis on the hepatic expression of CD36 proteins in two-month-old male CA-AhR mice. **(D)** Real-time PCR analysis on intestinal CD36 expression. N=3 for each group. **(E and F)** Real-time PCR analysis on the liver (E) and skeletal muscle (F) mRNA expression of CD36 in 8 week-old female C57BL/6J mice treated with vehicle or TCDD (30 μg/kg, p.o.) for 3 days (3d, n=4 for each group) or 7 days (7d, n=8 for each group). (G) The induction of CD36 by TCDD (10 μg/kg TCDD, 1day) was abolished in $AhR^{-/-}$ mice.

livers from CA-AhR mice. The regulation of *CD36* was transgene-dependent, because the induction was abolished after DOX treatment (Figure 11A), presumably due to the silencing of the transgene. Interestingly, AhR-mediated *CD36* regulation appeared to be tissue specific, because the intestinal *CD36* expression remained unchanged (Figure 11D), despite the transgene expression and *Cyp1a2* induction in this tissue (Figure 8). The hepatic induction of *CD36* was also observed in C57BL/6J mice treated with TCDD (Figure 11E). Again, the regulation appeared to be tissue-specific, because TCDD had little effect on *CD36* expression in skeletal muscle (Figure 11F). The induction of *CD36* by TCDD was largely abolished in $AhR^{-/-}$ mice, as was the induction of *Cyp1a2* (Figure 11G). These results demonstrated that the TCDD effect on *CD36* gene expression was AhR-dependent. In addition to CD36, the hepatic uptake of fatty

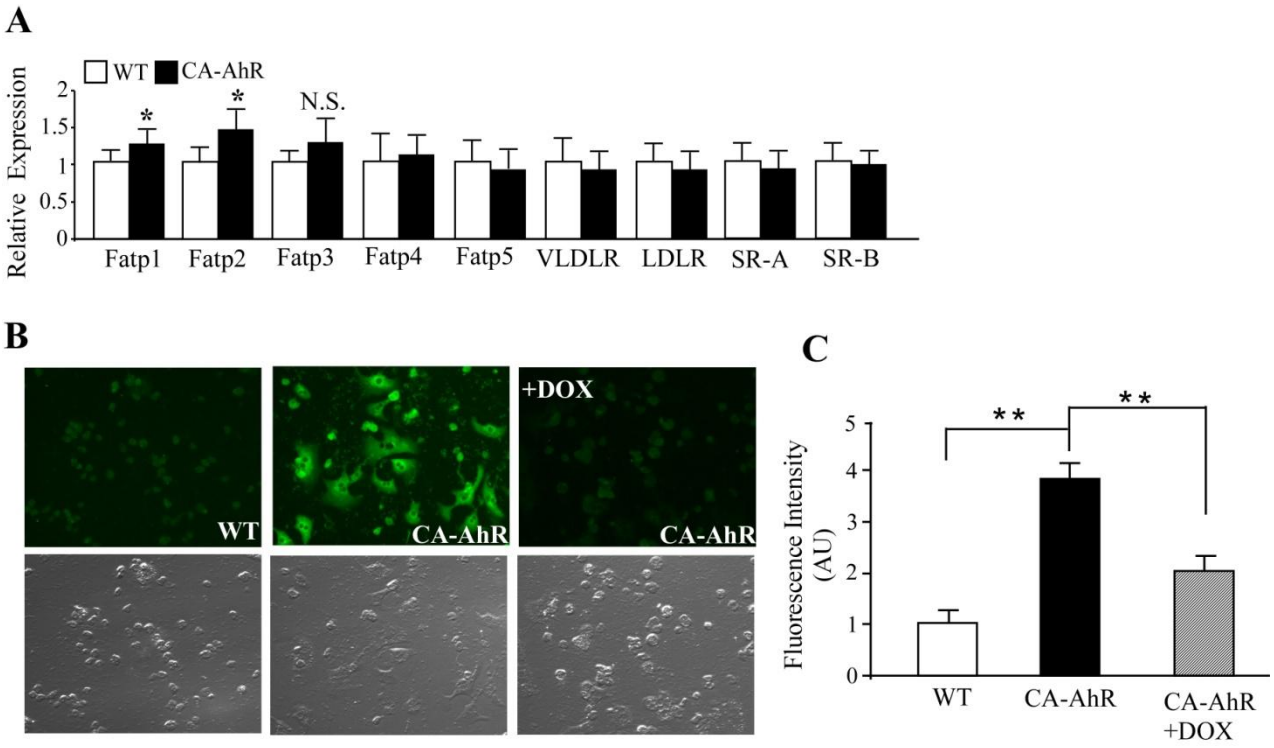

Figure 12 Activation of AhR induced the free fatty acid uptake in mouse hepatocytes. **(A)** Real-time PCR analysis on the hepatic expression of free fatty acid transporter proteins (Fatps), very-low density lipoprotein receptor (VLDLR), low density lipoprotein receptor (LDLR), scavenger receptor A and B (SR-A and SR-B) in CA-AhR mice (n=6 for each group). **(B and C)** Free fatty acid uptake in primary mouse hepatocytes is monitored by the uptake of 4,4-difluoro-5,7-dimethyl-4-bora-3α, 4α-diaza-s-indacene-3-hexadecanoic acid (BODIPY-C16). (B) Top and bottom panels are fluorescence and phase contrast images of the cells, respectively. DOX concentration is 1 μg/ml. (C) Quantification of BODIPY-C16 uptake in (B). AU, arbitrary unit.

acids can also be facilitated by the intracellular fatty acid transfer proteins (FATPs) (Goldberg and Ginsberg, 2006). Cell surface lipoprotein receptors, such as VLDLR, LDLR, SR-A and SR-B, also contribute to the hepatic uptake of lipids. As shown in Figure 12A, the expression of *Fatp1* and *Fatp2* was modestly, but significantly, increased in transgenic mice; whereas the expression of *Fatps 3-5*, *VLDLR*, *LDLR*, *SR-A* and *SR-B* was not affected.

To determine whether the elevated expression of CD36, Fatp1 and Fatp2 led to an increased hepatic fatty acid uptake, primary hepatocytes were isolated and evaluated for fatty acid uptake by incubating cells with 4,4-difluoro-5,7-dimethyl-4-bora-3α, 4α-diaza-*s*-indacene-3-hexadecanoic acid (BODIPY-C16), a fluorescent fatty acid analog (Shaffer et al., 1994). As

shown in Figure 12B and 12C, the BODIPY-C16 uptake by hepatocytes derived from the transgenic mice was markedly increased compared to those isolated from the WT mice. The transgenic effect on BODIPY-C16 uptake was largely abrogated upon DOX treatment.

2.3.5 Treatment of AhR ligands induced CD36 and increased free fatty acid uptake in human liver cells

Treatment of primary human hepatocytes (Figure 13A) or Huh-7 human hepatoma cells (Figure 13B) with TCDD (10 nM) for 24 hrs induced the mRNA expression of *CD36*, suggesting that the AhR effect on CD36 gene expression is conserved in human liver cells. In the same TCDD-treated cells, the respective expression of *CYP1A1* and *CYP3A4* was induced and reduced as expected (Shaban et al., 2005). Activation of CD36 gene expression was also observed in Huh-7 cells treated with the various AhR ligands including endogenous AhR agonists Indigo (Adachi et al., 2001) and FICZ (Rannug et al., 1995) (Figure 13C). Moreover, the induction of *CD36* by FICZ in Huh-7 cells was significantly inhibited when cells were transfected with AhR siRNA (Figure 13D). The efficiency of AhR siRNA knockdown was confirmed by real-time PCR and Western blot analysis (Figure 13E). Also in Huh-7 cells, treatment with TCDD (10 nM) increased the uptake of BODIPY-C16, but this effect was abolished when cells were transfected with AhR siRNA (Figure 13F and 13G).

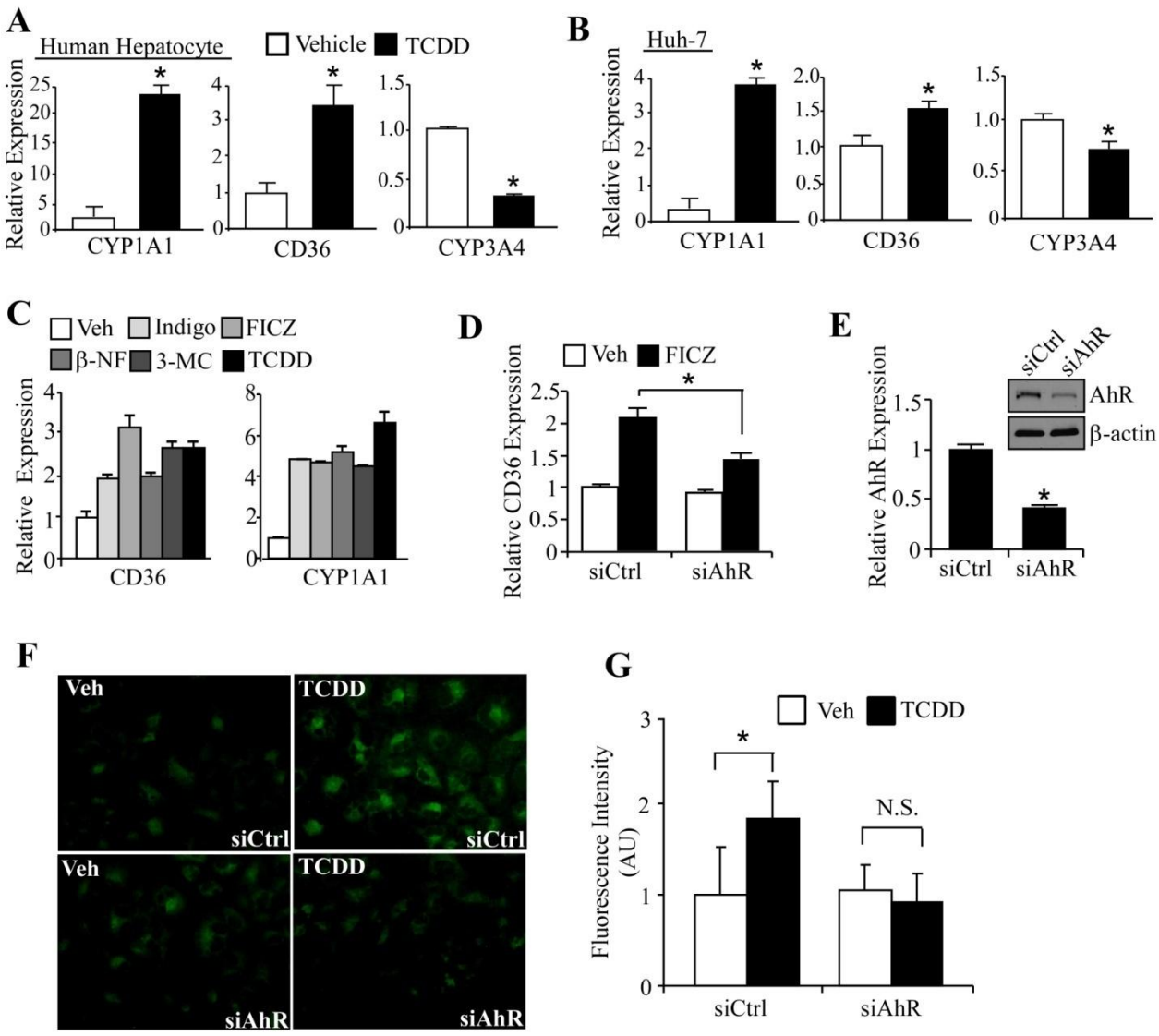

Figure 13 Treatment of human hepatocytes with AhR agonists induced the expression of CD36 and increased free fatty acid uptake. **(A-C)** Primary human hepatocyte (A) and Huh-7 human hepatoma cells (B and C) were treated with indicated drugs for 24 hrs before RNA harvesting and real-time PCR analysis. **(D)** The FICZ-inducible activation of CD36 gene expression was abolished in Huh-7 cells transfected with AhR siRNA. **(E)** The knockdown of AhR in siAhR-transfected cells was confirmed by real-time PCR and Western blot analysis (insert). **(F)** Fatty acid uptake is monitored by the uptake of BODIPY-C16. **(G)** Quantification of BODIPY-C16 uptake in (F). The drug concentrations are TCDD, 10 nM; FICZ, 200 nM; Indigo, 10 μM; β-NF, 10μM; 3-MC, 2 μM.

2.3.6 The mouse and human CD36 gene promoters are transcriptional targets of AhR

To determine the molecular mechanism by which AhR regulates *CD36*, the mouse (nt -1411 to +56) and human (nt -1961 to +57) *CD36* gene promoters were cloned and analyzed for their regulation by AhR. Inspection of the promoter sequences revealed several putative DREs (Figure 14A) whose binding to AhR-Arnt heterodimers was confirmed by EMSA (Figure 14B). Consistent with the EMSA results, luciferase reporter genes containing the mouse (pGL-mCD36) or human (pGL-hCD36) *CD36* promoters were activated by wild type AhR in response to the various AhR agonist (Figure 14C). Both the mouse and human CD36 gene promoters were also activated by CA-AhR without an exogenously added ligand (Figure 14D and 14E). Mutation of DREs abrogated AhR-dependent transactivation (Figure 14D and 14E).

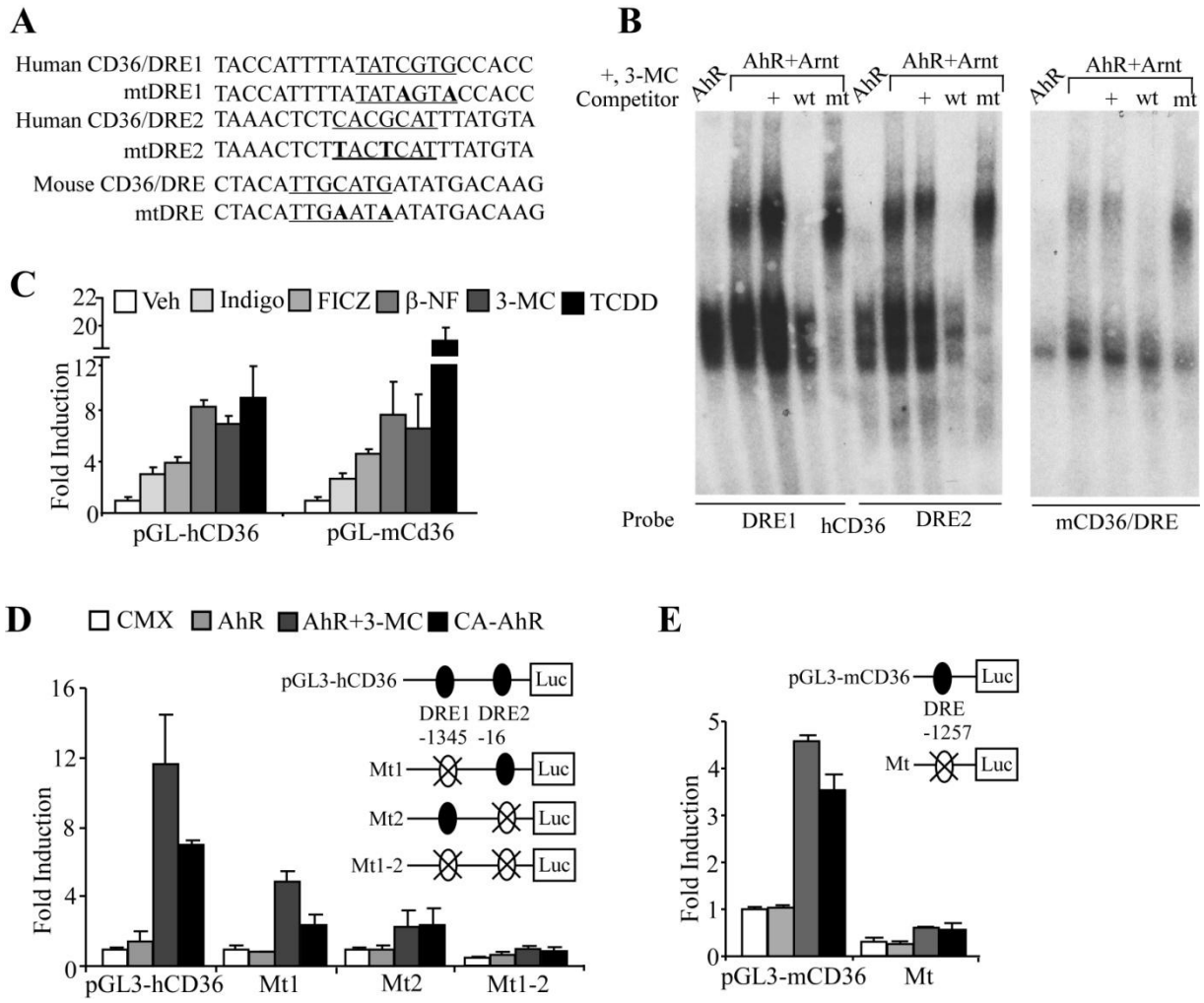

Figure 14 The human and mouse CD36 genes are transcriptional targets of AhR. **(A)** The sequences of dioxin responsive elements (DREs) in the human and mouse CD36 gene promoters. **(B)** EMSA was performed using in vitro transcribed and translated proteins and ^{32}P-labeled DREs. **(C)** Activation of hCD36 and mCD36 promoter reporter genes by the exogenous and endogenous AhR agonists. **(D and E)** Mutation of DREs in hCD36 and mCD36 promoter reporter genes abolished AhR-dependent transactivation in the presence of 3-MC or CA-AhR-dependent transactivation without an exogenously added ligand. HepG2 cells were co-transfected with indicated reporters and receptors. Transfected cells were treated with vehicle (DMSO), Indigo (10μM), FICZ (200nM), β-NF (10μM), TCDD (10nM) or 3-MC (2 μM) for 24 hrs before luciferase assay. The transfection efficiency was normalized against the co-transfected β-gal activity.

2.3.7 Loss of CD36 in mice inhibited the steatotic effect of an AhR agonist

Having established *CD36* as an AhR target gene, we went on to determine whether the expression and regulation of *CD36* were required for the steatotic effect of AhR. In this experiment, we first determined whether the expression of CD36 is required for fatty acid uptake dependent on AhR activation. As shown in Figure 15A and 15B, the BODIPY-C16 uptake by primary hepatocytes derived from the WT was significantly increased in the presence of TCDD. In sharp contrast, the BODIPY-C16 uptake was abolished in TCDD-treated hepatocytes derived from $CD36^{-/-}$ mice (Figure 15A and 15B).

To assess if the lack of CD36 expression could rescue the steatotic effect by AhR in vivo, WT and $CD36^{-/-}$ female mice were treated with a single dose of TCDD (30 μg/kg) and the mice were sacrificed 7 days later. Treatment of WT mice with TCDD induced hepatomegaly and hepatic steatosis as shown by Oil-red O staining (Figure 15C) and measurement of tissue triglyceride content (Figure 15D). These results were consistent with those observed in the CA-AhR transgenic mice, as well as those published by others (Boverhof et al., 2006). Interestingly, hepatic steatosis phenotypes were inhibited in $CD36^{-/-}$ mice (Figure 15C and 15D). In female mice, increase of hepatic triglyceride levels in TCDD-treated $CD36^{-/-}$ mice were abolished compared their WT counterparts, whereas loss of CD36 alone, in the absence of TCDD, had little effect on the liver triglyceride content (Figure 15C). These results suggest that CD36 acts as a hepatic fatty acid translocator in the response of AhR activation. Interestingly, the lack of TCDD-induced triglyceride increase in liver was more prominent in female than male $CD36^{-/-}$ mice (data not shown). TCDD treatment significantly decreased plasma triglyceride levels in both female (Figure 15E). However, the decrease of triglyceride levels by TCDD was not seen in

CD36$^{-/-}$ female mice (Figure 15E). These results suggest that CD36 is required for the steatotic effect of AhR agonists.

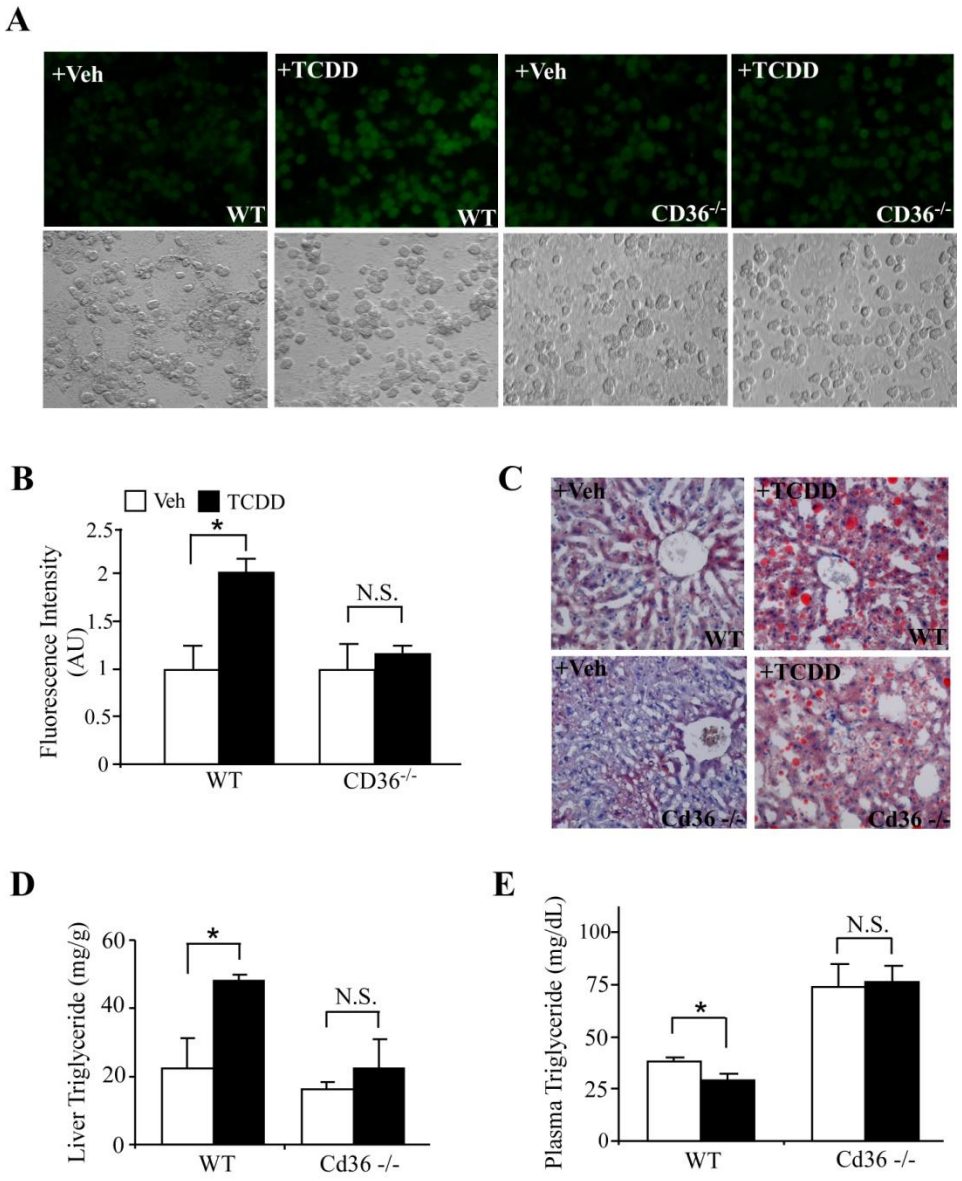

Figure 15 Loss of CD36 in mice inhibited the steatotic effect of an AhR agonist. **(A and B)** Free fatty acid uptake in primary mouse hepatocytes from WT and CD36$^{-/-}$ treated with vehicle (Veh) or TCDD is monitored by the uptake of BODIPY-C16. Top and bottom panels are fluorescence and phase contrast images of the cells, respectively (A). TCDD concentration is 10 nM. (B) Quantification of BODIPY-C16 uptake in (A). AU, arbitrary unit. **(C)** Oil-red O staining on liver sections of WT or CD36$^{-/-}$ mice treated with vehicle (Veh) or TCDD. **(D)** Measurements of hepatic triglyceride levels. **(E)** Measurements of plasma triglyceride levels. Two-month old female mice were gavaged with a single dose of TCDD (30 μg/kg) for 7 days and sacrificed after 16 hrs of fasting

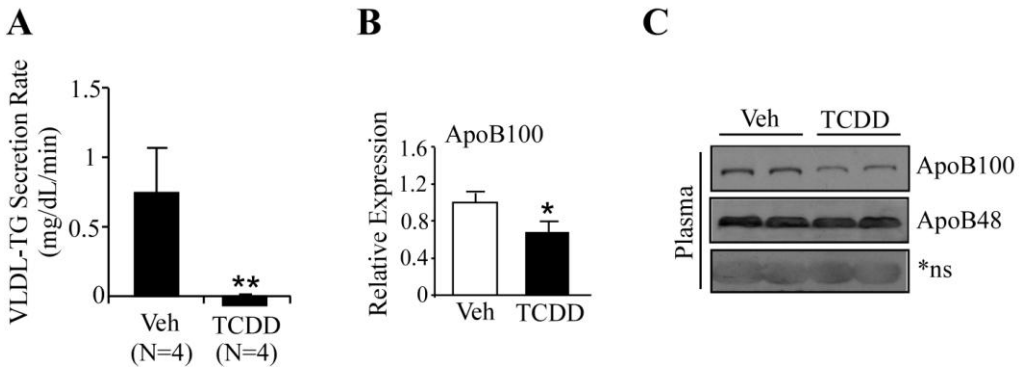

Figure 16 Treatment with TCDD inhibited VLDL-triglyceride secretion. **(A)** Two-month old female mice were treated with a single dose of TCDD (30 μg/kg) for 7 days before measuring the VLDL-triglyceride (TG) secretion. Mice were fasted for 16 hrs before the assay. **(B-C)** Measurements of hepatic *ApoB100* mRNA (B, shown is the real-time PCR result, n=3) and plasma ApoB protein (C, shown is the Western blot result) levels. *ns, non-specific band

2.3.8 Treatment with AhR agonist inhibited VLDL-triglyceride secretion

VLDL secretion is important for the export of triglycerides from hepatocytes. The accumulation of hepatic triglycerides and lack of increases in circulating triglycerides prompted us to determine whether the activation of AhR inhibits VLDL-triglyceride secretion. VLDL-triglyceride secretion rate in vivo was measured by injecting fasted mice with Triton WR1339 (500 mg/kg in saline) via the tail vein to inhibit lipoprotein lipase activity and thus preventing VLDL hydrolysis. Blood samples were collected at 0 and 90 min after Triton WR1339 injection and plasma triglyceride levels were measured. As shown in Figure 16A, treatment of WT mice with TCDD (30 μg/kg, single p.o. dose) for 7 days resulted in a significant inhibition of VLDL-triglyceride secretion. The hepatic mRNA expression of ApoB100, an apolipoprotein important for the structural integrity of VLDL (Fisher and Ginsberg, 2002), was significantly decreased in TCDD-treated WT mice (Figure 16B). The plasma levels of both ApoB100, but not ApoB48 proteins were decreased in TCDD-treated mice (Figure 16C). In contrast, we observed normal

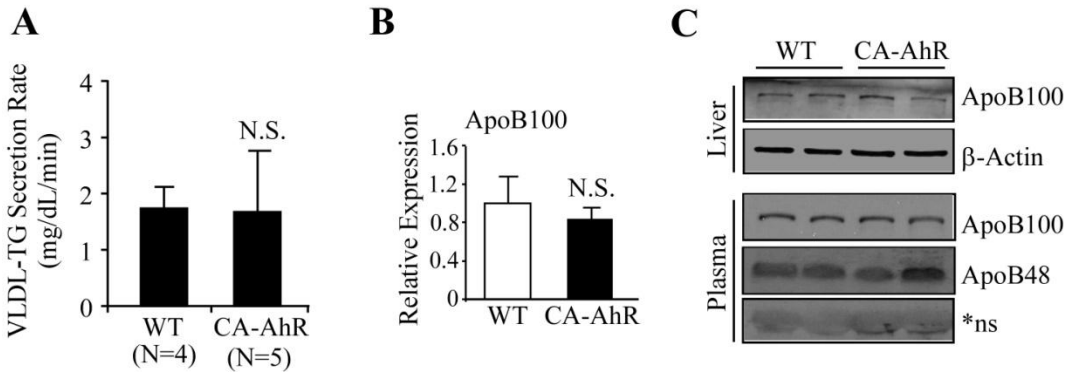

Figure 17 CA-AhR mice showed normal VLDL-triglyceride secretion. **(A)** VLDL-TG secretion, **(B)** hepatic *ApoB100* mRNA expression and **(C)** hepatic and plasma ApoB protein levels were measured in CA-AhR transgenic mice. *ns, non-specific band

VLDL-TG secretion rates in CA-AhR mice comparing to WT mice (Figure 17A). Neither the mRNA level of hepatic ApoB100, nor the protein levels of the hepatic and plasma ApoB100 were altered in CA-AhR mice (Figure 17B and 17C). The expression of microsomal triglyceride transfer protein (MTP), a protein required for assembling ApoB with triglyceride and cholesteryl esters, remained unchanged in both TCDD treated and CA-AhR mice comparing their controls (data not shown).

VLDL-triglyceride secretion *in vivo* remained impaired in $CD36^{-/-}$ mice in response to TCDD (data not shown). The decreased VLDL-triglyceride secretion may have accounted for the reduced plasma levels of triglyceride found in both WT and $CD36^{-/-}$ mice by TCDD whereas the observation was not seen in the CA-AhR mice.

2.3.9 Activation of AhR impaired hepatic peroxisomal fatty acid β-oxidation

The suppression of PPARα, a positive regulator of fatty acid oxidation, and its target genes acyl-coenzyme A oxidase 1 (Acox1), thiolase, long-chain Acyl CoA dehydrogenase (Lcad), and Cyp4a enzymes in transgenic mice was first suggested by the microarray analysis (Appendix B

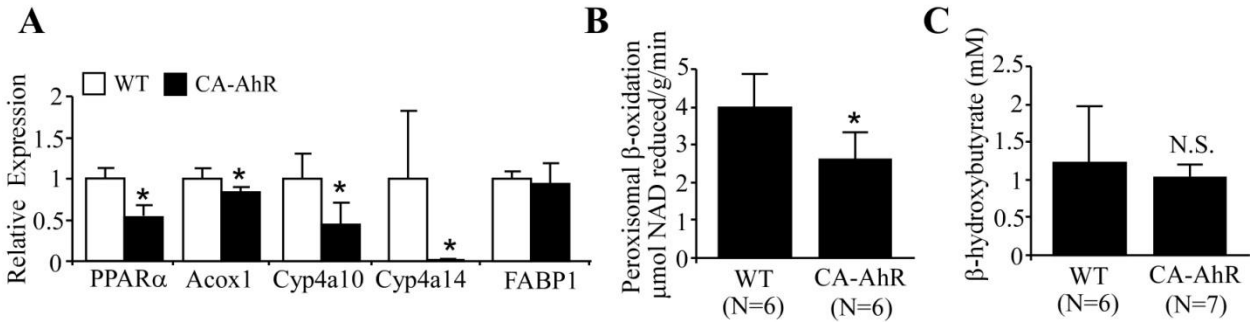

Figure 18 Activation of AhR in transgenic mice inhibited hepatic peroxisomal fatty acid β-oxidation. **(A)** Suppression of *PPARα* and its target genes involved in fatty acid oxidation in 2-month old female CA-AhR transgenic mice, as shown by real-time PCR analysis. N=6 for each group. **(B)** Inhibition of peroxisomal β-oxidation in the liver extracts of transgenic mice. Palmitoyl-CoA was used as the substrate. **(C)** Plasma levels of β-hydroxybutyrate. Two-month old male mice were fasted for 16hr prior to collect plasma.

and Table 1). The suppression of these genes was confirmed by real-time PCR analysis (Figure 18A). Consistent with suppression of Acox-1, the rate-limiting enzyme of peroxisomal β-oxidation, liver extracts from transgenic mice exhibited a significantly decreased peroxisomal β-oxidation when palmitoyl-CoA was used as the substrate (Figure 18B). Mitochondria β-oxidation determined by fasting plasma levels of β-hydroxybutyrate, which is one of ketone bodies produced by mitochondria β-oxidation, was not affected by activation of AhR (Figure 18C).

2.3.10 Activation of AhR decreased white adipose tissue (WAT) adiposity and increased WAT lypolysis

The decreased fat mass in CA-AhR transgenic mice was first suggested in MRI body composition analysis (Figure 10H). Necropsy showed smaller omental fat (Figure 19A) and adipocyte hypotrophy (Figure 19B and 19C) in the transgenic mice. Treatment of WT mice with TCDD also decreased the omental fat mass (Figure 19D), consistent with a previous report (Phillips et al., 1995). Consistent with the inhibition of WAT adiposity, we found the mRNA

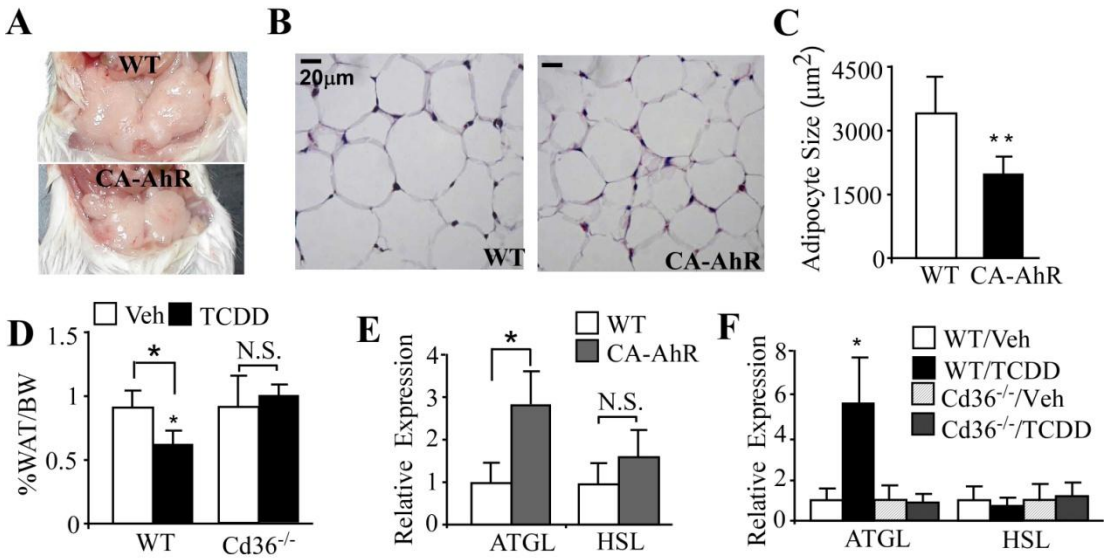

Figure 19 Activation of AhR in transgenic mice decreased white adipose tissue (WAT) adiposity, and increased WAT lipolysis. **(A)** Representative appearance of the omental fat in 8-week old female WT and transgenic mice. **(B)** H&E staining of epididymal fat. **(C)** Quantification of adipocyte size. **(D)** Omental fat tissue weight (WAT) was measured as percentage of total body weight (BW) in 2-month old male WT or CD36$^{-/-}$ mice gavaged with vehicle (Veh) or TCDD (30 μg/kg, p.o.) 7 days prior to being sacrificed (n=5 for each group). **(E and F)** Abdomen fat triglyceride lipase (*ATGL*) and hormone-sensitive lipase (*HSL*) mRNA expression as measured by real-time PCR analysis in transgenic mice (G, n=3 for each group), WT or CD36$^{-/-}$ mice treated with Veh or TCDD (H, n=5 for each group).

expression of adipose triglyceride lipase (*ATGL*) was significantly increased in the transgenic mice (Figure 19E) or TCDD-treated WT mice (Figure 19F), but the expression of hormone-sensitive lipase (*HSL*) was unchanged in either group. Interestingly, TCDD effect on decrease the omental fat mass and increase in ATGL expression was compromised in CD36$^{-/-}$ mice (Figure 19D and 19F).

2.3.11 The effect of AhR in hepatic oxidative stress, proliferation, apoptosis and dietary fat absorption.

To investigate whether activation of AhR affect on hepatic oxidative stress, we examined the status of various inflammatory parameters. Lipid peroxidation was measured by the thio-

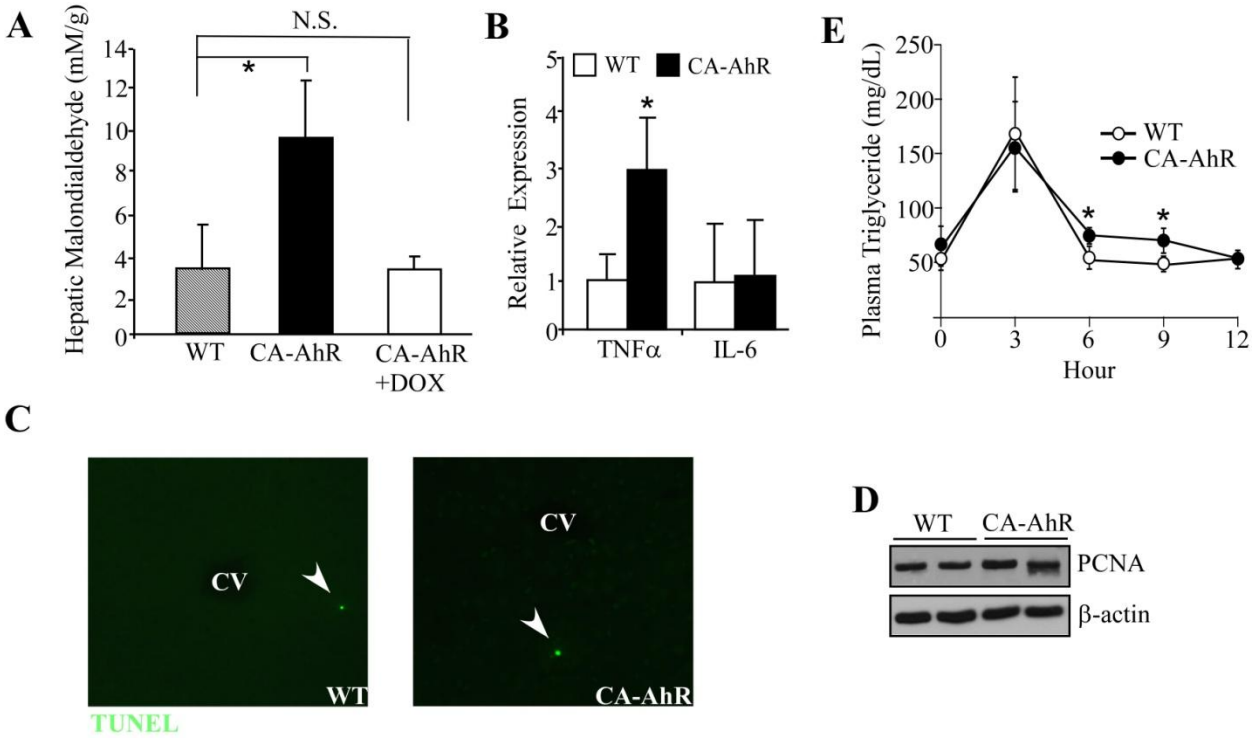

Figure 20 Effect of AhR in hepatic oxidative stress, proliferation, apoptosis and fat absorption. **(A)** Hepatic concentrations of malondialdehyde (MDA). Lipid homogenates were extracted from 5-6 week old female mice. DOX were treated for 2 weeks as indicated (n=3 each). **(B)** Hepatic mRNA expression of TNFα and IL-6 as measured by real-time PCR analysis (n=6 for each group). **(C)** Apoptosis in the liver was measured by TUNEL assay. CV represents central vein in the liver **(D)** Levels of PCNA as a proliferation marker in mouse liver extract were determined by Western blotting. **(E)** Intestinal fat absorption was determined by measuring plasma triglyceride levels after oral gavage of olive oil (10mL/kg). Two-month old female mice were fasted prior to administration of olive oil.

barbituric assay for malondialdehyde (MDA), which is an end product of lipid peroxidation. As shown in Figure 20A, activation of AhR caused three-fold increase of MDA concentrations in the liver. Enhanced lipid peroxidation in the liver of CA-AhR mice was abolished when DOX was administered in CA-AhR mice for 2 weeks, indicating that the effect is AhR dependent. Since cytokines are key mediators of hepatic inflammation and liver injury, we examined the effect of AhR in expression of cytokines, such as interleukin-6 (IL-6) and tumor necrosis factor α (TNF α), which are the 2 prototypical proinflammatory cytokines. As shown Figure 20B, we found increased expression of TNF α, not IL-6, in the liver of CA-AhR mice.

Apoptosis is a common mechanism of liver injury and patients with NASH compared with simple steatosis showed increased numbers of terminal deoxynucleotidyl transferase-mediated deoxyuridine triphosphate nick-end labeling (TUNEL)-positive cells (Tilg and Hotamisligil, 2006). At the age of 2 months in CA-AhR mice, no significant differences in hepatocytes apoptosis were observed (Figure 20C). Hepatic proliferation was evaluated by the proliferating cell nuclear antigen (PCNA) proliferation marker. As shown in Figure 20D, no enhanced expression of PCNA was observed in 2 month-old CA-AhR mice livers compared with WT controls.

To determine whether activation of AhR in intestine alters dietary fat digestion and/or absorption since the transgene is expressed in the intestine, we orally administered the mice with olive oil and evaluated intestinal fat absorption in vivo. Plasma triglyceride levels were immediately increased after olive oil administration in both WT and CA-AhR mice (Figure 20E). Elevated plasma triglyceride levels were decreased time-dependently in both WT and CA-AhR mice, however, CA-AhR mice had modestly enhanced fat absorption after a peak.

2.3.12 CA-AhR mice exhibited impaired glucose tolerance.

Hepatic steatosis and heightened oxidative stress are strongly associated with impaired insulin signaling and hepatic insulin resistance. To determine whether activation of AhR in liver is involved in insulin resistance, glucose tolerance was evaluated in mice, backcrossed for 3 generation from FVB to C57BL/6J, by intraperitoneal glucose tolerance test (GTT). Mice were fasted for 16hr and then challenged with i.p. injection of glucose (2g/kg). Blood samples were collected, and glucose levels were measured at 0, 15, 30, 60, 90, 120 180 min. As shown in

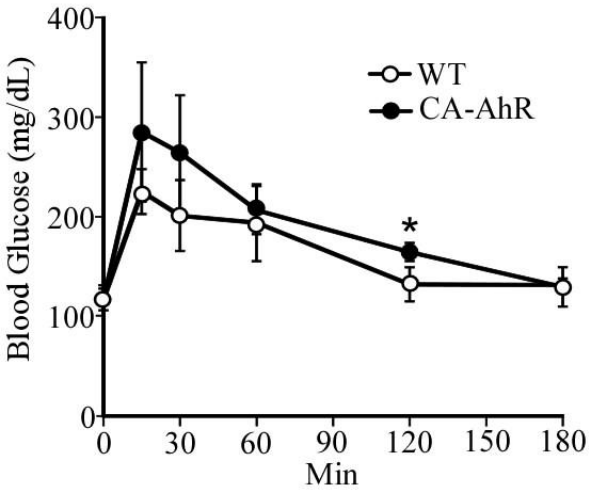

Figure 21 CA-AhR mice exhibited impaired glucose tolerance. Glucose intolerance test was performed in 16hr fasted 2-month-old WT or CA-AhR mice. Mice were backcrossed for 3 generation from FVB to C57BL/6J. Blood samples were collected at indicated time after i.p. injection of glucose (2g/kg).

Figure 21, CA-AhR mice demonstrated a higher peak glucose concentration at 15 min and reduced clearance of plasma glucose through glucose tolerance curve, suggesting that activation of AhR in liver decreased glucose tolerance during GTT.

2.4 DISCUSSION

In this study, we have uncovered a previously unrecognized endobiotic role of AhR in hepatic steatosis. Our results suggest that the AhR-induced fatty liver is likely a result of the combined effect of increased expression of fatty acid translocase CD36/FAT, suppression of fatty acid oxidation, inhibition of hepatic export of triglycerides, and an increase in peripheral fat mobilization. We showed that CD36 is a transcriptional target of AhR and activation of AhR in

liver cells induced *CD36* gene expression and enhanced fatty acid uptake in both mouse and human liver cells.

Activation of *CD36* gene expression is likely to have contributed to the steatotic effect of AhR, which was strongly supported by our observation that increased free fatty acid uptake by an AhR agonist was significantly inhibited in hepatocytes deficient of CD36. CD36 is a membrane fatty acid translocase capable of high affinity uptake of fatty acids. Emerging evidence has pointed at an important role for CD36 in controlling hepatic fatty acid uptake and steatosis. In patients with type 2 diabetes, food intake increases liver fatty acid uptake (Ravikumar et al., 2005), indicating the existence of a mechanism regulating hepatic fatty acid transport. An increased expression of CD36 was observed in the liver of high-fat diet fed mice (Inoue et al., 2005; Ito et al., 2007) and the *ob/ob* model of obesity and type 2 diabetes (Memon et al., 1999). Moreover, forced expression of CD36 in liver was sufficient to increase hepatic free fatty acid uptake and triglyceride storage (Koonen et al., 2007), suggesting a causative role for CD36 in the pathogenesis of hepatic steatosis.

A role for CD36 in hepatic steatosis was also supported by its liver-specific regulation by AhR. In both the genetic and pharmacological models, the activation of AhR induced the expression of *CD36* in liver, but not in other CD36-expressing tissues. The mechanism for the tissue-specific *CD36* regulation remains to be determined. Nevertheless, these results strongly suggest CD36 has a unique role in mediating hepatic steatosis.

The inhibition of hepatic fatty acid oxidation and VLDL-triglyceride secretion may have also contributed to the steatotic effect of AhR. The inhibition of fatty acid oxidation will lead to the storage of excess fatty acids as triglycerides. We showed that activation of AhR in transgenic mice inhibited peroxisomal β-oxidation of fatty acids. Peroxisomal β-oxidation is important

because peroxisomes are an exclusive site for β-oxidation of very-long chain fatty acids (Wanders et al., 2001). Although it represents a minor pathway relative to mitochondrial β-oxidation, peroxisomal β-oxidation becomes increasingly important during periods of increased delivery of fatty acids into the liver in pathogenic states, such as diabetes and fatty liver diseases (Hashimoto et al., 1999; Kroetz et al., 1998; Rao and Reddy, 2001). It is interesting that TCDD-mediated decrease in plasma triglyceride in WT mice was not seen in the CA-AhR mice. The inhibition of VLDL-triglyceride secretion in TCDD-treated mice was associated with decreased expression and production of ApoB100 resulting in low plasma triglyceride. The correlation between circulating levels of triglyceride and ApoB expression has been evidenced by mouse models. Heterozygous ApoB knockout mice had reduced hepatic, intestinal and plasma ApoB expression and reduced plasma levels of triglyceride (Farese et al., 1995). In contrast, transgenic mice overexpressing ApoB had a higher level of circulating triglycerides (McCormick et al., 1996).

The decreased WAT adiposity and adipocyte hypotrophy in AhR-activated mice were intriguing. This effect was abrogated in $CD36^{-/-}$ mice. The loss of fat mass might be explained by the activation of adipose ATGL, a predominant adipose lipase involved in fat mobilization. We reason the activation of *ATGL* gene expression may be secondary to the liver activation of AhR because: 1) the CA-AhR transgene was not targeted to the adipose tissue; and 2) expressing of CA-AhR under the fat specific aP2 gene promoter failed to activate ATGL (data not shown). It remains to be determined whether activation of AhR in the liver led to the production of hormonal factors, referred to as "hepatokines" such as FGF21, Fetuin A and retinol binding protein 4 (Stefan et al., 2008), which may subsequently affect extrahepatic tissues.

Results of this study are potentially implicated in human patients with non-alcoholic fatty liver disease (NAFLD), which is strongly associated with insulin resistance and metabolic syndrome (Kotronen and Yki-Jarvinen, 2008; Postic and Girard, 2008). If unmanaged, NAFLD may develop into nonalcoholic steatohepatitis (NASH), in which the fat accumulation is associated with inflammation (hepatitis) and scarring (fibrosis) of the liver (Green, 2003). The pathogenesis of NAFLD and NASH has been poorly understood. Although insulin resistance, influenced by genetic determinants, nutritional factors and lifestyle, plays a role in NAFLD and NASH, it is increasingly recognized that cytokines, including TNFα and IL6, are not only critically involved in hepatic inflammation, liver cell death, cholestasis and fibrosis, but also attenuate insulin action (Tilg and Hotamisligil, 2006). At age of 5-6 weeks, CA-AhR mice showed increased hepatic inflammatory signaling, which are evidenced by heightened lipid peroxidation and oxidative stress accompanying by induction of TNFα expression. While increase of TNFα by TCDD has been reported (Umannova et al., 2007), our transgenic mouse model revealed the direct link between AhR pathway and inflammatory liver injury. In addition to increase of TNFα, it remains to be determined whether AhR induces other inflammatory cytokines involved in NASH. Exposures to dioxin or polychlorinated biphenyls (PCBs) have been linked to insulin resistance and diabetes. It was reported that dioxin exposure is strongly associated with increased prevalence of fatty liver in human populations (Lee et al., 2006). In our study, we showed that treatment of human liver cells with an AhR agonist increased uptake of free fatty acids, providing a plausible mechanism by which polycyclic aromatic hydrocarbons, which can be generated during the food-cooking process, cigarette smoking, and industrial and military use of herbicides/pesticides, may promote fatty liver.

In summary, our study provides a novel and unexpected link between AhR-induced hepatic steatosis and the expression of fatty acid translocase CD36. The tetracycline inducible AhR transgenic mice, exhibiting fatty liver even when fed with a chow diet, represent a novel, convenient and reversible model of NAFLD. It is tempting for us to propose that AhR and its target CD36 may be novel therapeutic targets to manage NAFLD. It is encouraging to note that substantial progress has been made in the development and use of AhR antagonists (Casper et al., 1999; Dertinger et al., 2001; Lu et al., 1995; Puppala et al., 2008; Revel et al., 2003).

CHAPTER III

3.0 ANDROGEN DEPRIVATION BY LIVER X RECEPTOR-MEDIATED ACTIVATION OF PHASE II SULFOTRANSFERASE

3.1 BACKGROUND

Prostate is an androgen regulated exocrine gland of male reproductive system (Chatterjee, 2003). Androgens, including testosterone (T) and dihydrotestosterone (DHT), play an important role in the morphogenesis and physiology of normal prostate (Chatterjee, 2003; Denmeade and Isaacs, 2002; Long et al., 2005). In addition to its normal function, androgen is a risk factor for prostate cancer, the most commonly diagnosed and the second leading cause of cancer death in men (AmericanCancerSociety, 2006).

The production of testosterone in the testis, where more than 90 % of testosterone is synthesized from cholesterol, is regulated by the hypothalamus-pituitary axis (Figure 22). The adrenal gland can also produce androgens. The hypothalamus stimulates the production of luteinizing hormone (LH)-releasing hormone (LHRH), which travels into the pituitary gland and interacts with LHRH receptors. This interaction

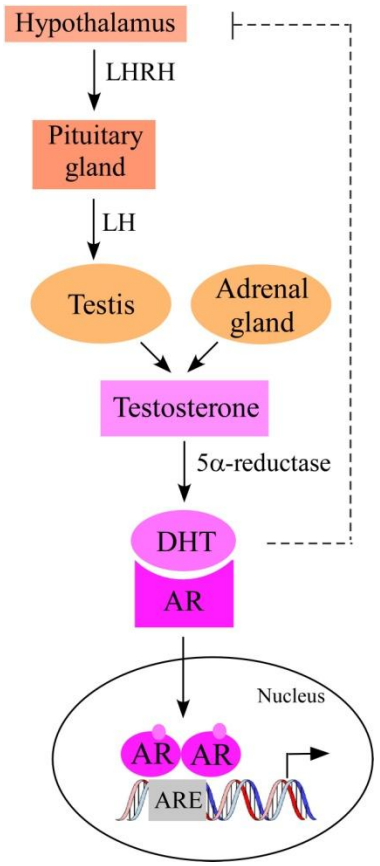

Figure 22 Androgen production and action. LHRH, luteinizing hormone (LH)-releasing hormone; DHT, dihydrotestosterone; AR, androgen receptor; ARE, AR responsive element

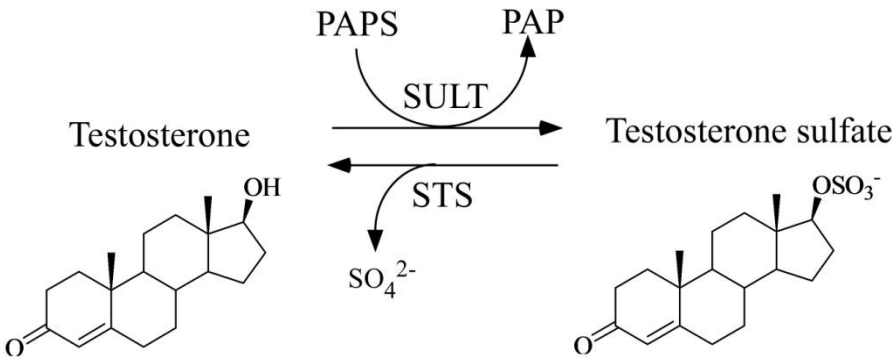

Figure 23 Testosterone sulfate formation and hydrolysis. SULT, sulfotransferase; STS, steroid sulfatase; PAP, 3'-phosphoadenosine-5'-phosphate; PAPS, 3'-phosphoadenosine-5'-phosposulfate.

stimulates the release of LH from the pituitary gland, which subsequently binds to LH receptors in the testis and stimulates the production of testosterone. In target tissues, such as the prostate, testosterone is converted into dihydrotestosterone, which is a more potent androgen, by the enzyme 5α-reductase. It is generally believed that most of the androgen actions are mediated by the androgen receptor (AR), a member of the nuclear hormone receptor superfamily (Heinlein and Chang, 2004; Trapman and Brinkmann, 1996). Upon activation by androgens, AR translocates from cytoplasm into the nucleus where it binds to the androgen responsive element (ARE) on target genes and recruits co-activators to facilitate gene regulation. The androgens-AR signaling stimulates a cascade of events that are required for prostate cancer development and progression. As such, the most effective endocrine therapy for prostate cancer has been androgen ablation. These include surgical or medical castration, as well as the use of anti-androgens (Denmeade and Isaacs, 2002). Upon androgen withdrawal or anti-androgen treatment, the growth of androgen-dependent prostate cancer cells is reduced and the cells undergo apoptosis, leading to tumor regression (Chatterjee, 2003).

Other than castration and the use of anti-androgens, an important pathway to metabolically deactivate androgens is through the sulfotransferase-mediated sulfonation (Figure

23). Sulfotransferases (SULTs), a family of Phase II drug metabolizing enzymes, catalyze the transfer of a sulfonyl group from the co-substrate 3'-phosphoadenosine-5'-phosposulfate (PAPS) to the acceptor substrates to form sulfate or sulfamate conjugates (Glatt et al., 2001; Nagata and Yamazoe, 2000; Strott, 1996, 2002). Sulfonation plays an important role in steroid hormone deactivation, since sulfonated hormones often fail to bind to their cognate receptors and thus lose their hormonal activities (Raftogianis et al., 1998; Strott, 2002). Sulfoconjugation also converts lipophilic steroid hormones to amphiphiles, which promotes their excretion (Raftogianis et al., 1998; Strott, 2002). The primary SULT isoform responsible for androgen sulfonation at physiological concentration is believed to be the hydroxysteroid sulfotransferase (SULT2A1) (Meloche et al., 2002; Strott, 2002). In humans, SULT2A1 is expressed in steroidogenic organs (adrenal and ovary), androgen-dependent tissue (prostate), tissues of the alimentary tract (stomach, small intestine, and colon) and liver (Strott, 2002). In rodents, Sult2a1/2a9 is predominantly expressed in the liver, although a lower level of its expression is also observed in several other tissues (Song et al., 1998).

The potential effect of SULT2A1 on androgen metabolism has been alluded to in previous reports. For instance, the androgen insensitivity in the livers of pre-puberty or aged rats were associated with an elevated hepatic expression of Sult2a1 (Chan et al., 1998), suggesting an important role for Sult2a1 in androgen homeostasis. On the other hand, the expression of SULT2A1 has been shown to be down-regulated by androgens (Chatterjee et al., 1996; Song et al., 1998), which may represent a regulatory mechanism to maintain a proper androgenic activity. Despite the potential role of SULT2A1 in androgen metabolism, the implication of SULT2A1 expression and regulation in prostate regeneration and prostate cancer have not been systemically evaluated. In addition to SULT2A1, other androgen metabolizing enzymes have

also been implicated in prostate cancer. For example, increased expression of enzymes converting adrenal androgens to testosterone, such as the aldo-keto reductase family 1, member C3 (AKR1C3), was detected in androgen-independent prostate cancer, which has been proposed to be a potential mechanism by which prostate cancer cells adapt to androgen deprivation (Stanbrough et al., 2006).

Other than SULT2A1, SULT2B1b may also contribute to androgen sulfation. It has been reported that recombinant SULT2B1b showed sulfonating activity toward T and DHT, although adrenal androgens such as androstenediol and DHEA are better substrates for this enzyme (Geese and Raftogianis, 2001; Strott, 2002). The steroid sulfatase (STS) also plays a role in androgen homeostasis. It is believed that the sulfonated androgens could be desulfonated within target tissues, such as the prostate, to be converted into active metabolites. Indeed, STS inhibitors have been explored as anti-cancer drugs for prostate cancer (Reed et al., 2005).

LXRs have been shown to possess diverse functions, ranging from cholesterol efflux to lipogenesis and anti-inflammation (Zelcer et al., 2006). More recently, we showed that LXR can promote bile acid detoxification and alleviate cholestasis (Uppal et al., 2007). The anti-cholestatic effect of LXR was associated with LXR-mediated activation of Sult2a1/2a9, which is also capable of sulfonating and detoxifying bile acids (Uppal et al., 2007). However, whether or not LXR plays a role in androgen homeostasis is unknown.

In this study, we showed that activation of LXR lowered circulating androgen level *in vivo* and inhibited androgen-dependent prostate regeneration and prostate cancer cell growth. We also showed that sulfonated androgens failed to activate AR and expression of SULT2A1 is both necessary and sufficient to deactivate androgens. We propose that LXR-mediated

SULT2A1activation represents a novel mechanism of androgen deprivation, which may have its utility in developing therapies for hormone-dependent prostate cancers.

3.2 METHODS

Animals and prostate regeneration experiment

The creation of FABP-VP-LXRα transgenic mice has been previously described in detail (Uppal et al., 2007). Transgenic mice and their wild type littermates have a mixed background of C57BL/6J and 129/SvImJ. For the prostate regeneration experiment, mice were surgically castrated at 8 weeks of age. Ten days after castration, mice received daily i.p. injection of testosterone propionate (TP, 5 mg/kg) for 10 days to allow the prostate to regenerate (Mukai et al., 2005). Mice were i.p. injected with bromodeoxyuridine (BrdU, 10 mg/kg) 6 hours before being sacrificed. When necessary, wild type mice received TO1317 treatment (daily gavage at 50 mg/kg) beginning 2 days before the TP treatment and continued until the completion of the experiment. The urogenital complex was removed and the anterior, ventral, lateral and dorsal prostate lobes were separated under a dissecting microscope and weighed. Ventral prostate lobes were processed for paraffin sections and subjected to immunostaining for BrdU or proliferating cell nuclear antigen (PCNA). Prostate lobes from each mouse were pooled for RNA extraction and gene expression analysis. Animals were sacrificed in a CO_2 chamber. The use of mice in this study was approved by the University of Pittsburgh Institutional Animal Care and Use Committee.

Sulfotransferase assay

Sulfotransferase assay using [^{35}S]-PAPS (Perkin Elmer) as the sulfate donor was performed as previously described (Gong et al., 2007; Saini et al., 2004; Uppal et al., 2005). In brief, 20μg/mL of total liver cytosolic extract was incubated with 5μM of testosterone substrate at 37 ℃. Reaction was terminated by the addition of ethyl acetate. Unconjugated substrate and free [^{35}S]-PAPS were extracted by vigorous mixing followed by centrifugation at 13,000 rpm for 5 min. The amount of radioactivity in the aqueous phase was determined by liquid scintillation. Each reaction was run in triplicate.

Cell proliferation assay

LNCaP and DU145 cells were maintained in RPMI-1640 medium supplemented with 10 % fetal bovine serum (FBS). LAPC4 cells were maintained in IMDM medium supplemented with 10 % FBS. Androgen independent LNCaP-derived LN05 and LAPC4-derived LA99 cells were maintained in phenol red-free RPMI-1640 and IMDM medium, respectively, supplemented with 10 % charcoal/dextran-stripped FBS. Cells were seeded onto 12-well cell culture plates at the density of 3×10^4/per well. After 24 hours of incubation, cells were replaced with medium supplemented with 10% charcoal/dextran-stripped FBS, in the absence or presence of androgens (testosterone or dihydrotestosterone, 10 nM each) and/or LXR ligands (22(*R*)-hydroxycholesterol, GW3965, or TO1317, 10 μM each). Cells were replaced with fresh medium daily. After 4 days of treatment, cells were trypsinized and counted with a hematocytometer. When necessary, cells were co-treated added 10 μM of dehydroepiandrosterone (DHEA).

TUNEL assay

LNCaP cells were seeded onto chamber slides at the density of 2.5×10^4/per well and incubated overnight before treatment with various LXR agonists, including 22R-hydroxycholesterol, GW3965 and TO1317 (10 μM each) for 3 days. Cells were then fixed with 4% paraformaldehyde (pH 7.4) for 30 mins. TUNEL assay were performed using an assay kit (Cat # 11 684 795 910) from Roche Diagnostics (Indianapolis, IN). Apoptotic cells were detected by fluorescein staining, and the nuclei were counterstained with DAPI.

Measurement of serum levels of testosterone and luteinizing hormone (LH)

The wild type and transgenic mice were castrated at 8 weeks. Ten days after castration, mice received a single i.p. injection of TP (5 mg/kg) 24 hours prior to being sacrificed and serum testosterone levels were measured. When necessary, wild type mice received GW3965 treatment (daily gavage at 20 mg/kg) beginning 2 days before the TP treatment and continued until the completion of the experiment. Serum testosterone levels were determined using a testosterone enzymatic immunoassay (EIA) kit from Cayman Chemical Company (Ann Arbor, MI). According the manufacturer's specification, this EIA assay is highly specific for testosterone (100 %), whereas its specificity for estered testosterone and testosterone sulfate is 0.11 % and 0.03 %, respectively. The specificity of this EIA assay to testosterone and its lack of specificity to testosterone propionate, testosterone sulfate, and testosterone glucuronide were experimentally confirmed by us (data not shown). The mouse blood samples were not extracted prior to assay. Non-interference was ruled out by serial dilution (data not shown). The LH levels were commercially measured by the University of Virginia Center for Research and Reproduction (www.healthsystem.virginia.edu/internet/crr/ligand.cfm).

Plasmid construct and transfection assay

Expression vector for AR (pcDNA-AR) and the PSA-Luc and ARE-Luc reporter genes were generous gifts from Dr. Hongwu Chen (Louie et al., 2003). The human SULT2A1 cDNA was cloned by RT-PCR using the following pair of oligonucleotides: 5'-CCGGAATTCATGTCGGACGATTTCTTATGG-3', and 5'-CTAGCTAGCTTATTCCCATGGGAACAGCTC-3'. The SULT2A1 cDNA was digested and inserted into the pCMX expression vector. The identity of the cDNA was verified by DNA sequencing. HepG2 and DU145 cells were transfected on 48-well cell culture plates using the polyethyleneimine polymer transfection agent and Lipofectamine 2000, respectively. For each triplicate transfection of HepG2 cells, 0.8 μg of reporter, 0.4 μg of pcDNA-AR and 0.25 μg of pCMX-βgal were used. For DU145 cell transfection, the amounts of reporter, AR and β-gal were 0.15 μg , 0.1 μg and 0.25 μg. Transfected cells were then treated with vehicle or androgens in medium containing 10% charcoal/dextran-stripped FBS for 24 hours before harvesting for luciferase and β-gal assays. The transfection efficiency was normalized against the β-gal activity.

Northern blot and real-time RT-PCR analysis

Total RNA was isolated from tissues or cell cultures using the TRIZOL reagent from Invitrogen (Carlsbad, CA). Northern hybridization using ^{32}P-labeled cDNA probe was carried out as described (Barish and Evans, 2004). In the real-time RT-PCR analysis, reverse transcription was performed with the random hexamer primers and the Superscript RT III enzyme from Invitrogen following the manufacturer's instruction. SYBR Green-based real-time PCR was performed with the ABI 7300 Real-Time PCR System. Data was normalized against the control of cyclophillin signals. Sequences of the real-time PCR probes are shown in Appendix D.

LXR ribonucleic acid interference experiment

The siRNA transfection was carried out using Lipofectamine 2000. The human LXRs and SULT2A1 siRNAs were added to the final concentration of 5 nM in transfection. The sequences of siRNAs are: LXRα 5'-AGCAGGGCUGCAAGUGGAA-3' (corresponding to nucleotides 1017-1039), LXRβ 5'-CAGAUCCGGAAGAAGAAGA-3' (corresponding to nucleotides 746-768) SULT2A1: 5'-CCCGAAGAACUGAACUUAA-3' (corresponding to nucleotides 699-721). All siRNAs, including the control scrambled siRNA, were ordered from QIAGEN (Valencia, CA). Cell were transfected for 5 hours before being replaced with medium containing 10% FBS.

BrdU and PCNA immunostaining

Tissues were fixed in 4% formaldehyde, embedded in paraffin, sectioned at 5 μm, and subjected to immunostaining with a rat monoclonal anti-BrdU antibody (Cat# OBT0030) from Accurate (Westbury, NY) (1:20) or an anti-PCNA antibody (Cat # VP-P980) from Vector (Burlingame, CA) (1:100) using *Vectastain Elite* ABC Kit from Vector. Diaminobenzidine tetrahydrochloride (DAB) was used as the chromogen, and sections were counterstained with Gill's hematoxylin.

3.3 RESULTS

3.3.1 Inhibition of androgen-dependent prostate regeneration by activation of LXR

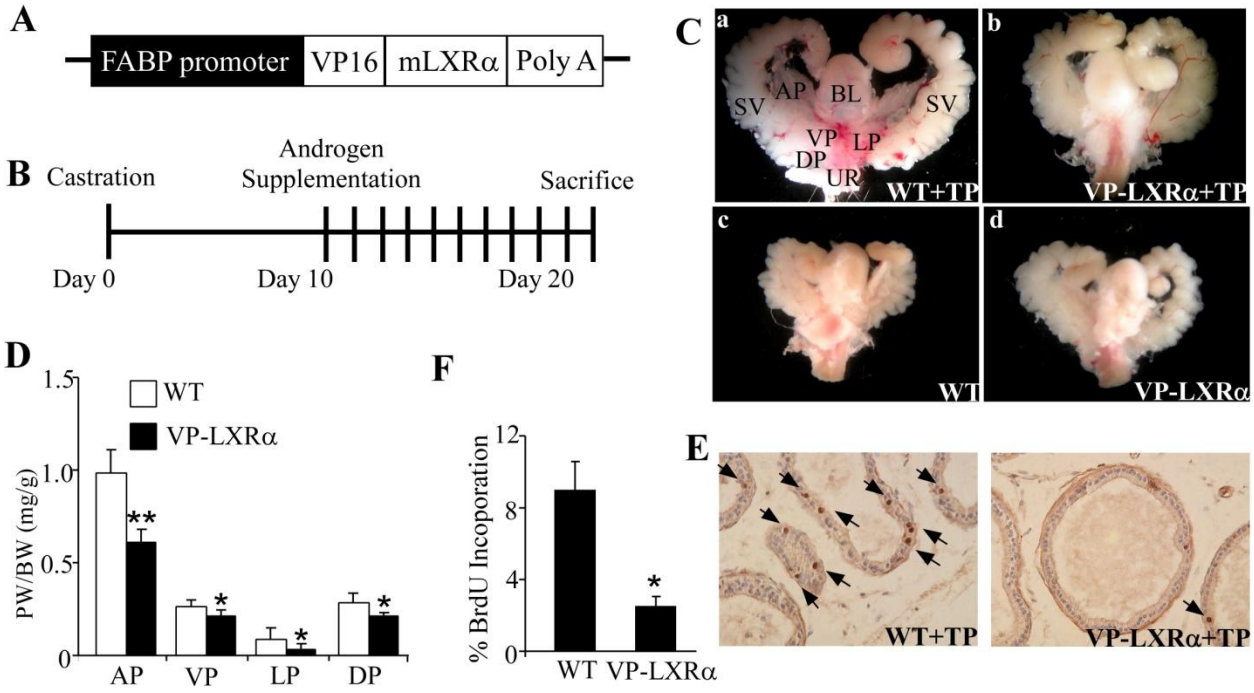

Figure 24 Genetic activation of LXR in mice inhibited androgen-dependent prostate regeneration. **(A)** Schematic representation of the FABP-VP-LXRα transgenic construct. FABP promoter, fatty acid binding protein promoter. VP, viral protein 16. Poly A, SV40 poly(A) sequences. **(B)** Outline of the prostate regeneration experiment **(C)** Urogenital complex of WT and VP-LXRα transgenic (VP-LXRα) mice. AP, anterior prostate; VP, ventral prostate; LP, lateral prostate; DP, dorsal prostate; BL, bladder; SV, seminal vesicle; UR, urethra. **(D-F)** Prostate weight (PW) normalized to body weight (BW) (D), prostate luminal epithelial cell proliferation was measured by BrdU immunostaining with the positive nuclei arrow-headed (E), and quantification of BrdU labeling index (F) in the WT and TG mice. In C-F, all mice, except those in C-c and C-d, were castrated at 8-weeks old, rested for 10 days, and then treated with testosterone propionate (TP, 5 mg/kg) for 10 days. Mice were labeled with BrdU (10 mg/kg) 6 hours prior to being sacrificed. Mice in C-a and C-b were castrated but not TP-treated. Each group has 7-8 mice.

Uppal et al. has recently created the FABP-VP-LXRα transgenic mice that express the activated LXRα (VP-LXRα) in the liver under the control of the rat liver fatty acid binding protein (FABP) promoter (Uppal et al., 2007). Figure 24A shows the schematic representation of the transgene. Created by fusing the VP16 activation domain of the herpes simplex virus to the amino-terminal of mouse LXRα, VP-LXRα activates LXR responsive genes in a constitutive manner (Uppal et al., 2007). The creation of this transgenic line also led to our recent identification of *Sult2a1/2a9* as a novel LXR target gene (Uppal et al., 2007).

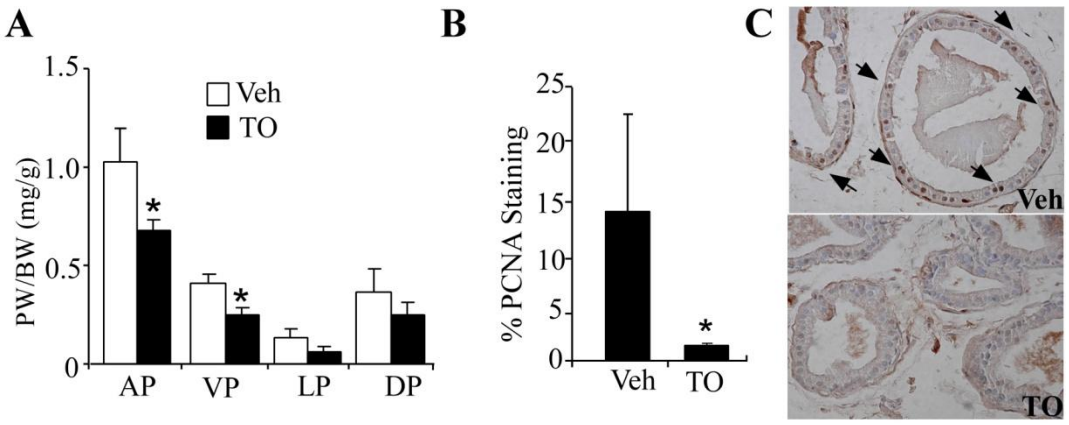

Figure 25 Pharmacological activation of LXR in mice inhibited androgen-dependent prostate regeneration. **(A-C)** WT mice were castrated at 8-weeks old, rested for 10 days, and then treated with TP for 10 days, in the presence of vehicle (Veh) or TO1317 (50 mg/kg, daily gavage). The TO1317 treatment started 2 days before the TP treatment and continued until the completion of the experiment. Shown are PW normalized to BW (A), prostate luminal epithelial cell proliferation was measured by PCNA immunostaining. (B) Quantification of PCNA-positive cells. (C) The positive nuclei stained with PCNA are arrow-headed. Each group contains three mice.

The potential effect of Sult2a1/2a9 on androgen metabolism prompted us to examine whether activation of LXR affects androgen homeostasis. We first evaluated the effect of LXR activation on androgen-dependent prostate regeneration (Figure 24B). In this experiment, wild type (WT) or FABP-VP-LXRα transgenic (VP-LXRα) mice were castrated at 8 weeks of age. Ten days post-castration, when the prostates have been degenerated (Figure 24C) (English et al., 1987; Karhadkar et al., 2004), mice were treated with testosterone propionate (TP, 5 mg/kg/day, i.p.) for 10 days to allow the prostate to regenerate. Six hours prior to being sacrificed, mice were labeled with bromodeoxyuridine (BrdU, 10 mg/kg, i.p.). The urogenital complexes were removed, and the anterior (AP), ventral (VP), lateral (LP) and dorsal (DP) lobes of prostate were dissected under a dissecting microscope and weighed. As shown in Figure 24C, the prostate lobes in TP-treated WT mice were notably larger that their transgenic counterparts. Indeed, the average weights of all prostate lobes, when measured as ratios of prostate weight (PW) to body weight (BW), were significantly lower in the VP-LXRα mice than the WT mice (Figure 24D). It appeared that LXR had most profound effect on the anterior prostate. The retarded prostate

regeneration in the VP-LXRα mice was accompanied by a decrease in prostate epithelial proliferation as measured by BrdU immunostaining (Figure 24E). The BrdU labeling index in the ventral prostate of VP-LXRα mice was 28% of the WT mice (Figure 24F).

The inhibition of androgen-dependent prostate regeneration was also observed in WT mice treated with the LXR agonist TO1317. In this experiment, 8-week old WT male mice were castrated. Ten days post-castration, mice were randomly divided into two groups, with one group receiving daily gavage of TO1317 (50 mg/kg) and the control group receiving vehicle until the completion of the experiments. Our pilot experiment showed that the 50 mg/kg dose of TO1317 is optimal to show the effect on prostate regeneration. Beginning at 12 days post-castration, all mice received daily i.p. injection of TP (5 mg/kg) for 10 days before being sacrificed and analyzed for prostate regeneration. As shown in Figure 25A, the regeneration of all lobes was inhibited in the TO1317-treated mice. Immunostaining of proliferating cell nuclear antigen (PCNA), another indicator of cell proliferation, showed that the percentage of PCNA-positive cells in the ventral prostate was higher in the vehicle-treated than the TO1317-treated mice (Figure 25B and 25C). Treatment of WT mice with GW3965, another synthetic LXR agonist, resulted in a similar inhibition of androgen-dependent prostate regeneration (data not shown).

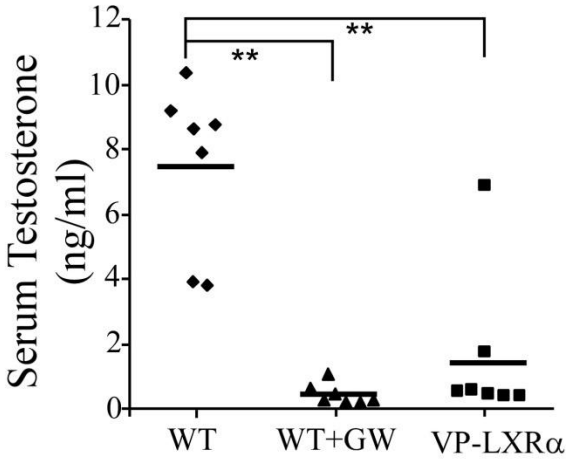

Figure 26 Activation of LXR lowered circulating level of active testosterone. Wild type (WT) and VP-LXRα transgenic (VP-LXRα) mice were castrated at 8 weeks, rested for 10 days, and then treated with a single i.p. injection of TP (5 mg/kg) 24 hours prior to being sacrificed. When applicable, the GW3965 (GW) treatment (20 mg/kg, daily gavage) started 2 days before the TP treatment and continued until the completion of the experiment. Data represent individual mice. Lines represent average testosterone levels in each group.

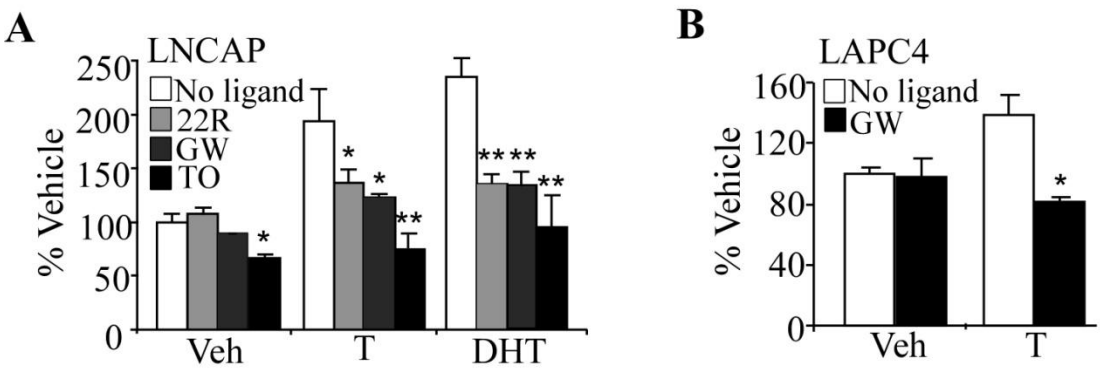

Figure 27 Treatment with LXR agonists inhibited androgen-dependent LNCAP and LAPC4 prostate cancer cell growth. **(A and B)** Treatment with 10 μM of LXR agonist 22(R)-hydroxycholesterol (22R), GW3965 (GW) and TO1317 (TO) inhibited testosterone (T, 10 nM) and dihydrotestosterone (DHT, 10nM) induced LNCaP (A) or LAPC4 (B) cell proliferation as measured by cell number counting. Cells were maintained in medium supplemented with 10% charcoal/dextran-stripped FBS during the 4-day treatment period.

3.3.2 Activation of LXR lowered the circulating testosterone levels

To understand the mechanism by which LXR inhibits prostate regeneration, we measured the levels of testosterone in the serum of VP-LXRα mice and GW3965-treated WT mice. In this experiment, mice were castrated at 8 weeks. Ten days after castration, mice were treated with a single dose of TP (5 mg/kg, i.p.) and the mice were sacrificed 24 hours after the TP injection. When the LXR ligand was used, the GW3965 treatment started 2 days before the TP treatment and continued until the completion of the experiment. As shown in Figure 26, the average serum testosterone concentration in TP-treated castrated WT mice was 7.4 ng/ml, similar to what has been reported (33). In a sharp contrast, the genetic (transgenic) or pharmacological (GW3965) activation of LXR resulted in significantly decreased serum concentrations of testosterone.

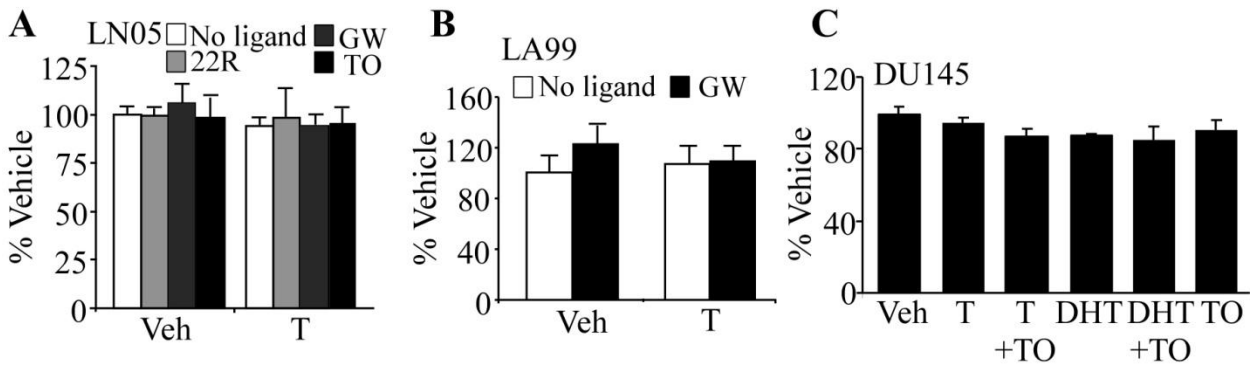

Figure 28 Treatment with LXR agonists had little effect on androgen-independent prostate cancer cell growth. **(A)** LNCaP-derived LN05, **(B)** LAPC4-derived LA99, and **(C)** DU145. Cell conditions are same as Figure 27.

3.3.3 Inhibition of androgen-dependent prostate cancer cell growth by treatment with LXR agonists

The inhibition of androgen-dependent prostate regeneration led us to determine whether activation of LXR affects androgen-dependent human prostate cancer cell growth. In this experiment, the AR-positive and androgen-dependent LNCaP and LAPC4 cells were treated with 22(*R*)-hydroxycholesterol, GW3965 or TO1317, in the absence or presence of the supplemented androgens, including testosterone (T) and dihydrotestosterone (DHT) in charcoal/dextran-stripped fetal bovine serum (FBS). As expected, treatment with T or DHT induced 2-3 fold increases in LNCaP cell numbers (Figure 27A). All three LXR agonists, when applied at 10 μM concentration, inhibited the androgen dependent-LNCaP cell proliferation with TO1317 had the most dramatic inhibition (Figure 27A). In the absence of androgens, 22(*R*)-hydroxycholesterol and GW3965 had little effect on LNCaP cell growth, but TO1317 has a modest but significant inhibitory effect. GW3965 also inhibited the proliferation of LAPC4 cells, another AR-positive and androgen-dependent human prostate cancer cells (Figure 27B). Under the same cell culture condition, LXR ligands had little effect on the growth of the androgen-independent LNCaP-

derived LN05, LAPC4-derived LA99 and DU145 cells, regardless of the androgen treatment (Figure 28).

The TO1317- and GW3965-induced LNCaP growth inhibition was accompanied by a suppression of the mRNA expression of the prostate-specific antigen (PSA) (Figure 29A) and increased apoptosis as revealed by TUNEL assay (Figure 29B and 29C). Consistent with the result of cell proliferation, TO1317 showed the most dramatic effect in inhibiting PSA expression and triggering apoptosis. The inhibitory effect of LXR agonists on LNCaP cells was LXR dependent, since this inhibition was abolished when both LXRα and LXRβ were knocked-down by siRNAs (Figure 29D). The down-regulation of LXR expression in siRNA-transfected cells was confirmed by real-time PCR analysis (Figure 29E).

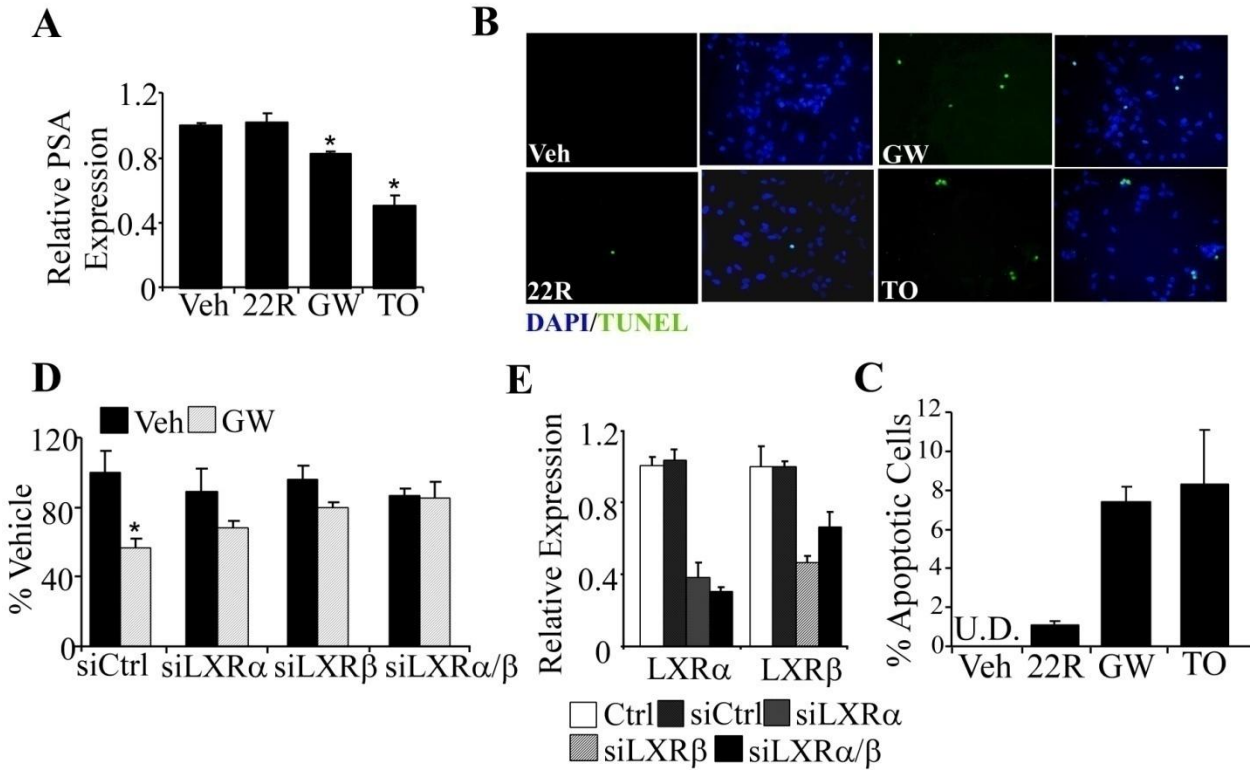

Figure 29 Treatment of LXR agonists decreases mRNA expression of prostate specific antigen (PSA) and induces apoptosis. **(A-C)** LNCaP cells were maintained in medium containing 10% FBS for 3 days in the presence of vehicle, 22R, GW or TO. Total RNA was isolated and the mRNA expression of PSA was measured by real-time PCR (A). Apoptosis was measured (B) and quantified (C) by TUNEL assay. UD, undetectable. **(D)** Down-regulation of LXRα and LXRβ by siRNAs abolished the growth inhibitory effect of GW3965 on LNCaP cells. The treatment conditions after siRNA transfection were identical to those described in (A and B). The LXR ligand concentration is 10 μM. The concentration for T or DHT is 10 nM. **(E)** The efficiencies of LXR knock-downs were confirmed by real-time PCR. Ctrl is lipofectamine alone control. Knockdown efficiency was presented as expression relative to that observed in Ctrl (arbitrarily set at 1).

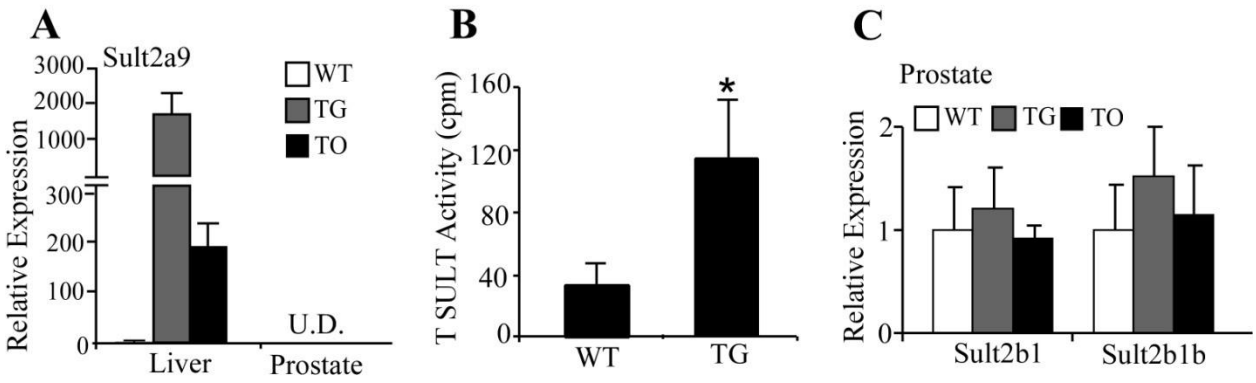

Figure 30 Activation of LXR induced the expression of SULT2a9 in the mouse liver. **(A)** Activation of hepatic Sult2a9 gene expression in VP-LXRα transgenic (VP-LXRα) mice and wild type (WT)-treated with TO1317 as shown by real-time PCR. Each group contains 3-5 mice. UD, undetectable. **(B)** Increased testosterone sulfotransferase activity in VP-LXRα mice. Cytosolic liver extracts from WT and VP-LXRα mice were incubated with testosterone as the substrate and [^{35}S]-PAPS as the sulfate donor. Radioactivity was determined by liquid scintillation. **(C)** Expression of Sult2b1 and Sult2b1b in the prostate of WT mice mock treated or treated with TO1317 as shown by real-time PCR. Mice were treated with TO1317 (50 mg/kg, gavage) for 10 days. Each group contains three mice.

3.3.4 Activation of LXR induced the expression of SULT2A1 and suppressed the expression of STS in mouse prostate and LNCaP cells

The VP-LXRα and TO1317-treated WT male mice showed markedly increased expression of *Sult2a1/2a9* in the liver (Figure 30A), consistent with our previous report (Uppal et al., 2007). The liver cytosol extracts of the VP-LXRα mice also exhibited a significantly higher sulfation activity toward testosterone, a known Sult2a1/2a9 substrate (Meloche et al., 2002; Strott, 2002) (Figure 30B). The basal expression of Sult2a1/2a9 in the prostate is nearly undetectable (Ct number was greater than 34 or the signals were "undetermined" in real-time PCR analysis), consistent with the notion that Sult2a1/2a9 is predominantly expressed in the liver in rodents (Song et al., 1998). The expressed of Sult2a1/2a9 in the prostate also failed to be induced in LXR ligand-treated mice (Figure 30A). Sult2b1 and Sult2b1b are expressed in the prostate, but their expression was not altered in response to TO1317 (Figure 30C).

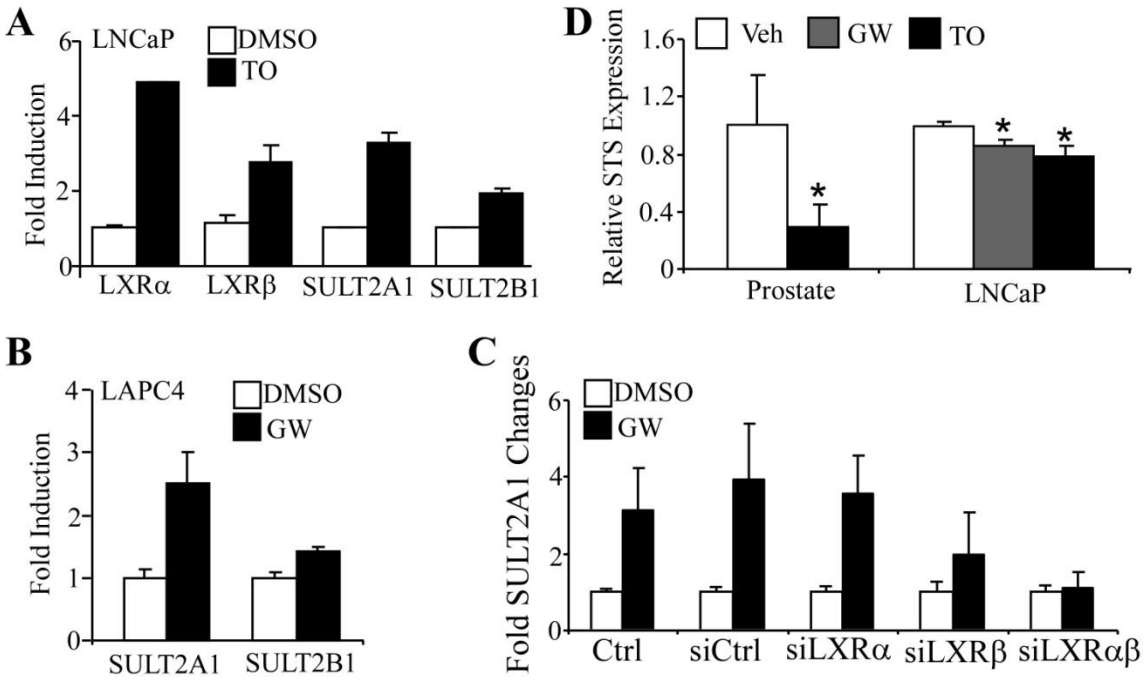

Figure 31 Activation of LXR induced the expression of SULT2A1 in androgen-dependent prostate cancer cells and suppressed the expression of STS in the mouse liver and LNCaP cells. **(A)** Effect of TO1317 on the mRNA expression of SULT2A1 and 2B1 in LNCaP cells. Cells were treated with vehicle (DMSO) or 10μM TO1317 for 2 days before RNA extraction and real-time PCR analysis. LXRα and LXRβ are included as positive controls of LXR target genes. **(B)** Effect of GW3965 on the mRNA expression of SULT2A1 and 2B1 in LAPC4. The same conditions in (A) were used. **(C)** Knocking-down of both LXRα and LXRβ abolished SULT2A1 activation in response to GW3965 in LNCaP cells as shown by real-time PCR analysis. **(D)** Effect of LXR ligands on the mRNA expression of STS in the mouse prostate and LNCaP cells as shown by real-time PCR. The same mice in Figure 29C were used. LNCaP cells were treated with Veh (DMSO), TO1317 or GW3965 (10 μM each) for 3 days.

We have previously shown that the expression of SULT2A1 was induced in primary human hepatocytes treated with TO1317 (Uppal et al., 2007). Here, we showed that the expression of SULT2A1 was also induced in LNCaP and LAPC4 cells treated with TO1317 or GW3965 (Figure 31A and 31B). The human SULT2B1 was also modestly but significantly induced by LXR agonists, consistent with a previous report on keratinocytes (Jiang et al., 2005). Although recombinant SULT2B1 is capable of sulfonating T and DHT, this enzyme has been shown to be more effective in sulfonating adrenal androgens, such as androstenediol and DHEA (Geese and Raftogianis, 2001; Strott, 2002). In TO1317-treated LNCaP cells, the expression of

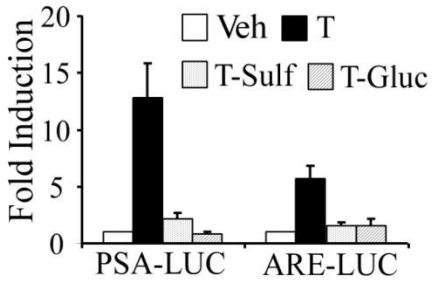

Figure 32 Sulfonated testosterone failed to activate AR. Sulfate conjugated-testosterone (T-Sulf) failed to activate AR in transient transfection and reporter gene assay. HepG2 cells were transfected with expression vector for AR and AR responsive PSA-LUC or ARE-LUC reporter gene as indicated. Cells were then treated with vehicle, testosterone (T), testosterone-sulfate (T-Sulf) or testosterone-glucuronide (T-Gluc) (10 nM each) for 24 hours before luciferase assay.

both LXR isoforms, known LXR target genes (Laffitte et al., 2001; Repa et al., 2000a; Schultz et al., 2000), was induced as expected (Figure 31A). The activation of SULT2A1 by GW3965 in LNCaP cells was LXR dependent, since knocking-down of both LXR isoforms abolished the SULT2A1 activation (Figure 31C).

We also measured the effect of LXR activation on the expression of steroid sulfatase (STS). As shown in Figure 30D, treatment with LXR agonists inhibited the expression of STS in both the mouse prostate and LNCaP cells. Interestingly, the effect of LXR on Sts expression appeared to be prostate-specific, since the VP-LXRα transgene had little effect on the hepatic expression of Sts (data not shown).

We used transient transfection and reporter gene assay to determine whether the sulfonated testosterone is indeed hormonally inactive. In this experiment, HepG2 cells were transiently transfected with AR, together with the AR-responsive natural PSA promoter reporter gene (PSA-LUC) or a synthetic report gene (ARE-LUC) that contains five copies of the AR response element (ARE) derived the PSA gene promoter. Transfected cells were then treated with testosterone (T), testosterone sulfate (T-Sulf), or testosterone glucuronide (T-Gluc) for 24 hours before luciferase assay. As shown in Figure 32, treatment with T induced the reporter gene

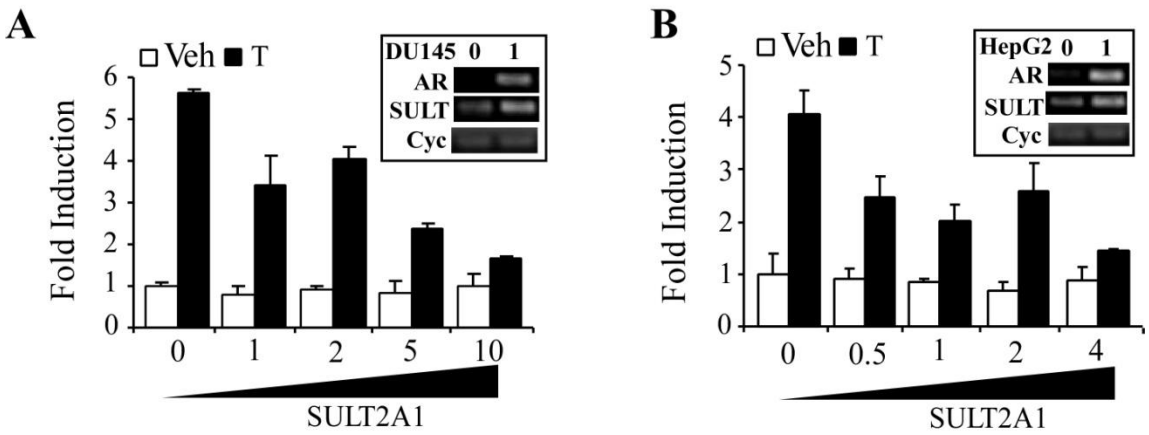

Figure 33 Overexpression of SULT2A1 was sufficient to deactivate androgens. **(A and B)** Ectopic expression of SULT2A1 in DU145 (A) or HepG2 (B) cells was sufficient to abolish the activity of the exogenously added T. Cells were transfected with AR, PSA-Luc and increasing concentrations of SULT2A1. The SULT2A1 to AR plasmid DNA ratios are labeled. Cells were then treated with T (1 nM) for 24 h before luciferase assay. Inserts in A and B show the expression of the endogenous and/or transfected AR and SULT2A1 mRNA was confirmed by RT-PCR. Cyclophillin (Cyc) is included as a loading control. Lane 0 represents control CMX vector-transfected cells, and Lane 1 represents cells transfected with both AR and SULT2A1 at 1:1 ratio.

activities as expected. In a sharp contrast, the activation of both reporter genes was largely abolished in T-Sulf-treated cells. T-Gluc was also ineffective to activate AR (Figure 32). The lack of T-Sulf and T-Gluc effect may also because these two compounds cannot be internalized by cells.

To determine whether activation of SULT2A1 is sufficient to deactivate androgens, DU145 (Figure 33A) and HepG2 (Figure 33B) cells were transfected with AR and PSA-LUC, together with increasing concentrations of expression vector for SULT2A1, before being treated with T for 24 hours. As shown in Figure 33A and 33B, co-transfection of SULT2A1 inhibited T-induced reporter gene activation in a dose-dependent manner in both cell lines.

To determine whether SULT2A1 activity is required for the growth inhibitory effect of LXR agonists, we repeated the experiment to examine the effect of TO1317 on LNCaP cell proliferation in the absence or presence of DHEA, a known SULT2A1-specific enzyme inhibitor (Lee et al., 2003; Rehse et al., 2002). As shown in Figure 34A, the inhibitory effect of TO1317

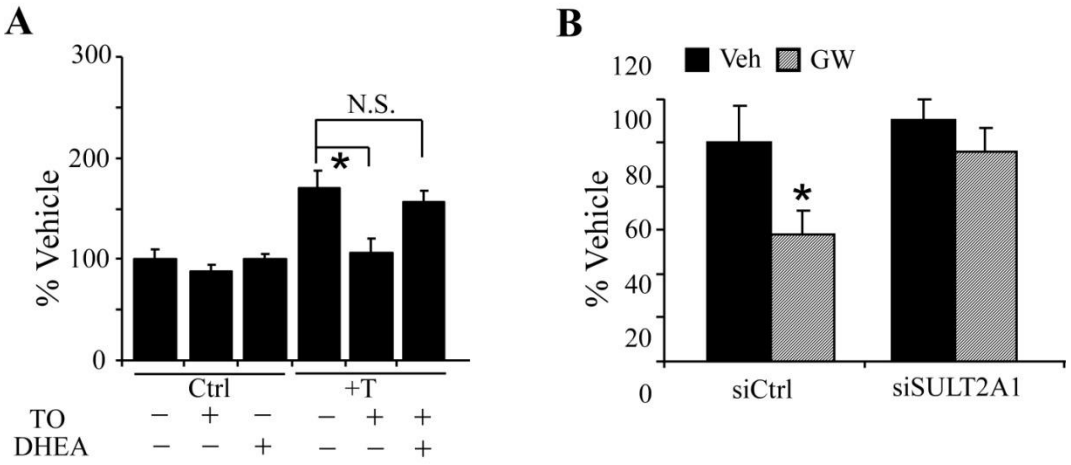

Figure 34 Activation of SULT2A1 was required for the growth inhibitory effect of LXR agonists. **(A)** The growth inhibitory effect of TO1317 on T-induced LNCaP cell proliferation was inhibited in the presence of the SULT2A1 inhibitor DHEA (10 μM). Proliferation was measured by cell countering. **(B)** Knocking-down of SULT2A1 by siRNA abolished the growth inhibitory effect of GW3965 in LNCaP cells.

on T-stimulated cell proliferation was largely abolished, whereas DHEA treatment alone had little effect on the cell growth. Knocking-down the endogenous SULT2A1 in LNCaP cells was also efficient to abolish the growth inhibitory effect of GW3965 (Figure 34B). The efficiency of SULT2A1 knockdown was confirmed by real-time PCR (data not shown).

3.3.5 Effect of LXR activation on androgen synthesis, AR expression, and pituitary hormone

We have measured the expression of androgen synthesizing enzymes in the testis and prostate. We have previous shown that the VP- LXRα transgene is expressed in the testis (Gong et al., 2007), which was confirmed by real-time PCR (Figure 34A). Among testicular androgen synthesizing enzymes, the expression of 3β- and 17β-hydroxysteroid dehydrogenases (3β-Hsd and 17β-Hsd) was modestly but significantly increased in the transgenic mice (Figure 35A). In

the prostate, TO1317 treatment had no significant effect on the expression of either AR or 5α-reductase (Figure 35B).

The synthesis of androgens is also under the influence of pituitary luteinizing hormone (LH). We showed that, in castrated mice that have been treated with TP for 24 hrs, neither GW3965 nor the transgene had significant effect on the serum level of LH (Figure 35C). In intact wild type male mice, treatment with GW3965 modestly but significantly induced the pituitary mRNA expression of Lhβ (Figure 35D). Both LXRα and LXRβ are expressed in the pituitary, but their expression was not affected by GW3965 (Figure 35D).

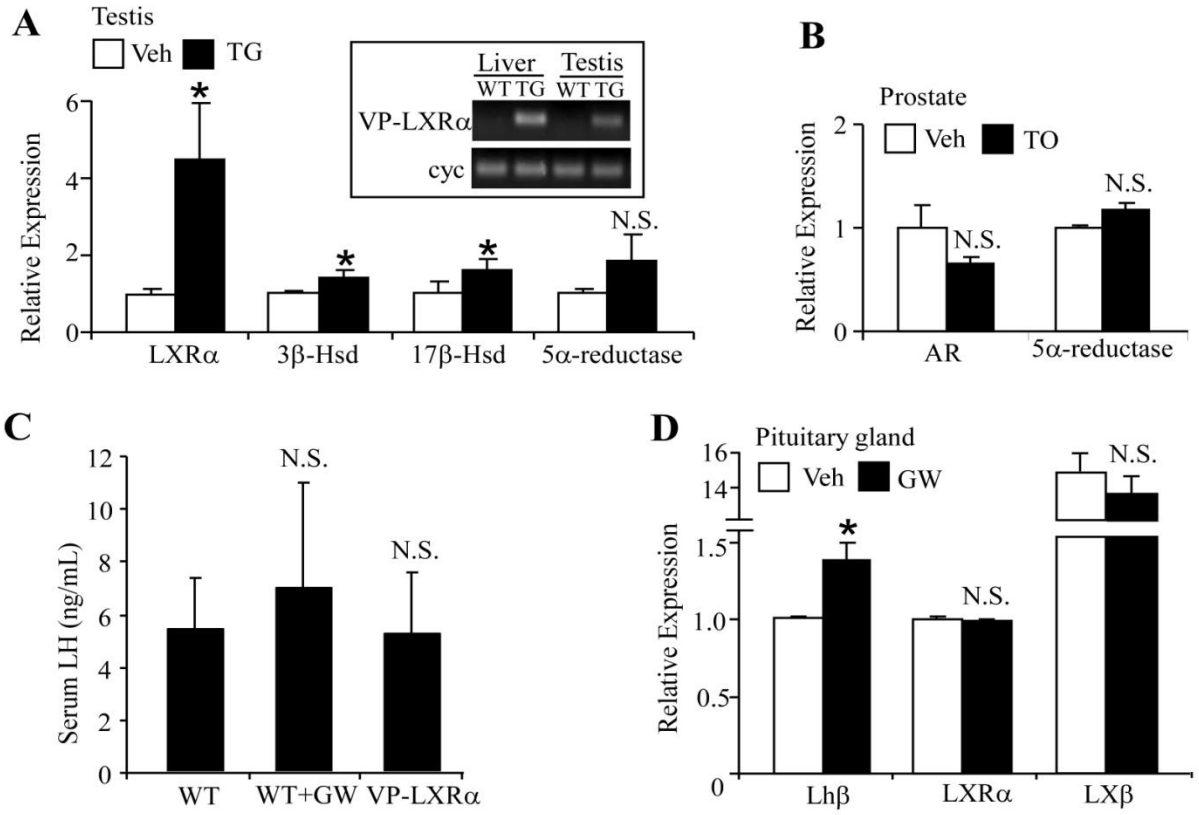

Figure 35 Effect of LXR activation on androgen synthesis, AR expression, and pituitary hormone. **(A)** The VP-LXRα transgene is expressed in the testis and induced the testicular expression of 3β-Hsd and 17β-Hsd. Each group contains 4-5 mice. Insert shows the expressions of VP-LXRα in the liver and testis of VP-LXRα (TG) mice as shown by RT-PCR. Cyclophillin (Cyc) is included as a loading control. **(B)** Prostatic mRNA expression of androgen receptor (AR) and 5α-reductase in WT mice treated with Veh or TO1317. Each group contains three mice. **(C)** Serum LH levels in castrated mice treated with TP for 24 h. The mice are from those described in Figure 25. **(D)** Pituitary expression of Lhβ, LXRα and LXRβ in WT male mice treated with GW3965 for 7 days. Each group contains six mice.

3.4 DISCUSSION

In Chapter II, we revealed a novel LXR-controlled and SULT2A1-mediated pathway of androgen deprivation. Genetic or pharmacological activation of LXR was sufficient to inhibit androgen-responsive prostate regeneration and prostate cancer cell proliferation.

Consistent with the notion that androgens play an important role in the initiation and progression of prostate cancer, androgen ablation has been an effective therapy for hormone-dependent prostate cancers. Strategies to lower testosterone level in prostate cancer patients include orchiectomy and the use of luteinizing hormone-releasing hormone (LHRH) agonists or antagonists. Orchiectomy is invasive and non-reversible. LHRH agonist therapy is widely used as a medical and reversible castration. Another strategy to inhibit androgenic effect is to use the anti-androgens. A clinical concern for the use of LHRH agonists and anti-androgens is the potential effect of these agents on the hypothalamic-pituitary-testicular axis after the cessation of the therapy. In several studies, the serum testosterone levels rose gradually upon long-term LHRH agonist therapy (Kinouchi et al., 2002; Morote et al., 2006). It was also reported that anti-androgens may eventually cross the blood-brain barrier, which will promote the release of LH into the circulation, leading to a subsequent increase in serum testosterone level (Denmeade and Isaacs, 2002). Therefore, it is necessary to continue to develop novel and effective androgen deprivation therapies for prostate cancer with fewer side effects. Here we show that activation of LXR is sufficient to inhibit androgenic activity both in vivo and in cultured prostate cancer cells. The inhibition of prostate regeneration in LXR-activated mice was in agreement with the marked drop in serum testosterone levels in these animals. The activation of SULT2A1, a known LXR target gene, is required for the androgen deprivation effect of LXR agonists. We propose that the LXR-SULT2A1 pathway represents a novel mechanism of androgen deprivation.

The expression of SULT2A1 is known to subject to androgen regulation. It has been shown that activation of AR suppressed SULT2A1 expression, and the level of SULT2A1 expression is lower in androgen- dependent prostate cancer cells (Chan et al., 1998). These results suggest that decreased expression of SULT2A1 may contribute to unchecked androgen stimulation and cancerous transformation. It is also conceivable that re-activation of SULT2A1 may represent a novel therapeutic strategy to inhibit androgen-dependent prostate cancer growth. Indeed, we showed that treatment with LXR agonists inhibited androgen-dependent prostate cancer cell growth in LXR- and SULT2A1-dependent manner. Interestingly, SULT2A1 regulation exhibits both tissue and species specificity. It appears that Sult2a1/2a9 activation by LXR in mice is liver specific. The mouse prostate has little basal or inducible expression of this Sult isoform, suggesting that the liver-mediated systemic androgen deprivation plays the major role in the prostate regeneration phenotype. In contrast, the human SULT2A1 regulation can be seen in both the liver and prostate cells. We have previously shown that treatment with LXR agonist induced the expression of SULT2A1 in primary cultures of human hepatocytes (Uppal et al., 2007). In the current study, we showed that LNCaP and LAPC4 cells exhibited both basal and inducible expression of SULT2A1 (Figure 30A and 30B).

Interestingly, activation of LXR also decreased the expression of STS in the mouse prostate and LNCaP cells (Figure 31D). The prostate is a major peripheral tissue where STS plays an important role in producing biologically active androgens from sufonated metabolites (Reed et al., 2005). Our results suggest that activation of Sult2a1 in the liver and suppression of Sts in the prostate may function in concert to ensure the LXR-mediated androgen deprivation.

Other than SULT2A1, other SULT isoforms, including the estrogen sulfotransferase (EST, or SULT1E1), are also capable of sulfonating steroid hormones. We have recently shown

that activation of LXR induced the expression of EST, and thus promoted estrogen deprivation. The expression of EST is required for the LXR effect on estrogens, since the estrogen deprivation phenotype was completely abolished in the EST null mice (Gong et al., 2007). EST is also expressed in the prostate (data not shown and ref (Takase et al., 2007)). We showed that GW3965 was efficient to inhibit prostate regeneration and lower the serum level of testosterone in the EST null mice (data not shown), suggesting that EST is not required for the androgen deprivation effect of LXR. Our results suggested that LXR affects androgen and estrogen metabolism through regulating distinct target genes. Nevertheless, the combined effect of LXR on androgen and estrogen metabolism suggests that LXR may function as a master regulator of steroid hormone homeostasis, an endocrine role distinct to the previously known sterol sensor role of this receptor (Tontonoz and Mangelsdorf, 2003).

Activation of LXR has been implicated in apoptosis. Interestingly, LXR could have an opposite effect on apoptosis depending on the cellular context. It was reported that activation of LXR prevented bacterial-induced macrophage apoptosis by regulating pro-apoptotic and anti-apoptotic regulators and effectors (Joseph et al., 2004; Valledor et al., 2004). In two other independent studies, LXR was found to induce β-cell apoptosis through LXR-mediated lipotoxicity (Choe et al., 2007; Wente et al., 2007). We have recently shown that TO1317 had little effect on apoptosis in the MCF-7 xenograft tumors (Gong et al., 2007). Using cells maintained in complete serum, Fukuchi and colleagues reported that TO1317 inhibited the growth of both androgen-dependent and independent prostate cancer cells and this inhibition was associated with increased expression of the cyclin-dependent kinase inhibitor $p27^{Kip-1}$ (Chuu et al., 2006; Fukuchi et al., 2004). The growth inhibitory effect of LXR agonists on androgen-independent prostate cancer cells, such as DU145 cells, was not observed in our experiments.

Instead, using culture conditions of charcoal/dextran-stripped serum and the addition of exogenous androgens, we showed clearly that the inhibitory effect of LXR agonists on LNCaP cells is androgen-dependent (Figure 27). The inhibitory effect by GW3965 was LXR-dependent. Expression of SULT2A1 was not only induced but also required for GW3965-mediated growth inhibition. Other than SULT2A1, there is a possibility that this growth inhibition may be associated with other pathway, including G1 cell cycle arrest (Fukuchi et al., 2004). We also showed that treatment with GW3965 and TO1317 suppressed the expression of CDK4 protein in LNCaP cells, but not in DU145 cells (Appendix E), consistent with the selective growth inhibition.

In vivo control of circulating androgens is subjected to the effect of the hypothalamic-pituitary-reproductive axis. No significant changes in serum LH were detected despite significant reduction in circulating testosterone levels in GW3965-treated wild type and VP-LXRα transgenic mice. It is possible that the LH secretion is not rapidly suppressed after testosterone treatment in castrated animals (Lindzey et al., 1998). In contrast, a significantly higher mRNA expression of Lhβ was found in the pituitary of GW3965 treated mice, consistent with a previous report that a combined loss of LXRs α and β in mice lowered plasma LH concentration and decreased the expression of androgen synthesizing enzymes (Volle et al., 2007). We can also not exclude the possibility that adrenal androgens may have also contributed the overall homeostasis of circulating androgens.

We recognize that there are several challenges in developing LXR as a therapeutic target for prostate cancer. It is known that intracellular conversion of testosterone to DHT is important for prostatic cell proliferation. Several studies have demonstrated that a high expression of androgen-producing enzymes, such as the 17β-Hsd and 5α-reductase, is correlated with poor

clinical outcome of prostate cancer (Nakamura et al., 2005). It has also been reported that castration decreases plasma concentration of testosterone by more than 90 %, however, androgen levels in prostate cancer tissues decreases by only 50-60 % due to the conversion of adrenal androgens into DHT in prostate cancer cells (Mizokami et al., 2004). Our results showed that LXR activated 17β-Hsd but had little effect on 5α-reductase. The lipogenic effect of LXR is another potential concern. Androgens stimulate lipogenesis by activating lipogenic enzymes (Freeman and Solomon, 2004; Swinnen et al., 2006). SREBP-1c and SREBP-2, key lipogenic transcription factors, are up-regulated in LNCaP xenograft tumors (Hager et al., 2006), suggesting that aberrant regulation of lipid metabolism may play a role in prostate cancer. It remains to be seen whether LXR promotes lipogenesis in the prostate. It has also been reported that some LXR agonists could have partial or gene-specific activity to avoid the unwanted lipogenic side effect (Kaneko et al., 2003; Song and Liao, 2001).

It has been reported that non-hepatic cells, including prostatic cells, can eliminate cholesterol by CYP27-mediated formation of 27-cholesterol and cholestenoic acid (Repa and Mangelsdorf, 1999). 27-hydroxycholesterol is an endogenous LXR ligand (Fu et al., 2001) and the expression of CYP27 decreased during the progression prostate cancer (Chuu et al., 2006). These results suggest that a decreased production of endogenous LXR ligands and attenuation of LXR signaling may contribute to the progression of prostate cancer.

In summary, we have revealed a novel function of LXR in androgen deprivation, which may establish this nuclear receptor as a therapeutic target for hormone-dependent prostate cancer. Our results also suggest that SULT2A1 is likely the LXR target gene responsible for the androgen deprivation effect. We anticipate that development of LXR agonists that have more

specific SULT2A1 activation property may have future clinical potentials to treat hormone-dependent prostate cancer.

CHAPTER IV

4.0 SUMMARY AND PERSPECTIVES

The present studies have revealed the primary contribution of AhR-mediated signaling in fatty acid metabolism and hepatic steatosis as summarized in Figure 36. Despite the rapidly accumulating evidence that exposure to dioxin results in numerous pathophysiological abnormalities, the transcriptional mechanisms of AhR have not been well documented, with exception of a few reports. In our current model, AhR can directly regulate the expression of the fatty acid translocase CD36. It is important to note that AhR-mediated CD36 regulation is liver-specific, further highlighting the unique and previously unnoticed role of CD36 in hepatic steatosis.

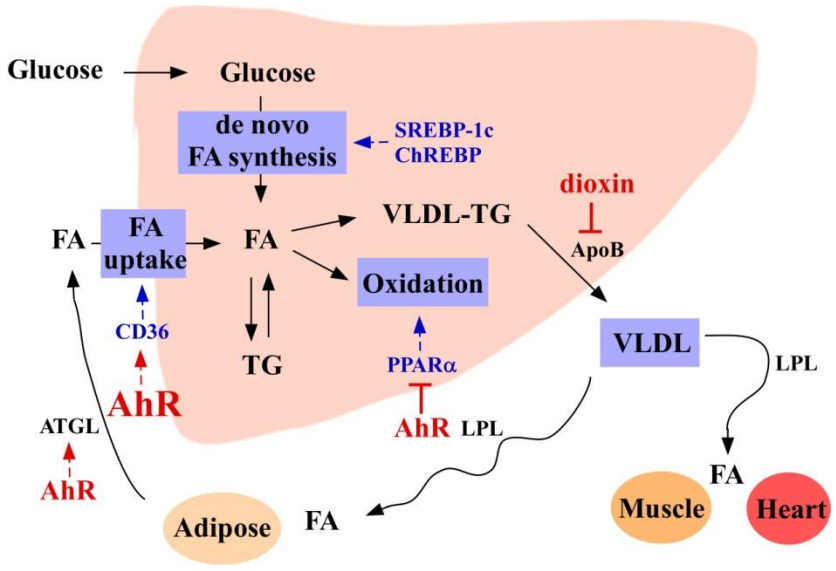

Figure 36 Model for AhR mediated mechanisms of hepatic steatosis

We revealed the LXR-mediated induction of SULT2A1 can contribute to androgen deprivation, which is summarized in Figure 37. LXRs have been explored as a therapeutic target for atherosclerosis, diabetics and Alzheimer's disease in animal models due to their potentials ranging from cholesterol efflux to lipogenesis and anti-inflammation. Our current studies have revealed a novel role of LXRs in regulating androgen metabolism in the liver and prostate.

The effects of AhR and LXRs on lipid and androgen homeostasis have opened debate on whether these regulatory pathways can be explored as therapeutic targets to manage human diseases. The ligand-dependent AhR and LXR are attractive targets for drug discovery, since their activities can be regulated by small lipophilic molecules. Moreover, in many cases, the receptor agonistic and antagonistic property of small molecules can be chemically defined and modified. It is tempting to speculate that inhibition of AhR and selective activation of LXR to induce SULT2A1 may represent novel strategies to prevent or relieve fatty liver disease and prostate cancer, respectively.

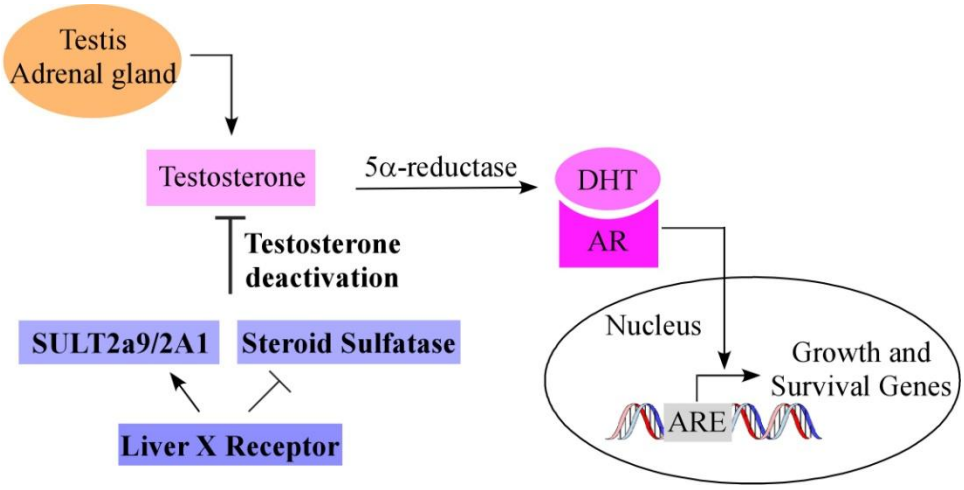

Figure 37 Model for LXR-mediated mechanisms of androgen deprivation

APPENDIX A

SEQUENCES OF REAL-TIME PCR PRIMERS

Gene	Primer Sequences	
	Forward	Reverse
Cd36	GGAACTGTGGGCTCATTGC	CATGAGAATGCCTCCAAACAC
Cyp1a1	GTGCATCGGAGAGACCATTG	GGTAGGAGTCATATCCACCTT
Cyp1a2	GCAGTGGAAAGACCCCTTTG	CCTTCTCGCTCTGGGTCTTG
Fatp1	CCGTATCCTCACGCATGTGT	CTCCATCGTGTCCTCATTGAC
Fatp2	CAACACACCGCAGAAACCA	ATTTCCCAGGGCTTTTTTCA
Fatp3	GGAGACACCTTCAGGTGGAA	GGCACCGTGACTCCATAGAT
Fatp4	CATGAGGAGAGTGTGGCTCA	GGCTAAGGGCTTATCCCAAG
Fatp5	TCGGATCTGGGAATTCTACG	AAGCTCAAAGGGAGTCAGCA
LDLR	TTCAGTGCCAATCGACTCAC	TGTGACCTTGTGGAACAGGA
VLDLR	GCGCCATGGACGAGCTG	TTGGCACCTGGGCTGCT
SR-A	GACGCTTCCAGAATTTCAGC	CCAGTGAATTCCCATGTTCC
SR-B	CACTACGCGCAGTATGTGCT	TGAATGGCCTCCTTATCCTG
ApoB100	TGTGGCAAAGGAAACAATGA	AATCCTGCAGATTGGAGTGG
PPARα	TGTCGAATATGTGGGGACAA	AATCTTGCAGCTCCGATCAC
Acox1	GAGCTGCTCACAGTGACTCG	CACGATCATCTTCCCATCCT
Cyp4a10	CCACAATGTGCATCAAGGAG	TTGGGTAAAGAGCGTCCATC
Cyp4a14	TTGCCAGAATGGAGGATAGG	CAGGAAATTCCACTGGCTGT
L-Fabp	AAATCGTGCATGAAGGGAAG	GTCTCCAGTTCGCACTCCTC
CA-AhR	CTGGGGCCATGTCCATGTATC	GTCCTTGGGGTCTTCTACCTTTCTC
cyclophillin	TGGAGAGCACCAAGACAGACA	TGGAGAGCACCAAGACAGACA
CD36	AAATAAACCTCCTTGGCCTGA	GCAACAAACATCACCACACC
CYP1A1	CTTCCGACACTCTTCCTTCG	GGTTGATCTGCCACTGGTTT
CYP3A4	TTGCCCAGTATGGAGATGTG	AGGGGTCTTGTGGATTGTTG
AHR	TAGTGGAGCCACAGCAACAG	TGCTGTGGACAATTGAAAGG
Cyclophillin	TTTCATCTGCACTGCCAAGA	TTGCCAAACACCACATGCT

APPENDIX B

MICROARRAY ANALYSIS ON THE LIVER OF CA-AHR TRANSGENIC MICE

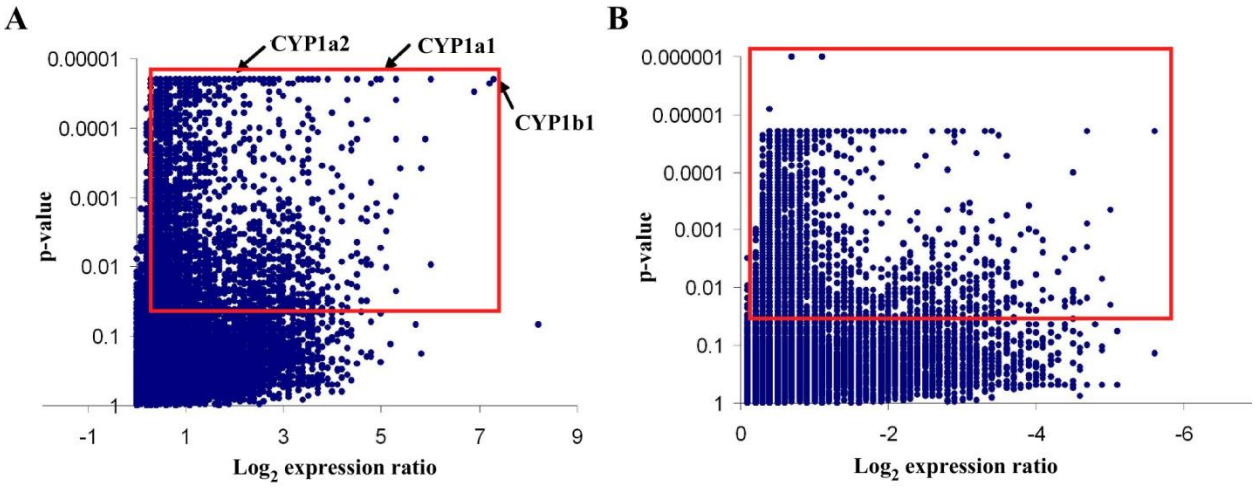

In livers of CA-AhR mice, 1292 genes are upregulated (A), and 1093 genes are downregulated (B). Positive controls including, induction of CYP1a1, 1a2 and 1b1, are shown in (A). $p<0.05$ was considered statistically significant (red rectangle).

B.1 PARTIAL LIST OF GENES FROM MICROARRAY ANALYSIS

CA-AhR vs WT, Liver

Gene	Functional Category	Fold Induction
Cytochrome P450, 1b1	Drug Metabolism	157.6
Cytochrome P450, 1a1		32
Cytochrome P450, 1a2		4.3
Cytochrome P450, 2d9		11.3
Glutathione S-transferase, alpha2 (Gsta2)		3.2
Glutathione S-transferase, mu2 (Gstm2)		3.0
Glutathione S-transferase, mu3 (Gstm3)		2.6
Glutathione S-transferase, pi 2 (Gstp2)		2.8
Sulfotransferase, estrogen preferring (Ste)		7.0
ATP-binding cassette, sub-family C, member9 (Abcc9)		2.5
Organic anion transpoter 6-S (mOAT6-S)		2.6
Lipoprotein Lipase (Lpl)	Fat Synthesis and Uptake	7.5
Stearoyl-Coenzyme A desaturase 2 (Scd2)		2.3
CD36 antigen (Cd36)		1.7
Fatty acid binding protein 5 (Fabp5)		1.6
Peroxisome proliferator-activated receptor alpha (Pparα)	Fat Oxidation	0.6
Acyl CoA oxidase 1 (Acox1)		0.6
Thiolase		0.5
Cytochrome P450, 4a10		0.4
Cytochrome P450, 4a14		0.1
Acyl CoA dehydrogenase, long-chain (Lcad)		0.7
Fatty acid binding protein 1 (L-Fabp)		0.7
Glucose-6-phosphatase, catalytic (G6pc)	Glucose Metabolism	1.6
Pyruvate kinase 3 (Pk3)		2.1
Insulin-like growth factor binding protein1 (Igfbp1)		2.8
Pyruvate kinase liver and red blood cell (Pklr)		0.6
Pyruvate carboxylase		0.7
Glucose-6-phosphatase, transport protein1 (G6pt1)		0.8

Table 1. Microarray analysis on the liver of CA-AhR transgenic mice

APPENDIX C

MICROARRAY ANALYSIS OF THE INTESTINE OF CA-AHR TRANSGENIC MICE

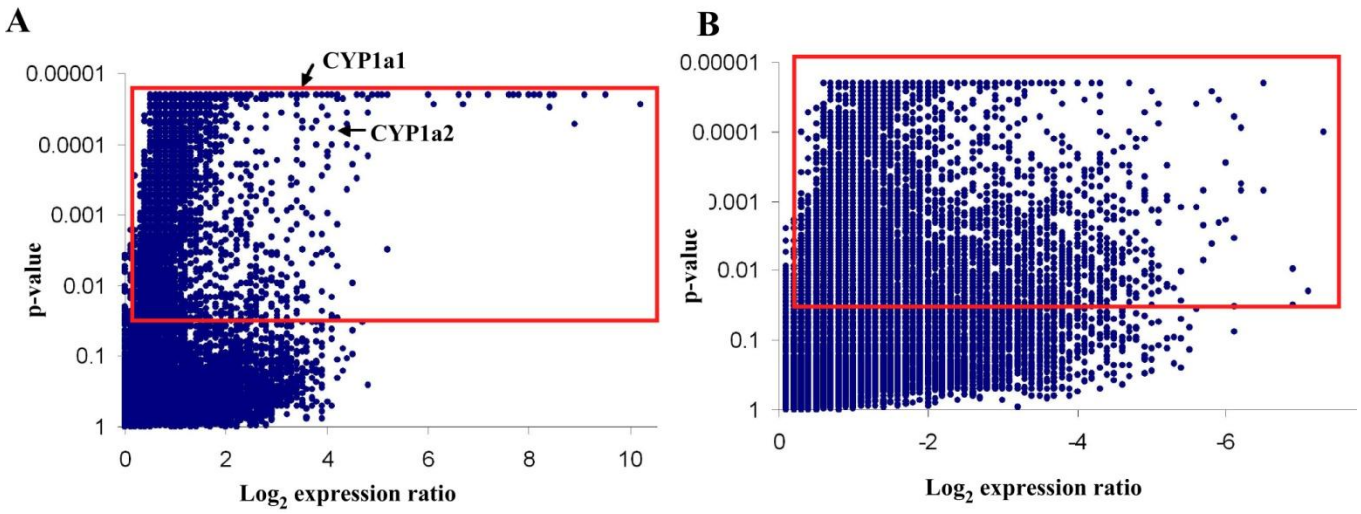

In intestines of CA-AhR mice, 2253 genes are upregulated (A), and 2203 genes are downregulated (B). Positive controls, including induction of CYP1a1 and 1a2, are shown in (A). $p<0.05$ was considered statistically significant (red rectangle).

C.1 PARTIAL LIST OF GENES IN MICROARRAY ANALYSIS

CA-AhR vs WT, Duodenum

Gene	Functional Category	Fold Induction
Cytochrome P450, 1a1	Drug Metabolism	11.3
Cytochrome P450, 1a2		17.1
Cytochrome P450, 2b10		2.8
Cytochrome P450, 3a13		4.3
Cytochrome P450, 4b1		2.1
ATP-binding cassette, sub-family B (MDRTAP), member2		2.0
ATP-binding cassette, sub-family D (ALD), member1		1.6
Stearoyl-Coenzyme A desaturase 2 (Scd2)	Fat Synthesis	3.5
Fatty acid synthase (Fas)		3.0
Fatty acid binding protein 5 (Fabp5)		3.5
Pancreatic lipase related protein 1 (Pnliprp1)	Fat Digestion and Absorption	32.0
Pancreatic lipase-related protein 2 (Pnliprp2)		11.3
Carboxyl ester lipase		11.3
Phospholipase A2, group 1B, pancreas		21.1
Diacylglycerol acyltransferase		1.9

Table 2 Microarray analysis on the intestine of CA-AhR transgenic mice

APPENDIX D

SEQUENCES OF REAL-TIME PCR PRIMERS

Gene	Primer Sequences	
	Forward	Reverse
AR (mouse)	CAGTGGATGGGCTGAAAAAT	CTTGAGCAGGATGTGGGATT
3β-Hsd	GCTTCCTGCTACGTCCAGTC	CCAGATCTCGCTGAGCTTTC
17β-Hsd	GTTATGAGCAAGCCCTGAGC	AAGCGGTTCGTGGAGAAGTA
5α-reductase	ACCTTTGTCTTGGCCTTCCT	GGGTTACCCAGTCTTCAGCA
Sult2a9	CTGGCTGTCCATGAGAGAAT	GGCTTGGAAAGAGCTGTACT
Lxrα	AGGAGTGTCGACTTCGCAAA	CTCTTCTTGCCGCTTCAGTTT
Lxrβ	AAGCAGGTGCCAGGGTTCT	TGCATTCTGTCTCGTGGTTGT
Lhβ	ATCACCTTCACCACCAGCAT	GTAGGTGCACACTGGCTGAG
Sts	AGCACGAGTTCCTGTTCCAC	GTTGGGCGTGAAGTAGAAGG
Sult2b1	TGCTGGGCAATTAAAGGACC	AGCCCTTGATGTGGTCAAAC
Sult2b1b	CTGTGGAGCTCGTCTGAGAA	GTGAGTACATGCCGACAGGA
VP-LXRα	GGCCGACTTCGAGTTTGAGC	GCAGAATCAGGAGAAACATC
cyclophillin	TGGAGAGCACCAAGACAGACA	TGCCGGAGTCGACAATGAT
AR (human)	GAATTCCTGTGCATGAAAGCA	CGAAGTTGATGAAAGAATTTTTGATT
LXRα	CCCTTCAGAACCCACAGAGAT	GCTCCTTCCCCAGCATTTT
LXRβ	CGCTAAGCAAGTGCCTGGTT	GCCTGGCTGTCTCTAGCAGC
SULT2A1	GGTGTATCTGGGGACTGGAA	GGAACAGCTCTCGAGGAAGA
SULT2B1	GGAGCTGCAGCAGGACTTAC	GCGTGTAGTTGGACATGGTG
PSA	CATCAGGAACAAAAGCGTGA	ATATCGTAGAGCGGGTGTGG
Cyclophillin	TTTCATCTGCACTGCCAAGA	TTGCCAAACACCACATGCT

APPENDIX E

EFFECT OF LXR ON CELL CYCLE

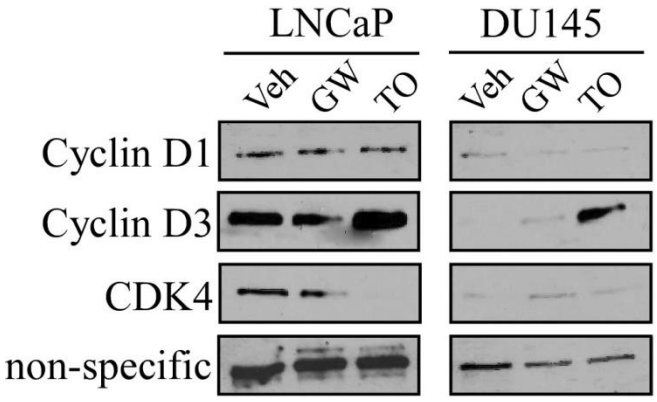

LXR ligands, when applied at 10 μM concentration, suppressed the expression of CDK4 in the androgen-dependent LNCaP cells. Cell extracts were subjected to Western blot analysis using indicated antibodies purchased from Santa Cruz Biotechnology INC. Cells were maintained in medium supplemented with 10% FBS during the 3-day treatment period.

BIBLIOGRAPHY

Adachi, J., Mori, Y., Matsui, S., Takigami, H., Fujino, J., Kitagawa, H., Miller, C.A., 3rd, Kato, T., Saeki, K., and Matsuda, T. (2001). Indirubin and indigo are potent aryl hydrocarbon receptor ligands present in human urine. J Biol Chem *276*, 31475-31478.

Alberti, S., Schuster, G., Parini, P., Feltkamp, D., Diczfalusy, U., Rudling, M., Angelin, B., Bjorkhem, I., Pettersson, S., and Gustafsson, J.A. (2001). Hepatic cholesterol metabolism and resistance to dietary cholesterol in LXRbeta-deficient mice. J Clin Invest *107*, 565-573.

AmericanCancerSociety (2006). Cancer Facts and Figures.

Andersson, P., McGuire, J., Rubio, C., Gradin, K., Whitelaw, M.L., Pettersson, S., Hanberg, A., and Poellinger, L. (2002). A constitutively active dioxin/aryl hydrocarbon receptor induces stomach tumors. Proc Natl Acad Sci U S A *99*, 9990-9995.

Andersson, P., Ridderstad, A., McGuire, J., Pettersson, S., Poellinger, L., and Hanberg, A. (2003). A constitutively active aryl hydrocarbon receptor causes loss of peritoneal B1 cells. Biochem Biophys Res Commun *302*, 336-341.

Barish, G.D., and Evans, R.M. (2004). PPARs and LXRs: atherosclerosis goes nuclear. Trends Endocrinol Metab *15*, 158-165.

Boverhof, D.R., Burgoon, L.D., Tashiro, C., Sharratt, B., Chittim, B., Harkema, J.R., Mendrick, D.L., and Zacharewski, T.R. (2006). Comparative toxicogenomic analysis of the hepatotoxic effects of TCDD in Sprague Dawley rats and C57BL/6 mice. Toxicol Sci *94*, 398-416.

Bradbury, M.W. (2006). Lipid metabolism and liver inflammation. I. Hepatic fatty acid uptake: possible role in steatosis. Am J Physiol Gastrointest Liver Physiol *290*, G194-198.

Carlson, D.B., and Perdew, G.H. (2002). A dynamic role for the Ah receptor in cell signaling? Insights from a diverse group of Ah receptor interacting proteins. J Biochem Mol Toxicol *16*, 317-325.

Casper, R.F., Quesne, M., Rogers, I.M., Shirota, T., Jolivet, A., Milgrom, E., and Savouret, J.F. (1999). Resveratrol has antagonist activity on the aryl hydrocarbon receptor: implications for prevention of dioxin toxicity. Mol Pharmacol *56*, 784-790.

Cha, J.Y., and Repa, J.J. (2007). The liver X receptor (LXR) and hepatic lipogenesis. The carbohydrate-response element-binding protein is a target gene of LXR. J Biol Chem *282*, 743-751.

Chan, J., Song, C.S., Matusik, R.J., Chatterjee, B., and Roy, A.K. (1998). Inhibition of androgen action by dehydroepiandrosterone sulfotransferase transfected in PC-3 prostate cancer cells. Chem Biol Interact *109*, 267-278.

Chatterjee, B. (2003). The role of the androgen receptor in the development of prostatic hyperplasia and prostate cancer. Mol Cell Biochem *253*, 89-101.

Chatterjee, B., Song, C.S., Jung, M.H., Chen, S., Walter, C.A., Herbert, D.C., Weaker, F.J., Mancini, M.A., and Roy, A.K. (1996). Targeted overexpression of androgen receptor with a liver-specific promoter in transgenic mice. Proc Natl Acad Sci U S A *93*, 728-733.

Chawla, A., Repa, J.J., Evans, R.M., and Mangelsdorf, D.J. (2001). Nuclear receptors and lipid physiology: opening the X-files. Science *294*, 1866-1870.

Chiaro, C.R., Morales, J.L., Prabhu, K.S., and Perdew, G.H. (2008). Leukotriene A4 metabolites are endogenous ligands for the Ah receptor. Biochemistry *47*, 8445-8455.

Choe, S.S., Choi, A.H., Lee, J.W., Kim, K.H., Chung, J.J., Park, J., Lee, K.M., Park, K.G., Lee, I.K., and Kim, J.B. (2007). Chronic activation of liver X receptor induces beta-cell apoptosis through hyperactivation of lipogenesis: liver X receptor-mediated lipotoxicity in pancreatic beta-cells. Diabetes *56*, 1534-1543.

Chu, K., Miyazaki, M., Man, W.C., and Ntambi, J.M. (2006). Stearoyl-coenzyme A desaturase 1 deficiency protects against hypertriglyceridemia and increases plasma high-density lipoprotein cholesterol induced by liver X receptor activation. Mol Cell Biol *26*, 6786-6798.

Chuu, C.P., Hiipakka, R.A., Kokontis, J.M., Fukuchi, J., Chen, R.Y., and Liao, S. (2006). Inhibition of tumor growth and progression of LNCaP prostate cancer cells in athymic mice by androgen and liver X receptor agonist. Cancer Res *66*, 6482-6486.

Collins, J.L., Fivush, A.M., Watson, M.A., Galardi, C.M., Lewis, M.C., Moore, L.B., Parks, D.J., Wilson, J.G., Tippin, T.K., Binz, J.G., *et al.* (2002). Identification of a nonsteroidal liver X receptor agonist through parallel array synthesis of tertiary amines. J Med Chem *45*, 1963-1966.

Collot-Teixeira, S., Martin, J., McDermott-Roe, C., Poston, R., and McGregor, J.L. (2007). CD36 and macrophages in atherosclerosis. Cardiovasc Res *75*, 468-477.

Denison, M.S., and Nagy, S.R. (2003). Activation of the aryl hydrocarbon receptor by structurally diverse exogenous and endogenous chemicals. Annu Rev Pharmacol Toxicol *43*, 309-334.

Denmeade, S.R., and Isaacs, J.T. (2002). A history of prostate cancer treatment. Nat Rev Cancer *2*, 389-396.

Dertinger, S.D., Nazarenko, D.A., Silverstone, A.E., and Gasiewicz, T.A. (2001). Aryl hydrocarbon receptor signaling plays a significant role in mediating benzo[a]pyrene- and cigarette smoke condensate-induced cytogenetic damage in vivo. Carcinogenesis *22*, 171-177.

English, H.F., Santen, R.J., and Isaacs, J.T. (1987). Response of glandular versus basal rat ventral prostatic epithelial cells to androgen withdrawal and replacement. Prostate *11*, 229-242.

Farese, R.V., Jr., Ruland, S.L., Flynn, L.M., Stokowski, R.P., and Young, S.G. (1995). Knockout of the mouse apolipoprotein B gene results in embryonic lethality in homozygotes and protection against diet-induced hypercholesterolemia in heterozygotes. Proc Natl Acad Sci U S A *92*, 1774-1778.

Febbraio, M., Abumrad, N.A., Hajjar, D.P., Sharma, K., Cheng, W., Pearce, S.F., and Silverstein, R.L. (1999). A null mutation in murine CD36 reveals an important role in fatty acid and lipoprotein metabolism. J Biol Chem *274*, 19055-19062.

Febbraio, M., and Silverstein, R.L. (2007). CD36: implications in cardiovascular disease. Int J Biochem Cell Biol *39*, 2012-2030.

Fernandez-Salguero, P., Pineau, T., Hilbert, D.M., McPhail, T., Lee, S.S., Kimura, S., Nebert, D.W., Rudikoff, S., Ward, J.M., and Gonzalez, F.J. (1995). Immune system impairment and hepatic fibrosis in mice lacking the dioxin-binding Ah receptor. Science *268*, 722-726.

Fisher, E.A., and Ginsberg, H.N. (2002). Complexity in the secretory pathway: the assembly and secretion of apolipoprotein B-containing lipoproteins. J Biol Chem *277*, 17377-17380.

Freeman, M.R., and Solomon, K.R. (2004). Cholesterol and prostate cancer. J Cell Biochem *91*, 54-69.

Fu, X., Menke, J.G., Chen, Y., Zhou, G., MacNaul, K.L., Wright, S.D., Sparrow, C.P., and Lund, E.G. (2001). 27-hydroxycholesterol is an endogenous ligand for liver X receptor in cholesterol-loaded cells. J Biol Chem *276*, 38378-38387.

Fukuchi, J., Kokontis, J.M., Hiipakka, R.A., Chuu, C.P., and Liao, S. (2004). Antiproliferative effect of liver X receptor agonists on LNCaP human prostate cancer cells. Cancer Res *64*, 7686-7689.

Geese, W.J., and Raftogianis, R.B. (2001). Biochemical characterization and tissue distribution of human SULT2B1. Biochem Biophys Res Commun *288*, 280-289.

Glass, C.K., and Ogawa, S. (2006). Combinatorial roles of nuclear receptors in inflammation and immunity. Nat Rev Immunol *6*, 44-55.

Glatt, H., Boeing, H., Engelke, C.E., Ma, L., Kuhlow, A., Pabel, U., Pomplun, D., Teubner, W., and Meinl, W. (2001). Human cytosolic sulphotransferases: genetics, characteristics, toxicological aspects. Mutat Res *482*, 27-40.

Goldberg, I.J., and Ginsberg, H.N. (2006). Ins and outs modulating hepatic triglyceride and development of nonalcoholic fatty liver disease. Gastroenterology *130*, 1343-1346.

Gong, H., Guo, P., Zhai, Y., Zhou, J., Uppal, H., Jarzynka, M.J., Song, W.C., Cheng, S.Y., and Xie, W. (2007). Estrogen deprivation and inhibition of breast cancer growth in vivo through activation of the orphan nuclear receptor liver X receptor. Mol Endocrinol *21*, 1781-1790.

Green, R.M. (2003). NASH--hepatic metabolism and not simply the metabolic syndrome. Hepatology *38*, 14-17.

Gronemeyer, H., Gustafsson, J.A., and Laudet, V. (2004). Principles for modulation of the nuclear receptor superfamily. Nat Rev Drug Discov *3*, 950-964.

Gu, Y.Z., Hogenesch, J.B., and Bradfield, C.A. (2000). The PAS superfamily: sensors of environmental and developmental signals. Annu Rev Pharmacol Toxicol *40*, 519-561.

Hager, M.H., Solomon, K.R., and Freeman, M.R. (2006). The role of cholesterol in prostate cancer. Curr Opin Clin Nutr Metab Care *9*, 379-385.

Han, J.Y., Choo, K.H., and Shaffer, L.G. (1994). Molecular cytogenetic characterization of 17 rob(13q14q) Robertsonian translocations by FISH, narrowing the region containing the breakpoints. Am J Hum Genet *55*, 960-967.

Hashimoto, T., Fujita, T., Usuda, N., Cook, W., Qi, C., Peters, J.M., Gonzalez, F.J., Yeldandi, A.V., Rao, M.S., and Reddy, J.K. (1999). Peroxisomal and mitochondrial fatty acid beta-oxidation in mice nullizygous for both peroxisome proliferator-activated receptor alpha and peroxisomal fatty acyl-CoA oxidase. Genotype correlation with fatty liver phenotype. J Biol Chem *274*, 19228-19236.

Heinlein, C.A., and Chang, C. (2004). Androgen receptor in prostate cancer. Endocr Rev *25*, 276-308.

Hoffman, E.C., Reyes, H., Chu, F.F., Sander, F., Conley, L.H., Brooks, B.A., and Hankinson, O. (1991). Cloning of a factor required for activity of the Ah (dioxin) receptor. Science *252*, 954-958.

Horton, J.D., Goldstein, J.L., and Brown, M.S. (2002). SREBPs: activators of the complete program of cholesterol and fatty acid synthesis in the liver. J Clin Invest *109*, 1125-1131.

Hubbard, B., Doege, H., Punreddy, S., Wu, H., Huang, X., Kaushik, V.K., Mozell, R.L., Byrnes, J.J., Stricker-Krongrad, A., Chou, C.J., *et al.* (2006). Mice deleted for fatty acid transport protein 5 have defective bile acid conjugation and are protected from obesity. Gastroenterology *130*, 1259-1269.

Inoue, M., Ohtake, T., Motomura, W., Takahashi, N., Hosoki, Y., Miyoshi, S., Suzuki, Y., Saito, H., Kohgo, Y., and Okumura, T. (2005). Increased expression of PPARgamma in high fat diet-induced liver steatosis in mice. Biochem Biophys Res Commun *336*, 215-222.

Ito, M., Suzuki, J., Tsujioka, S., Sasaki, M., Gomori, A., Shirakura, T., Hirose, H., Ito, M., Ishihara, A., Iwaasa, H., *et al.* (2007). Longitudinal analysis of murine steatohepatitis model induced by chronic exposure to high-fat diet. Hepatol Res *37*, 50-57.

Jiang, Y.J., Kim, P., Elias, P.M., and Feingold, K.R. (2005). LXR and PPAR activators stimulate cholesterol sulfotransferase type 2 isoform 1b in human keratinocytes. J Lipid Res *46*, 2657-2666.

Joseph, S.B., Bradley, M.N., Castrillo, A., Bruhn, K.W., Mak, P.A., Pei, L., Hogenesch, J., O'Connell R, M., Cheng, G., Saez, E., *et al.* (2004). LXR-dependent gene expression is important for macrophage survival and the innate immune response. Cell *119*, 299-309.

Joseph, S.B., Castrillo, A., Laffitte, B.A., Mangelsdorf, D.J., and Tontonoz, P. (2003). Reciprocal regulation of inflammation and lipid metabolism by liver X receptors. Nat Med *9*, 213-219.

Joseph, S.B., Laffitte, B.A., Patel, P.H., Watson, M.A., Matsukuma, K.E., Walczak, R., Collins, J.L., Osborne, T.F., and Tontonoz, P. (2002). Direct and indirect mechanisms for regulation of fatty acid synthase gene expression by liver X receptors. J Biol Chem *277*, 11019-11025.

Kaneko, E., Matsuda, M., Yamada, Y., Tachibana, Y., Shimomura, I., and Makishima, M. (2003). Induction of intestinal ATP-binding cassette transporters by a phytosterol-derived liver X receptor agonist. J Biol Chem *278*, 36091-36098.

Karhadkar, S.S., Bova, G.S., Abdallah, N., Dhara, S., Gardner, D., Maitra, A., Isaacs, J.T., Berman, D.M., and Beachy, P.A. (2004). Hedgehog signalling in prostate regeneration, neoplasia and metastasis. Nature *431*, 707-712.

Kinouchi, T., Maeda, O., Ono, Y., Meguro, N., Kuroda, M., and Usami, M. (2002). Failure to maintain the suppressed level of serum testosterone during luteinizing hormone-releasing hormone agonist therapy in a patient with prostate cancer. Int J Urol *9*, 359-361.

Koonen, D.P., Jacobs, R.L., Febbraio, M., Young, M.E., Soltys, C.L., Ong, H., Vance, D.E., and Dyck, J.R. (2007). Increased hepatic CD36 expression contributes to dyslipidemia associated with diet-induced obesity. Diabetes *56*, 2863-2871.

Kotronen, A., and Yki-Jarvinen, H. (2008). Fatty liver: a novel component of the metabolic syndrome. Arterioscler Thromb Vasc Biol *28*, 27-38.

Kroetz, D.L., Yook, P., Costet, P., Bianchi, P., and Pineau, T. (1998). Peroxisome proliferator-activated receptor alpha controls the hepatic CYP4A induction adaptive response to starvation and diabetes. J Biol Chem *273*, 31581-31589.

Laffitte, B.A., Joseph, S.B., Walczak, R., Pei, L., Wilpitz, D.C., Collins, J.L., and Tontonoz, P. (2001). Autoregulation of the human liver X receptor alpha promoter. Mol Cell Biol *21*, 7558-7568.

Lahvis, G.P., Lindell, S.L., Thomas, R.S., McCuskey, R.S., Murphy, C., Glover, E., Bentz, M., Southard, J., and Bradfield, C.A. (2000). Portosystemic shunting and persistent fetal vascular structures in aryl hydrocarbon receptor-deficient mice. Proc Natl Acad Sci U S A *97*, 10442-10447.

Lazarow, P.B., and De Duve, C. (1976). A fatty acyl-CoA oxidizing system in rat liver peroxisomes; enhancement by clofibrate, a hypolipidemic drug. Proc Natl Acad Sci U S A *73*, 2043-2046.

Lee, C.C., Yao, Y.J., Chen, H.L., Guo, Y.L., and Su, H.J. (2006). Fatty liver and hepatic function for residents with markedly high serum PCDD/Fs levels in Taiwan. J Toxicol Environ Health A *69*, 367-380.

Lee, J.H., Gong, H., Khadem, S., Lu, Y., Gao, X., Li, S., Zhang, J., and Xie, W. (2008a). Androgen deprivation by activating the liver x receptor. Endocrinology *149*, 3778-3788.

Lee, J.H., Zhou, J., and Xie, W. (2008b). PXR and LXR in hepatic steatosis: a new dog and an old dog with new tricks. Mol Pharm *5*, 60-66.

Lee, K.A., Fuda, H., Lee, Y.C., Negishi, M., Strott, C.A., and Pedersen, L.C. (2003). Crystal structure of human cholesterol sulfotransferase (SULT2B1b) in the presence of pregnenolone and 3'-phosphoadenosine 5'-phosphate. Rationale for specificity differences between prototypical SULT2A1 and the SULT2B1 isoforms. J Biol Chem *278*, 44593-44599.

Lindzey, J., Wetsel, W.C., Couse, J.F., Stoker, T., Cooper, R., and Korach, K.S. (1998). Effects of castration and chronic steroid treatments on hypothalamic gonadotropin-releasing hormone content and pituitary gonadotropins in male wild-type and estrogen receptor-alpha knockout mice. Endocrinology *139*, 4092-4101.

Long, R.M., Morrissey, C., Fitzpatrick, J.M., and Watson, R.W. (2005). Prostate epithelial cell differentiation and its relevance to the understanding of prostate cancer therapies. Clin Sci (Lond) *108*, 1-11.

Louie, M.C., Yang, H.Q., Ma, A.H., Xu, W., Zou, J.X., Kung, H.J., and Chen, H.W. (2003). Androgen-induced recruitment of RNA polymerase II to a nuclear receptor-p160 coactivator complex. Proc Natl Acad Sci U S A *100*, 2226-2230.

Lu, Y.F., Santostefano, M., Cunningham, B.D., Threadgill, M.D., and Safe, S. (1995). Identification of 3'-methoxy-4'-nitroflavone as a pure aryl hydrocarbon (Ah) receptor antagonist and evidence for more than one form of the nuclear Ah receptor in MCF-7 human breast cancer cells. Arch Biochem Biophys *316*, 470-477.

McCormick, S.P., Ng, J.K., Veniant, M., Boren, J., Pierotti, V., Flynn, L.M., Grass, D.S., ConnollyA, and Young, S.G. (1996). Transgenic mice that overexpress mouse apolipoprotein B. Evidence that the DNA sequences controlling intestinal expression of the apolipoprotein B gene are distant from the structural gene. J Biol Chem *271*, 11963-11970.

McGuire, J., Okamoto, K., Whitelaw, M.L., Tanaka, H., and Poellinger, L. (2001). Definition of a dioxin receptor mutant that is a constitutive activator of transcription: delineation of overlapping repression and ligand binding functions within the PAS domain. J Biol Chem *276*, 41841-41849.

McKenna, N.J., and O'Malley, B.W. (2002). Combinatorial control of gene expression by nuclear receptors and coregulators. Cell *108*, 465-474.

McMillan, B.J., and Bradfield, C.A. (2007). The aryl hydrocarbon receptor is activated by modified low-density lipoprotein. Proc Natl Acad Sci U S A *104*, 1412-1417.

Meloche, C.A., Sharma, V., Swedmark, S., Andersson, P., and Falany, C.N. (2002). Sulfation of budesonide by human cytosolic sulfotransferase, dehydroepiandrosterone-sulfotransferase (DHEA-ST). Drug Metab Dispos *30*, 582-585.

Memon, R.A., Fuller, J., Moser, A.H., Smith, P.J., Grunfeld, C., and Feingold, K.R. (1999). Regulation of putative fatty acid transporters and Acyl-CoA synthetase in liver and adipose tissue in ob/ob mice. Diabetes *48*, 121-127.

Merkel, M., Weinstock, P.H., Chajek-Shaul, T., Radner, H., Yin, B., Breslow, J.L., and Goldberg, I.J. (1998). Lipoprotein lipase expression exclusively in liver. A mouse model for metabolism in the neonatal period and during cachexia. J Clin Invest *102*, 893-901.

Mizokami, A., Koh, E., Fujita, H., Maeda, Y., Egawa, M., Koshida, K., Honma, S., Keller, E.T., and Namiki, M. (2004). The adrenal androgen androstenediol is present in prostate cancer tissue after androgen deprivation therapy and activates mutated androgen receptor. Cancer Res *64*, 765-771.

Moennikes, O., Loeppen, S., Buchmann, A., Andersson, P., Ittrich, C., Poellinger, L., and Schwarz, M. (2004). A constitutively active dioxin/aryl hydrocarbon receptor promotes hepatocarcinogenesis in mice. Cancer Res *64*, 4707-4710.

Morote, J., Esquena, S., Abascal, J.M., Trilla, E., Cecchini, L., Raventos, C.X., Catalan, R., and Reventos, J. (2006). Failure to maintain a suppressed level of serum testosterone during long-acting depot luteinizing hormone-releasing hormone agonist therapy in patients with advanced prostate cancer. Urol Int *77*, 135-138.

Mukai, M., Dong, Q., Hardy, M.P., Kiyokawa, H., Peterson, R.E., and Cooke, P.S. (2005). Altered prostatic epithelial proliferation and apoptosis, prostatic development, and serum testosterone in mice lacking cyclin-dependent kinase inhibitors. Biol Reprod *73*, 951-958.

Nagata, K., and Yamazoe, Y. (2000). Pharmacogenetics of sulfotransferase. Annu Rev Pharmacol Toxicol *40*, 159-176.

Nakamura, Y., Suzuki, T., Nakabayashi, M., Endoh, M., Sakamoto, K., Mikami, Y., Moriya, T., Ito, A., Takahashi, S., Yamada, S., *et al.* (2005). In situ androgen producing enzymes in human prostate cancer. Endocr Relat Cancer *12*, 101-107.

Newberry, E.P., Xie, Y., Kennedy, S.M., Luo, J., and Davidson, N.O. (2006). Protection against Western diet-induced obesity and hepatic steatosis in liver fatty acid-binding protein knockout mice. Hepatology *44*, 1191-1205.

Nohara, K., Pan, X., Tsukumo, S., Hida, A., Ito, T., Nagai, H., Inouye, K., Motohashi, H., Yamamoto, M., Fujii-Kuriyama, Y., *et al.* (2005). Constitutively active aryl hydrocarbon receptor expressed specifically in T-lineage cells causes thymus involution and suppresses the immunization-induced increase in splenocytes. J Immunol *174*, 2770-2777.

Pascussi, J.M., Gerbal-Chaloin, S., Duret, C., Daujat-Chavanieu, M., Vilarem, M.J., and Maurel, P. (2008). The tangle of nuclear receptors that controls xenobiotic metabolism and transport: crosstalk and consequences. Annu Rev Pharmacol Toxicol *48*, 1-32.

Peet, D.J., Turley, S.D., Ma, W., Janowski, B.A., Lobaccaro, J.M., Hammer, R.E., and Mangelsdorf, D.J. (1998). Cholesterol and bile acid metabolism are impaired in mice lacking the nuclear oxysterol receptor LXR alpha. Cell *93*, 693-704.

Phillips, M., Enan, E., Liu, P.C., and Matsumura, F. (1995). Inhibition of 3T3-L1 adipose differentiation by 2,3,7,8-tetrachlorodibenzo-p-dioxin. J Cell Sci *108 (Pt 1)*, 395-402.

Postic, C., and Girard, J. (2008). Contribution of de novo fatty acid synthesis to hepatic steatosis and insulin resistance: lessons from genetically engineered mice. J Clin Invest *118*, 829-838.

Puppala, D., Lee, H., Kim, K.B., and Swanson, H.I. (2008). Development of an aryl hydrocarbon receptor antagonist using the proteolysis-targeting chimeric molecules approach: a potential tool for chemoprevention. Mol Pharmacol *73*, 1064-1071.

Raftogianis, R.B., Zalatoris, J.J., and Walther, S.F. (1998). The role of pharmacogenetis in cancer therapy, prevention, and risk. Fox Chase Cancer Center Scientific Report, 243-247.

Rannug, U., Rannug, A., Sjoberg, U., Li, H., Westerholm, R., and Bergman, J. (1995). Structure elucidation of two tryptophan-derived, high affinity Ah receptor ligands. Chem Biol *2*, 841-845.

Rao, M.S., and Reddy, J.K. (2001). Peroxisomal beta-oxidation and steatohepatitis. Semin Liver Dis *21*, 43-55.

Ravikumar, B., Carey, P.E., Snaar, J.E., Deelchand, D.K., Cook, D.B., Neely, R.D., English, P.T., Firbank, M.J., Morris, P.G., and Taylor, R. (2005). Real-time assessment of postprandial fat storage in liver and skeletal muscle in health and type 2 diabetes. Am J Physiol Endocrinol Metab *288*, E789-797.

Reddy, J.K., and Hashimoto, T. (2001). Peroxisomal beta-oxidation and peroxisome proliferator-activated receptor alpha: an adaptive metabolic system. Annu Rev Nutr *21*, 193-230.

Reed, M.J., Purohit, A., Woo, L.W., Newman, S.P., and Potter, B.V. (2005). Steroid sulfatase: molecular biology, regulation, and inhibition. Endocr Rev *26*, 171-202.

Rehse, P.H., Zhou, M., and Lin, S.X. (2002). Crystal structure of human dehydroepiandrosterone sulphotransferase in complex with substrate. Biochem J *364*, 165-171.

Repa, J.J., Liang, G., Ou, J., Bashmakov, Y., Lobaccaro, J.M., Shimomura, I., Shan, B., Brown, M.S., Goldstein, J.L., and Mangelsdorf, D.J. (2000a). Regulation of mouse sterol regulatory

element-binding protein-1c gene (SREBP-1c) by oxysterol receptors, LXRalpha and LXRbeta. Genes Dev *14*, 2819-2830.

Repa, J.J., and Mangelsdorf, D.J. (1999). Nuclear receptor regulation of cholesterol and bile acid metabolism. Curr Opin Biotechnol *10*, 557-563.

Repa, J.J., and Mangelsdorf, D.J. (2002). The liver X receptor gene team: potential new players in atherosclerosis. Nat Med *8*, 1243-1248.

Repa, J.J., Turley, S.D., Lobaccaro, J.A., Medina, J., Li, L., Lustig, K., Shan, B., Heyman, R.A., Dietschy, J.M., and Mangelsdorf, D.J. (2000b). Regulation of absorption and ABC1-mediated efflux of cholesterol by RXR heterodimers. Science *289*, 1524-1529.

Revel, A., Raanani, H., Younglai, E., Xu, J., Rogers, I., Han, R., Savouret, J.F., and Casper, R.F. (2003). Resveratrol, a natural aryl hydrocarbon receptor antagonist, protects lung from DNA damage and apoptosis caused by benzo[a]pyrene. J Appl Toxicol *23*, 255-261.

Reyes, H., Reisz-Porszasz, S., and Hankinson, O. (1992). Identification of the Ah receptor nuclear translocator protein (Arnt) as a component of the DNA binding form of the Ah receptor. Science *256*, 1193-1195.

Saini, S.P., Sonoda, J., Xu, L., Toma, D., Uppal, H., Mu, Y., Ren, S., Moore, D.D., Evans, R.M., and Xie, W. (2004). A novel constitutive androstane receptor-mediated and CYP3A-independent pathway of bile acid detoxification. Mol Pharmacol *65*, 292-300.

Schmidt, J.V., Su, G.H., Reddy, J.K., Simon, M.C., and Bradfield, C.A. (1996). Characterization of a murine Ahr null allele: involvement of the Ah receptor in hepatic growth and development. Proc Natl Acad Sci U S A *93*, 6731-6736.

Schultz, J.R., Tu, H., Luk, A., Repa, J.J., Medina, J.C., Li, L., Schwendner, S., Wang, S., Thoolen, M., Mangelsdorf, D.J., *et al.* (2000). Role of LXRs in control of lipogenesis. Genes Dev *14*, 2831-2838.

Seidel, S.D., Winters, G.M., Rogers, W.J., Ziccardi, M.H., Li, V., Keser, B., and Denison, M.S. (2001). Activation of the Ah receptor signaling pathway by prostaglandins. J Biochem Mol Toxicol *15*, 187-196.

Seo, J.B., Moon, H.M., Kim, W.S., Lee, Y.S., Jeong, H.W., Yoo, E.J., Ham, J., Kang, H., Park, M.G., Steffensen, K.R., *et al.* (2004). Activated liver X receptors stimulate adipocyte differentiation through induction of peroxisome proliferator-activated receptor gamma expression. Mol Cell Biol *24*, 3430-3444.

Shaban, Z., Soliman, M., El-Shazly, S., El-Bohi, K., Abdelazeez, A., Kehelo, K., Kim, H.S., Muzandu, K., Ishizuka, M., Kazusaka, A., *et al.* (2005). AhR and PPARalpha: antagonistic effects on CYP2B and CYP3A, and additive inhibitory effects on CYP2C11. Xenobiotica *35*, 51-68.

Shaffer, L.G., McCaskill, C., Han, J.Y., Choo, K.H., Cutillo, D.M., Donnenfeld, A.E., Weiss, L., and Van Dyke, D.L. (1994). Molecular characterization of de novo secondary trisomy 13. Am J Hum Genet *55*, 968-974.

Shi, Y., and Burn, P. (2004). Lipid metabolic enzymes: emerging drug targets for the treatment of obesity. Nat Rev Drug Discov *3*, 695-710.

Shimizu, Y., Nakatsuru, Y., Ichinose, M., Takahashi, Y., Kume, H., Mimura, J., Fujii-Kuriyama, Y., and Ishikawa, T. (2000). Benzo[a]pyrene carcinogenicity is lost in mice lacking the aryl hydrocarbon receptor. Proc Natl Acad Sci U S A *97*, 779-782.

Song, C., and Liao, S. (2001). Hypolipidemic effects of selective liver X receptor alpha agonists. Steroids *66*, 673-681.

Song, C.S., Jung, M.H., Kim, S.C., Hassan, T., Roy, A.K., and Chatterjee, B. (1998). Tissue-specific and androgen-repressible regulation of the rat dehydroepiandrosterone sulfotransferase gene promoter. J Biol Chem *273*, 21856-21866.

Stanbrough, M., Bubley, G.J., Ross, K., Golub, T.R., Rubin, M.A., Penning, T.M., Febbo, P.G., and Balk, S.P. (2006). Increased expression of genes converting adrenal androgens to testosterone in androgen-independent prostate cancer. Cancer Res *66*, 2815-2825.

Stefan, N., Kantartzis, K., and Haring, H.U. (2008). Causes and metabolic consequences of Fatty liver. Endocr Rev *29*, 939-960.

Strott, C.A. (1996). Steroid sulfotransferases. Endocr Rev *17*, 670-697.

Strott, C.A. (2002). Sulfonation and molecular action. Endocr Rev *23*, 703-732.

Swinnen, J.V., Brusselmans, K., and Verhoeven, G. (2006). Increased lipogenesis in cancer cells: new players, novel targets. Curr Opin Clin Nutr Metab Care *9*, 358-365.

Takase, Y., Luu-The, V., Poisson-Pare, D., Labrie, F., and Pelletier, G. (2007). Expression of sulfotransferase 1E1 in human prostate as studied by in situ hybridization and immunocytochemistry. Prostate *67*, 405-409.

Talukdar, S., and Hillgartner, F.B. (2006). The mechanism mediating the activation of acetyl-coenzyme A carboxylase-alpha gene transcription by the liver X receptor agonist T0-901317. J Lipid Res *47*, 2451-2461.

Tauchi, M., Hida, A., Negishi, T., Katsuoka, F., Noda, S., Mimura, J., Hosoya, T., Yanaka, A., Aburatani, H., Fujii-Kuriyama, Y., *et al.* (2005). Constitutive expression of aryl hydrocarbon receptor in keratinocytes causes inflammatory skin lesions. Mol Cell Biol *25*, 9360-9368.

Tilg, H., and Hotamisligil, G.S. (2006). Nonalcoholic fatty liver disease: Cytokine-adipokine interplay and regulation of insulin resistance. Gastroenterology *131*, 934-945.

Tontonoz, P., and Mangelsdorf, D.J. (2003). Liver X receptor signaling pathways in cardiovascular disease. Mol Endocrinol *17*, 985-993.

Trapman, J., and Brinkmann, A.O. (1996). The androgen receptor in prostate cancer. Pathol Res Pract *192*, 752-760.

Uchiyama, S., Shimizu, T., and Shirasawa, T. (2006). CuZn-SOD deficiency causes ApoB degradation and induces hepatic lipid accumulation by impaired lipoprotein secretion in mice. J Biol Chem *281*, 31713-31719.

Umannova, L., Zatloukalova, J., Machala, M., Krcmar, P., Majkova, Z., Hennig, B., Kozubik, A., and Vondracek, J. (2007). Tumor necrosis factor-alpha modulates effects of aryl hydrocarbon receptor ligands on cell proliferation and expression of cytochrome P450 enzymes in rat liver "stem-like" cells. Toxicol Sci *99*, 79-89.

Uppal, H., Saini, S.P., Moschetta, A., Mu, Y., Zhou, J., Gong, H., Zhai, Y., Ren, S., Michalopoulos, G.K., Mangelsdorf, D.J., *et al.* (2007). Activation of LXRs prevents bile acid toxicity and cholestasis in female mice. Hepatology *45*, 422-432.

Uppal, H., Toma, D., Saini, S.P., Ren, S., Jones, T.J., and Xie, W. (2005). Combined loss of orphan receptors PXR and CAR heightens sensitivity to toxic bile acids in mice. Hepatology *41*, 168-176.

Uyeda, K., and Repa, J.J. (2006). Carbohydrate response element binding protein, ChREBP, a transcription factor coupling hepatic glucose utilization and lipid synthesis. Cell Metab *4*, 107-110.

Valledor, A.F., Hsu, L.C., Ogawa, S., Sawka-Verhelle, D., Karin, M., and Glass, C.K. (2004). Activation of liver X receptors and retinoid X receptors prevents bacterial-induced macrophage apoptosis. Proc Natl Acad Sci U S A *101*, 17813-17818.

Volle, D.H., Mouzat, K., Duggavathi, R., Siddeek, B., Dechelotte, P., Sion, B., Veyssiere, G., Benahmed, M., and Lobaccaro, J.M. (2007). Multiple roles of the nuclear receptors for oxysterols liver X receptor to maintain male fertility. Mol Endocrinol *21*, 1014-1027.

Wada, T., Kang, H.S., Angers, M., Gong, H., Bhatia, S., Khadem, S., Ren, S., Ellis, E., Strom, S.C., Jetten, A.M., *et al.* (2008). Identification of oxysterol 7alpha-hydroxylase (Cyp7b1) as a novel retinoid-related orphan receptor alpha (RORalpha) (NR1F1) target gene and a functional cross-talk between RORalpha and liver X receptor (NR1H3). Mol Pharmacol *73*, 891-899.

Walisser, J.A., Glover, E., Pande, K., Liss, A.L., and Bradfield, C.A. (2005). Aryl hydrocarbon receptor-dependent liver development and hepatotoxicity are mediated by different cell types. Proc Natl Acad Sci U S A *102*, 17858-17863.

Wanders, R.J., Vreken, P., Ferdinandusse, S., Jansen, G.A., Waterham, H.R., van Roermund, C.W., and Van Grunsven, E.G. (2001). Peroxisomal fatty acid alpha- and beta-oxidation in humans: enzymology, peroxisomal metabolite transporters and peroxisomal diseases. Biochem Soc Trans *29*, 250-267.

Wente, W., Brenner, M.B., Zitzer, H., Gromada, J., and Efanov, A.M. (2007). Activation of liver X receptors and retinoid X receptors induces growth arrest and apoptosis in insulin-secreting cells. Endocrinology *148*, 1843-1849.

Willy, P.J., Umesono, K., Ong, E.S., Evans, R.M., Heyman, R.A., and Mangelsdorf, D.J. (1995). LXR, a nuclear receptor that defines a distinct retinoid response pathway. Genes Dev *9*, 1033-1045.

Yoshikawa, T., Shimano, H., Amemiya-Kudo, M., Yahagi, N., Hasty, A.H., Matsuzaka, T., Okazaki, H., Tamura, Y., Iizuka, Y., Ohashi, K., *et al.* (2001). Identification of liver X receptor-retinoid X receptor as an activator of the sterol regulatory element-binding protein 1c gene promoter. Mol Cell Biol *21*, 2991-3000.

Youssef, J.A., Song, W.O., and Badr, M.Z. (1997). Mitochondrial, but not peroxisomal, beta-oxidation of fatty acids is conserved in coenzyme A-deficient rat liver. Mol Cell Biochem *175*, 37-42.

Zelcer, N., and Tontonoz, P. (2006). Liver X receptors as integrators of metabolic and inflammatory signaling. J Clin Invest *116*, 607-614.

Zhang, Y., Repa, J.J., Gauthier, K., and Mangelsdorf, D.J. (2001). Regulation of lipoprotein lipase by the oxysterol receptors, LXRalpha and LXRbeta. J Biol Chem *276*, 43018-43024.

Zhou, J., Zhai, Y., Mu, Y., Gong, H., Uppal, H., Toma, D., Ren, S., Evans, R.M., and Xie, W. (2006). A novel pregnane X receptor-mediated and sterol regulatory element-binding protein-independent lipogenic pathway. J Biol Chem *281*, 15013-15020.